NOVEL MODIFICATIONS OF ELEMENTAL NITROGEN AND THEIR MOLECULAR STRUCTURES – A QUANTUM-CHEMICAL CALCULATION

Denis V. Chachkov[a,b] and Oleg V. Mikhailov [a,b]*

Keywords: Nitrogen modifications; molecular structure; quantum-chemical calculation; QCISD; G3.

Using the quantum-chemical calculation methods QCISD and G3, the possibility of the existence of nitrogen molecules with the composition N_4, N_6, N_8 and N_{10} has been discussed. On the basis of the data obtained, the conclusion about possibility of existence of three novel polymorphic modifications of elemental nitrogen with an even number of atoms in molecules, namely N_4 with rectangular and regular tetrahedron shapes, and N_6 in a form remotely resembling an "open book", has been made. The values of bond lengths, valence and torsion angles, and oscillations frequencies in each of the above-mentioned forms of elemental nitrogen have been presented.

* Corresponding Authors
E-Mail: olegmkhlv@gmail.com
[a] Kazan National Research Technological University, K. Marx Street 68, 420015 Kazan, Russia
[b] Kazan Department of Joint Supercomputer Center of Russian Academy of Sciences – Branch of Federal Scientific Center"Scientific Research Institute for System Analysis of the RAS", Lobachevski Street 2/31, 420111 Kazan, Russia

INTRODUCTION

Molecule of elemental nitrogen is known to consist of two atoms with a triple bond between them.[1] The length of this bond is only 109.5 pm, and, owing to this, the N_2 molecule (dinitrogen) is characterized by a very high dissociation energy (941.64 kJ mol^{-1}) and by very less chemical activity.

Three crystalline modifications of N_2 are known. In the temperature range 36.61-63.29 K, β-N_2 phase having a hexagonal dense packing, a space $P6_3$ mmc^{-2} group, lattice parameters a = 3.93 Å and c = 6.50 Å, exists. At a temperature lower than 36.61 K, a stable α-N_2 phase having cubic lattice, a space $P2_13$ group and a period of a = 5.660 Å, occurs. At a pressure of more than 3500 atmospheres and a temperature below 83.0 K, a hexagonal phase of dinitrogen, namely γ-N_2, is formed.

There are some theoretical indications that other nitrogen oligomers and polymers may be possible. These nitrogen modifications may have potential applications as materials with a very high energy density and as powerful propellants or explosives.[1] For most neutral polynitrogens are not expected to have a large barrier towards decomposition, and that the few exceptions would be even more challenging to synthesize than the tetranitrogen N_4 which is an analogue of tetrahedrane C_4, and has potential as a high-performance energetic material.[2] Nevertheless, cationic and anionic polynitrogens, namely cations of triazenium (N_3^+), tetrazenium (N_4^+), pentazenium (N_5^+), and azide-anione (N_3^-), pentazolide-anione (cyclic aromatic N_5^-) have been characterized.[1,3-9] However, all these nitrogen compounds have a positive or negative charge. Up to now, however, there is no information in the literature on the existence of other neutral simple substances consisting solely of nitrogen atoms.[10-12] In this connection, in the this article the possibility of the existence of polyatomic molecules of nitrogen with an even number of atoms, namely nitrogen molecules of N_4, N_6, N_8 and N_{10} compositions will be discussed.

CALCULATION METHOD

The calculation of molecular structures of polyatomic nitrogen molecules of N_4, N_6, N_8 and N_{10} compositions was carried out using the QCISD(T)/TZVP method, as described in detail earlier,[13] in combination with the Gaussian09 software package.[14] The initial structures of the N_4, N_6, N_8 and N_{10} molecules for carrying out quantum-chemical calculations are shown in figure 1.

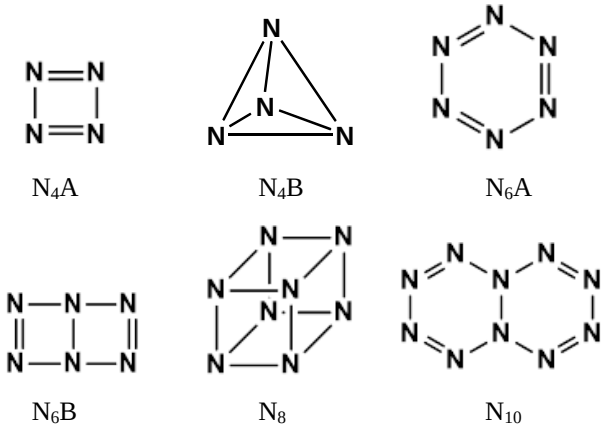

Figure 1. The assumed initial structures of nitrogen molecules.

The choice of these initial structures was determined by two factors. First, the valence possibilities of the nitrogen atom (which capable to bind with one, two or three neighboring atoms by means of three chemical bonds according to the exchange mechanism) and secondly, with the greatest typicality of these structures compared with other structures with a corresponding number of atoms. In this connection, the regular octahedron in the case of N_6, the

hexagonal bipyramid and the dodecahedron in the case of N_8, the two-capped cube or the two-capped dodecahedron in the case of N_{10} were not included in the number of initial structures. The correspondence of the found stationary points to energy minima was proved in all cases by the calculation of the second derivatives of energy with respect to the atom coordinates All equilibrium structures corresponding to the minima on the potential energy surfaces has only positive frequencies. The values of the standard thermodynamic characteristics of the nitrogen-containing compounds under examination were calculated using the G3 method described in earlier in detail.[15] All quantum-chemical calculations were carried out in the Joint Supercomputer Center, Kazan Branch of RAS – Branch of Federal Scientific Center "Research Institute for System Studies of the Russian Academy of Sciences" (http://www.jscc.ru).

RESULTS AND DISCUSSION

According to the results of our calculations, only three of the six structures of polyatomic nitrogen molecules mentioned above are stable, namely the N_4A structure in the form of a rectangle, N_4B in the form of a regular tetrahedron, and the N_6B structure in the form of an "open book". All these modifications have been shown in figure 2.

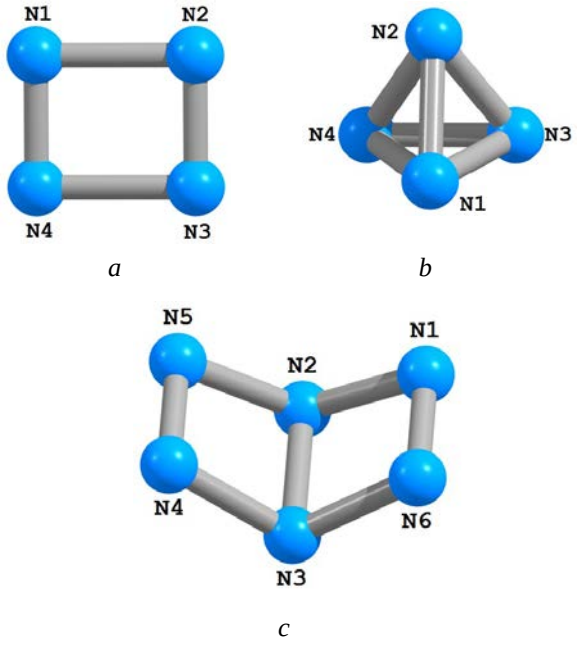

Figure 2. Molecular structures of three theoretically possible polymorphic modifications of elemental nitrogen.

The geometric parameters of these above-mentioned stable structures (bond lengths, valence and torsion angles) have been presented in the Table 1. As can be seen from these data, in the polyatomic nitrogen molecules under examination, the nitrogen–nitrogen bond lengths are much larger than those in the N_2 molecule; it is quite natural, because the theoretically expected multiplicity of bonds in them should be lesser than one in a dinitrogen molecule. It should be noted in this connection that for the N_2 molecule itself, according to the QCISD(T)/TZVP method, the bond length (N1N2) is 110.3 pm that is very close to the experimental value of (109.5-110.0) pm.[1] It is interesting that, according to our calculations, for a "planar" version of the tetranitrogen molecule N_4A, not a square or orthorhombic structure is realized, as might be expected, but a rectangular structure, with rather considerably different "longitudinal" and "transverse" bond lengths (154.6 and 127.1 pm, respectively) (Figure 2). At the same time, for the "tetrahedral" variant N_4B, the structure of the regular tetrahedron, where all the lengths of nitrogen-nitrogen bonds are exactly the same and have an intermediate values between the nitrogen- nitrogen bond lengths in the structure of N_4A.

Table 1. Parameters of the molecular structure of four- and six-atom nitrogen molecules.

Molecule N_4A			
N-N bond lengths, pm		**Valence angles, deg**	
(N1N2)	154.6	(N1N2N3)	90.0
(N2N3)	127.1	(N2N3N4)	90.0
(N3N4)	154.6	(N3N4N1)	90.0
(N4N1)	127.1	(N4N1N2)	90.0
Torsion (dihedral) angles, deg			
(N1N2N3N4)	0.0	(N2N3N4N1)	0.0
(N3N4N1N2)	0.0	(N4N1N2N3)	0.0
Molecule N_4(B)			
N-N bond lengths, pm		**Valence angles, deg**	
(N1N2)	146.7	(N1N2N3)	60.0
(N1N3)	146.7	(N1N2N4)	60.0
(N1N4)	146.7	(N1N3N2)	60.0
(N2N3)	146.7	(N1N3N4)	60.0
(N2N4)	146.7	(N1N4N2)	60.0
(N3N4)	146.7	(N1N4N3)	60.0
Torsion (dihedral) angles, deg			
(N1N2N3N4)	70.6	(N2N3N4N1)	–70.5
(N3N4N1N2)	–70.6	(N4N1N2N3)	–70.5
Molecule N_6(B)			
N-N bond lengths, pm		**Valence angles, deg**	
(N1N2)	147.8	(N1N2N5)	109.1
(N2N3)	153.0	(N2N5N4)	95.3
(N3N6)	147.7	(N5N4N3)	95.3
(N6N1)	125.8	(N4N3N6)	109.1
(N2N5)	147.7	(N3N6N1)	95.3
(N5N4)	125.8	(N6N1N2)	95.3
(N4N3)	147.7	(N2N3N4)	84.7
		(N2N3N6)	84.7
		(N3N2N1)	84.7
		(N3N2N5)	84.7
Torsion (dihedral) angles, deg			
(N1N2N5N4)	–82.5	(N6N3N4N5)	82.5
(N1N6N3N4)	–82.6	(N6N1N2N5)	82.5
(N1N2N3N6)	0.0	(N5N2N3N4)	0.0
(N2N3N6N1)	0.0	(N2N3N4N5)	0.0
(N3N6N1N2)	0.0	(N3N4N5N2)	0.0
(N6N1N2N3)	0.0	(N4N5N2N3)	0.0
(N5N2N3N6)	–109.8	(N1N2N3N4)	109.8

The structure of N_6B, as it should be expected, is non-coplanar. There are three different kinds of nitrogen-nitrogen bonds having different lengths in it. Two of them

are relatively short (125.8 pm) and correspond to the double N=N bond; the other five in own length correspond to a single N-N bond, but one of them forming sui generis "binding" of this "open book" itself, is noticeably longer than the other four, 153.0 and 147.7 pm, respectively.

Table 2. The oscillation frequencies in the N_4A, N_4B and N_6B.

Oscillation frequency, cm^{-1}	Assignment of oscillation frequency
Molecule N_4(A)	
402	Wagging
493	Stretching (*asym.*) with participation of atoms (N1N2) and (N3N4)
904	Stretching (*sym.*) with participation of atoms (N1N2) and (N3N4)
998	Scissoring
1296	Stretching (*asym.*) with participation of atoms (N1N4) and (N2N3)
1526	Stretching (*sym.*) with participation of atoms (N1N4) and (N2N3)
Molecule N_4(B)	
695	Scissoring with change of all valence angles
695	Scissoring with participation of atoms (N1N4) and (N2N3), concerning (N2N4) bond
915	Stretching (*asym.*) with change of (N1N4), (N1N3) and (N2N3) bond lengths
915	Stretching with change of (N1N3), (N1N4), (N2N3) and (N2N4) bond lengths
917	Scissoring with change of angles (N3N1N4) and (N3N2N4)
1288	Stretching (*sym.*) with participation of all participation of all N atoms
Molecule N_6(B)	
383	Conjugation of two rocking oscillations of (N4N3N6) and (N1N2N5)
447	Scissoring with participation of atom groupings (N3N4N6) and (N1N2N5)
468	Scissoring with participation of atom grouping (N3N4N6)
578	Stretching (*sym.*) with change of bond lengths in pairs (N2N5), (N1N2) and (N4N3), (N3N6)
716	Stretching (*asym.*) with change of bond lengths in pairs (N2N5), (N1N2) and (N4N3), (N3N6)
749	Stretching (*sym.*) with change of bond lengths in pairs(N1N2), (N2N5), and (N4N3), (N3N6), and (N2N3), too
841	Scissoring with participation of atom groupings (N1N2N5) and (N3N4N6)
917	Rocking with participation of atom groupings (N1N2N5) and (N3N4N6)
946	Scissoring with change of bond length (N2N3)
1030	Conjugation of several scissoring oscillations
1447	Stretching (*asym.*) with change of bond lengths (N1N6) and (N4N5)
1510	Stretching (*sym.*) with change of bond lengths (N1N6) and (N4N5)

As a result of the above differences, both sides of the "cover" of this "open book" are in fact not rectangles, as might be expected at first glance, but are identical isosceles trapezoids. The sum of the valence angles (N3N6N1) + (N6N1N2) + (N1N2N3) + (N2N3N6) and (N4N3N2) + (N3N2N5) + (N2N5N4) + (N5N4N3) are the same and are equal to exactly 360.0°. What is remarkable, the values of the valence angles (N1N2N5) and (N4N3N6) are much closer to 90° than to 180°, so the degree of non-coplanarity of the molecular structure of N_6B should be considered as very significant.

Oscillation frequencies of polynitrogen molecules N_4A, N_4B and N_6B are depicted in Table 2. According to theoretical expectations, 6 oscillations must be active in the IR spectrum in the case of N_4A and N_4B, and 12, in the case of N_6B. Our calculated values match the theoretical expectations.(Table 2). As may be seen from these data, the sets of vibrational frequencies in polynitrogen molecules are quite different among themselves. At the same time, what is interesting, in N_4B, there are two pairs of oscillations of different nature with the almost identical in frequency, 695 and 915 cm^{-1} whereas in N_4B and N_6B, nothing like this occurs.

Table 3. Calculated standard thermodynamic parameters of formation of N_4A, N_4B and N_6B molecules from dinitrogen.

Compound	$\Delta_f H^0$, kJ mol^{-1}	S^0, J mol^{-1} K^{-1}	$\Delta_f G^0$, kJ mol^{-1}
N_4A	771.6	248.6	810.8
N_4B	771.0	230.9	815.6
N_6B	1009.5	278.2	1096.7

The values of standard thermodynamic characteristics, namely $\Delta_f H^0$ (kJ mol^{-1}), S^0 (J mol^{-1} K^{-1}) and $\Delta_f G^0$ (kJ mol^{-1}), of the formation of N_4A, N_4B and N_6B were calculated with using of G3 method and are presented in the Table 3. As follows from the data given in it, they all have positive values. In this connection, this fact attracts its attention that the values of these standard parameters for compounds N_4A and N_4B despite the very significant difference in their molecular structures, are nevertheless extremely close to each other. It is easy may be shown with using of these data and well-known values of $\Delta_f H^0$ and S^0 for dinitrogen (0 kJ mol^{-1} and 191.6 J mol^{-1} K^{-1}, respectively,[16] they cannot be formed directly from N_2 within the framework of the isobar process by general eqns. (1-3)

$$2N_2\,(gas) \rightarrow N_4A\,(gas) \quad (1)$$

$$2N_2\,(gas) \rightarrow N_4B\,(gas) \quad (2)$$

$$3N_2\,(gas) \rightarrow N_6\,(gas) \quad (3)$$

Table 5. Calculated standard thermodynamic parameters of formation of N_4A, N_4B and N_6B molecules from atomic nitrogen.

Reaction	ΔH^0, kJ	S^0, J K^{-1}
4N (gas) → N_4A (gas)	–1119.6	–364.6
4N (gas) → N_4B (gas)	–1120.2	–382.3
6N (gas) → N_6 (gas)	–1827.3	–641.6

The point is that for each of these processes, the value of the standard enthalpy of the reaction (ΔH^0_{298}) is positive, and, on the contrary, the standard entropy (S^0_{298}) is negative (Table 4), and in accordance with the classical Gibbs-Helmholtz equation $\Delta G^0 = \Delta H^0 - T\Delta S^0$, their synthesis directly from the "ordinary" dinitrogen N_2 is thermodynamically forbidden process. However, from the thermodynamic point of view, the formation of N_4A, N_4B and N_6B from atomic nitrogen according to schemes (4-6) is perfectly permissible and, nevertheless, as can be shown using the values of $\Delta_f H^0$ and S^0 for atomic nitrogen (472.8 kJ mol^{-1} and 153.3 J mol^{-1} K^{-1}, respectively),[16] for each of reactions (4-6) ΔH^0 as well as ΔS^0 are *negative* (Table 5) so that in a certain temperature range each of them are thermodynamically resolved. It should be noted in this connection that according to our calculation using the G3 method, the standard enthalpy of the N_2(gas) → 2N (gas) process, in fact, the energy of N≡N bond in the dinitrogen molecule is 936.60 kJ mol^{-1}, which is in very good agreement with the experimental value of 941.64 kJ mol^{-1}. How to synthesize these novel polymorphic modifications of nitrogen is another problem, the discussion of which is beyond the scope of this paper, and further researches are needed for it.

4N (gas) →N_4(A) (gas) (4)

4N (gas) → N_4(B) (gas) (5)

6N (gas) → N_6 (gas) (6)

FUNDING INFORMATION

All quantum-chemical calculations were performed at the Kazan Department of Joint Supercomputer Center of Russian Academy of Sciences – Branch of Federal Scientific Center “Scientific Research Institute for System Analysis of the RAS”. Contribution of author Chachkov D.V. was funded by the state assignment to the Federal State Institution "Scientific Research Institute for System Analysis of the Russian Academy of Sciences" for scientific research.

CONFLICT OF INTEREST

The authors declare that they have no conflict of interest, financial or otherwise.

REFERENCES

[1]Wikipedia. Web-site https://en.wikipedia.org/wiki/Nitrogen

[2]Zhou, G., Zhang, J.L, Wong, N-B., *J. Mol. Struct.* (*Theochem*), **2004**, *668*, 189-195. https://doi.org/10.1016/j.theochem.2003.10.054

[3]Christe, K. O., Wilson, W. W., Sheehy, J. A., Boatz, J. A., $_5^+$: A Novel Homoleptic Polynitrogen Ion as a High Energy Density Material,, *Angew. Chem., Int. Ed*., **1999**, *38*, 2004-2009. https://doi.org/10.1002/(SICI)1521-3773(19990712)38:13/14%3C2004::AID-ANIE2004%3E3.0.CO;2-7

[4]Ashwani, V., Wilson, W. W, Vandana, V., Tham, F. S., Sheehy, J. A, Christe, K. O., Polynitrogen Chemistry. Synthesis, Characterization, and Crystal Structure of Surprisingly Stable Fluoroantimonate Salts of N_5^+, *J. Am. Chem. Soc*., **2001**, *123*, 6308-6313. https://doi.org/10.1021/ja010141g

[5]Burke, L. A., Fazen, P. J., Correlation analysis of the interconversion and nitrogen loss reactions of aryl pentazenes and pentazoles derived from aryl diazonium and azide ions, *Int. J. Quant. Chem*., **2009**, *109*, 3613-3618. https://doi.org/10.1002/qua.22408

[6]Steele, B. A., Stavrou, E., Crowhurst, J. C., Zaug, J. M., Prakapenka, V. B., Oleynik, I. I., High-Pressure Synthesis of a Pentazolate Salt, *Chem. Mater*. **2017**, *29*, 735-741. https://doi.org/10.1021/acs.chemmater.6b04538

[7]Zhang, C., Sun, C., Hu, B., Yu, C., Lu, M., Synthesis and characterization of the pentazolate anion cyclo-N_5^- in $(N_5)_6(H_3O)_3(NH_4)_4Cl$, *Science*, **2017**, *355(6323)*, 374-376. https://doi.org/10.1126/science.aah3840

[8]Tosi, P., Lu, W. Y,, Bassi, D., Tarroni, R., The reaction $N_2^+ + N_2 \rightarrow N_3^+ + N$ from thermal to 25 eV, *J. Chem. Phys*., **2001**, *114*, 2149‑2153. https://doi.org/10.1063/1.1336808

[9]Junk, G., The presence of N_3^+ and N_4^+ in the mass spectra of molecular nitrogen, *J. Am. Chem. Soc.*, **1958**, *80*, 2908–2909. https://doi.org/10.1021/ja01544a085

[10]Cacace, F., de Petris, G., Troiani, A., Experimental Detection of Tetranitrogen, *Science*, **2002**, *295(5554)*, 480–481.https://doi.org/10.1126/science.1067681

[11]Zarko, V. E., Searching for ways to create energetic materials based on polynitrogen compounds, *Combust. Explosion Shock Waves*, **2010**, *46*, 121–131. https://doi.org/10.1007/s10573-010-0020-x

[12]Nguyen, M. T., Polynitrogen compounds: 1. Structure and stability of N_4 and N_5 systems, *Coord. Chem. Revs.*, **2003**, *244*, 93–113. https://doi.org/10.1016/S0010-8545(03)00101-2

[13]Pople, J.A., Head-Gordon, M., Raghavachari, K., Quadratic configuration interaction. A general technique for determining electron correlation energies, *J. Chem. Phys*., **1987**, *87*, 5968-5975.https://doi.org/10.1063/1.453520

[14]Gaussian 09, Revision A.01, Frisch, M.J.; Trucks, G.W.; Schlegel, H.B.; Scuseria, G.E.; Robb, M.A.; Cheeseman, J.R.; Scalmani, G.; Barone, V.; Mennucci, B.; Petersson, G.A.; Nakatsuji, H.; Caricato, M.; Li, H.; Hratchian, H.P.; Izmaylov, A.F.; Bloino, J.; Zheng, G.; Sonnenberg, J.L.; Hada, M.; Ehara, M.; Toyota, K.; Fukuda, R.; Hasegawa, J.; Ishida, M.; Nakajima, T.; Honda, Y.; Kitao, O.; Nakai, H.; Vreven, T.; Montgomery, J.A. Jr.; Peralta, J.E.; Ogliaro, F.; Bearpark, M.; Heyd, J.J.; Brothers, E.; Kudin, K.N.; Staroverov, V.N.; Kobayashi, R.; Normand, J.; Raghavachari, K.; Rendell, A.; Burant, J.C.; Iyengar, S.S.; Tomasi, J.; Cossi, M.; Rega, N.; Millam, J.M.; Klene, M.; Knox, J.E.; Cross, J.B.; Bakken, V.; Adamo, C.; Jaramillo, J.; Gomperts, R.; Stratmann, R.E.; Yazyev, O.; Austin, A.J.; Cammi, R.; Pomelli, C.; Ochterski, J.W.; Martin, R.L.; Morokuma, K.; Zakrzewski, V.G.; Voth, G.A.; Salvador, P.; Dannenberg, J.J.; Dapprich, S.; Daniels, A.D.; Farkas, O.; Foresman, J.B.; Ortiz, J.V.; Cioslowski, J.; and Fox, D.J. Gaussian, Inc., Wallingford CT, 2009.

[15]Curtiss, A., Raghavachari, K., Redfern, P.C., Rassolov, V., Pople, J.A., *J. Chem. Phys.*, **1998**, *109*, 7764-7776. https://doi.org/10.1063/1.477422

[16]Standard thermodynamic properties of chemical substances. Web-site http://www.update.uu.se/ ~jolkkonen/pdf/CRC_TD.

Received: 15.01.2020.
Accepted: 13.03.2020.

Au-MOPS(3-MORPHOLINOPROPANE-1-SULFONIC ACID) COUPLED CATALYST FOR THE SYNTHESIS OF 3-AMINOALKYLATED INDOLES

Suryakant B. Sapkal,[a]* Sadanand Y. Guhe,[a] Sanjay N. Harke,[b] Balaji R. Madje[c] and Suchita S. Gadekar[c]

Keywords: Gold nanoparticles; catalytic performance; amino alkylated indoles; 3-morpholinopropane-1-sulfonic acid (MOPS).

Gold nanoparticles (Au NPs) coupled with 3-morpholinopropane-1-sulfonic acid (MOPS) for catalytic performance to the cyclocondensation reaction of aromatic/heteroaromatic/aliphatic aldehydes, indole and aromatic/heteroaromatic amines have been demonstrated for the first time in favour of 3-aminoalkylated indoles in ethyl alcohol at reflux temperature. Reaction conditions are just like ambient nevertheless all chemical transformations completed smoothly contributing worthwhile for the synthesis of 3-aminoalkylated indoles.

*Corresponding Authors
E-Mail: sapkalsb@gmail
[a] MGM's Jawaharlal Nehru Engineering College, Aurangabad-431 004, India,
[b] MGM's Institute of Bioscience and Technology, Aurangabad-431 004, India,
[c] Vasantrao Naik College, Aurangabad-431 004, India.

INTRODUCTION

In recent years, an emphasis of scientists and scientific communities is infusing to nurture the science and technology for human development and environment sustainability. For this accomplishment we need to use either clean and green recourses or processes or design such protocols that should not generate waste materials.[1,2] In this regards, we proposed this permissive protocol that covers the green chemistry features.

Literature assessment revealed that nanocatalysts are successfully utilized for various organic transformations. Nanomaterials provide active surface area and having high surface to volume ratio. Hence, that accelerate rate of chemical transformation while reducing activation energy of reactants.[3-6] MOPS help to involve reacting precursors in the chemical reaction by protonating them at the appropriate site. Henceforth, coupled nanocatalyst that is Au-MOPS could be a dedicated catalyst for beneficent synthetic route to 3-amino alkylated indoles. Literally, several chemical, biochemical applications of MOPS have been found as it is an excellent buffer for many biological systems [7-10] at near-neutral pH with a pK_a of 7.20. Chemical structure of MOPS contains a morpholine ring having propane sulfonic acid as a substituent at nitrogen atom. Herein, this protocol acquires benefits of both Au NPs as well as MOPS as a coupled catalyst.

As we know in many natural products a pharmacodynamic nucleus of indole exhibited characteristic activities, therefore indole moiety gaining considerable importance.[11-13] In particular, 3-C-functionalized indoles are highly applicable for the synthesis of various indole impurities in support of active pharmaceutical ingredients (APIs) such as antibacterial,[14] anti-inflammatory and analgesic agent,[15] anticonvulsant,[16] cardiovascular,[17] HIV-1 inhibitor,[18] antimigraine and to cure breast cancer.[19] Because of such widespread medicinal applications of 3-substituted indole nucleus the chemists and pharmacists are consistently engaged in the development of competent methodologies for proposed nucleus by applying several conditions such as β-cyclodextrin,[20] Silver triflate (AgOTf),[21] ionic liquids,[22] indium/HCl,[23] PMA-SiO_2/CH_3CN.[24] Moreover, 3-substituted indoles via reactive intermediates alkylidene indoleamine have also been attempted through state of the art conditions with considerable yields of the product in hand.[25] Herein, we have proposed beneficent and user friendly synthetic route to the 3-aminoalkylated indole nucleus in the presence of Au-MOPS coupled catalyst in ethyl alcohol at reflux temperature.

EXPERIMENTAL

All the reagents and solvents were used for the reactions and column chromatography were purchased from HiMedia, Finechem, Spectrochem and Rankem Chemical Companies and used directly without further purification. The progress of the reactions was monitored by thin-layer chromatography 60 F254 (TLC). 1H NMR spectra were recorded on 300 MHz FT-NMR spectrometer in $CDCl_3$ as a solvent and chemical shifts were reported in parts per million (ppm) relative to tetramethyl silane $(CH_3)_4Si$.

Preparation of Au NPs

Solutions of 0.025 M gold(III) chloride as a precursor and 0.5 M L-Ascorbic acid solution as a reducing and capping agent are prepared in a doubled distilled water. Gold(III) chloride solution is heated with continuous stirring on magnetic stirrer up to its boiling point. L-Ascorbic acid reducing agent is added drop by drop to the gold(III) chloride solution. Colour of the solution changes from colourless to ruby red indicates the formation of gold nanoparticles (Au NPs) which are cooled and stored in airtight glass container and used with MOPS as a catalyst for the said reaction.

Characterization of Au NPs

The UV-VIS absorption of gold nanoparticles was measured in single beam spectrophotometer and absorption maxima was noted

at different wavelength (523-551 nm).the gold colloidal gold synthesis in experiment shown heavy absorption at 523 nm. Four runs taken of samples with different reducing agent which are L-ascorbic acid and trisodium citrate and different concentration of it were taken *i.e.* in limited and excess amount. Baseline for UV-Vis was distilled water.

The size of gold nanoparticles has been determined by measuring the diameter of whole particles on TEM images. The average diameter of colloidal gold was around 25 nm and minimum size being around 7 nm.

Preparation of 3-aminoalkylated indoles

In hard glass test tube vanillin (0.306 g, 0.002 mol) and aniline (0.186 g, 0.002 mol) and MOPS (0.06 g, 1 mmol) in 25 mL ethyl alcohol was stirred at 60-65 °C for one hour. To this solution, Indole (0.234g, 0.002 mol) was added portion wise with continued stirring at same temperature. The progress of the reaction was monitored after interval of each half hour by TLC. The reaction is completed after specified period of time. After completion the reaction mixture was poured on crushed ice, the obtained solid was filtered, dried and purified by column chromatography on silica gel using ethyl acetate/n-hexane solvent system to yield a pure product. Similar procedure was applied for the synthesis of other derivatives. All compounds were characterized by spectroscopic analysis.

N-((1*H*-Indol-3-yl)(phenyl)methyl)benzeneamine (4a)

^{1}H NMH (200 MHz, $CDCl_3$): δ 9.95 (1H, s, NH), 7.90(1H, s, Ar-H), 6.7-7.5 (9H, m, Ar-H), 6.3-6.5 (5H, m, Ar-H), 5.85 (1H, s, C3H), 3.9 (1H, s, NH); ^{13}C NMR (50 MHz, $CDCl_3$): δ 144.14, 136.80, 128.88, 128.84, 128.33, 127.19, 126.24, 123.76, 122.01, 120.04, 119.80, 119.32, 111.17, 40.30.LC MS: m/z 298.15.

N-((4-Chlorophenyl)(1*H*-indol-3-yl)methyl)benzeneamine (4b)

^{1}H NMH (200 MHz, $CDCl_3$): δ 10.09 (1H, s, NH), 5.34 (1H, s, C-H), 6.43–7.04 (5H, m, Ar-H), 7.01–7.38 (8H, m, Ar-H), 6.81(1H ,s, Ar-H), 3.95 (1H, s, NH),. ^{13}C NMR (50 MHz, $CDCl_3$): δ: 61.7, 111.1, 112.0, 113.3, 117.2, 118.9, 119.9, 122.1, 123.0,127.1, 128.0, 128.5, 129.3, 132.9, 136.4, 140.2, 147.5; .LC MS: m/z 332.99.

N-((4-Hydroxyphenyl)(1*H*-indol-3-yl)methyl)benzeneamine (4c)

^{1}H NMH (200 MHz, $CDCl_3$): δ 10.1 (1H, s, NH), 5.16 (1H, s, C-H), 6.43–7.04 (5H, m, Ar-H), 6.61–7.4 (8H, m, Ar-H), 6.43 (1H ,s, Ar-H), 3.91 (1H, s, NH), 5.32 (1H, s OH). ^{13}C NMR (50 MHz, $CDCl_3$): δ: 61.9, 110.9, 112.1, 113.5, 115.2, 118.9, 119.9, 121.8, 124.0,127.4, 127.9, 129.3, 134.9, 136.6, 147.6, 156.7; .LC MS: m/z 314.09.

N-((1*H*-Indol-3-yl)(p-tolyl)methyl)benzeneamine (4d)

^{1}H NMH (200 MHz, $CDCl_3$): δ 7.81 (1H, brs), 7.30 (2H, d, J = 8.0 Hz, Ar-H), 7.00-7.10 (7H, m), 6.90 (2H, t, J = 8.0 Hz), 6.79 (2H, t, J = 8.0 Hz), 6.40 (2H, brs), 5.71 (1H, brs), 2.39 (3H, s); ^{13}C NMR (50 MHz, $CDCl_3$): δ 142.16, 135.80, 135.19, 130.00, 129.8, 128.01, 123.32, 121.5, 120.00, 119.6, 119.00, 109.90, 40.70, 22.05; .LC MS: m/z 312.11.

N-((4-hydroxy,3-methoxyphenyl)(1*H*-indol-3-yl)methyl)-benzeneamine (4e)

^{1}H NMH (200 MHz, $CDCl_3$): δ 9.39 (1H, s, NH), 5.6 (1H, s, C-H), 6.5–7.2 (8H, m, Ar-H), 7.1–7.6 (4H, m, Ar-H), 6.70 (1H ,s, Ar-H), 4.41 (1H, s, NH), 5.49 (1H, s OH), 3.89 (3H, S, C-H) ^{13}C NMR (50 MHz, $CDCl_3$): δ: 57.01, 62.4, 111.9, 112.3, 113.1,113.8, 116.2, 117.9, 119.7, 120.4, 121.0, 122.0, 122.9, 127.9, 129.8, 135.8, 136.5, 144.0, 148.7, 152.0; .LC MS: m/z 344.20.

N-((3-Chlorophenyl)(1*H*-indol-3-yl)methyl)benzeneamine (4f)

^{1}H NMH (200 MHz, $CDCl_3$): δ 10.09 (1H, s, NH), 5.34 (1H, s, C-H), 6.43–7.04 (5H, m, Ar-H), 7.01–7.38 (8H, m, Ar-H), 6.81(1H ,s, Ar-H), 3.95 (1H, s, NH),. ^{13}C NMR (50 MHz, $CDCl_3$): δ: 61.7, 111.1, 112.0, 113.3, 117.2, 118.9, 119.9, 122.1, 123.0,127.1, 128.0, 128.5, 129.3, 132.9, 136.4, 140.2, 147.5; .LC MS: m/z 332.99.

N-((2-Chlorophenyl)(1*H*-indol-3-yl)methyl)benzeneamine (4g)

^{1}H NMH (200 MHz, $CDCl_3$): δ 10.80 (1H, s, NH), 5.61 (1H, s, C-H), 6.63–7.75 (13H, m, Ar-H), 6.11(1H ,s, Ar-H), 4.15 (1H, s, NH),. ^{13}C NMR (50 MHz, $CDCl_3$): δ: 61.7, 111.1, 112.0, 113.3, 117.2, 118.9, 119.9, 122.1, 123.0,127.1, 128.0, 128.5, 129.3, 132.9, 136.4, 140.2, 147.5; .LC MS: m/z 332.99.

N-((4-(Dimethylamino)phenyl)(1*H*-indol-3-yl)methyl)benzene-amine (4h)

^{1}H NMH (200 MHz, $CDCl_3$): δ 10.10 (1H, s, NH), 5.11 (1H, s, C-H), 6.47–7.40 (13H, m, Ar-H), 6.71(1H ,s, Ar-H), 4.05 (1H, s, NH),.2.85 (6H, S, C-H); ^{13}C NMR (50 MHz, $CDCl_3$): δ: 40.3, 61.9, 110.19, 111.9, 113.5, 114.2, 117.1, 119.3, 120.3, 122.1, 123.0,127.1, 128.0, 128.5, 129.3, 131.9, 136.4, 147.9; .LC MS: m/z 341.17.

N-(1-(1*H*-Indol-3-yl)ethyl)benzeneamine (4i)

^{1}H NMH (200 MHz, $CDCl_3$): δ 10.00 (1H, s, NH), 7.40(1H, s, Ar-H), 6.7-7.5 (5H, m, Ar-H), 6.3-6.5 (4H, m, Ar-H), 5.15 (1H, s, C3H), 4.0 (1H, s, NH), 1.90 (3H, s, CH3); ^{13}C NMR (50 MHz, $CDCl_3$): δ 145.30, 137.00, 130.50, 128.30, 123.20, 123.00, 119.40, 114.05, 55.40, 23.01; .LC MS: m/z 236.17.

N-((1*H*-Indol-3-yl)(phenyl)methyl)benzeneamine (4j)

^{1}H NMH (200 MHz, $CDCl_3$): δ 8.99 (1H, s, NH), 6.90(1H, s, Ar-H), 6.24-7.08 (8H, m, Ar-H), 7.18-7.5 (4H, m, Ar-H), 5.45 (1H, s, C-H), 4.2 (1H, s, NH); ^{13}C NMR (50 MHz, $CDCl_3$): δ 65.2, 106.80, 110.08, 111.84, 112.33, 127.19, 113.24, 117.06, 119.01, 120.04, 122.80, 122.92, 127.17, 129.30, 136.5, 142.1, 147.5, 152.50; LC MS: m/z 288.15.

N-(Furan-2-yl)methyl)(1*H*-indol-3-yl)(phenyl)methanamine (4k)

^{1}H NMH (200 MHz, $CDCl_3$): δ 10.05 (1H, s, NH), 6.90 (1H, s, Ar-H), 6.7-7.14 (12H, m, Ar-H), 5.19 (1H, s, C-H), 2.50 (1H, s, NH); ^{13}C NMR (50 MHz, $CDCl_3$): 47.2, 58.9, 106.19, 111.9, 112.5, 119.2, 120.1, 122.1, 123.0,127.1, 128.0, 128.6, 136.5, 148.8; LC MS: m/z 320.15.

RESULTS AND DISCUSSION

Gold NPs were prepared in the reaction of a hot 0.025 M gold(III) chloride as a precursor and 0.5 M L-ascorbic acid solution as a reducing and capping agent added dropwise. The UV spectra of ruby-red solution indicates the formation of gold nanoparticles (Au NPs). UV-VIS spectrophotometry is an important method in characterization of gold nanoparticles. With increase in particle size the absorption peak shifts to longer wavelength and the width of absorption spectra is related to size distribution range. Generally gold nanoparticles display a single absorption peak in visible range between 510-550 nm this gives ruby red color to gold nanoparticles which varies according to their size.

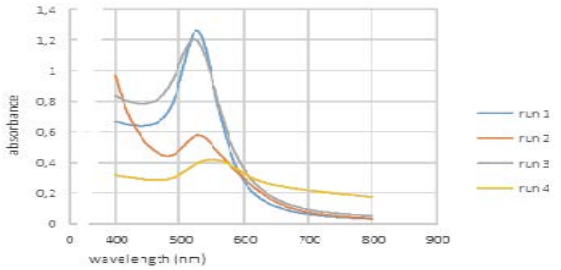

Figure1. UV-Visible absorbance spectra of Au NPs.

If coagulation is not permitted, the nuclei formed at the earliest time will grow to the largest size, and no particle can be larger than that. The particle size distribution result shows the size of nanoparticles in the solution with average size of 28 nm.

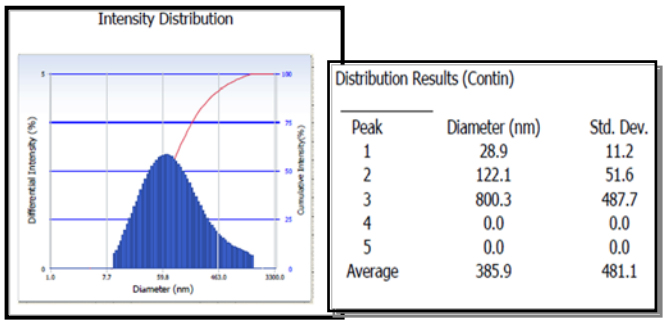

Figure 2. Particle size distribution (PSD) analysis of Au NPs.

Coagulation leads to formation of larger particles, and hence, the size distribution has become broader which is reflected in the Figure 3.

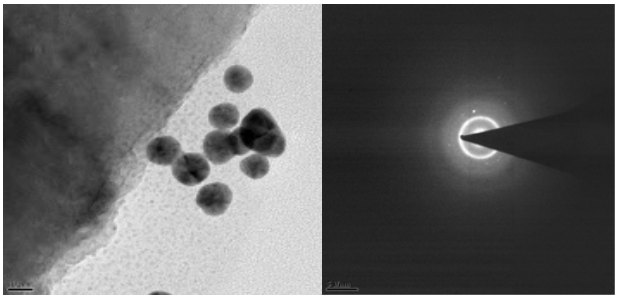

Figure 3. Transmission electron microscopy (TEM) image of as synthesized Au NPs at low magnification and its surface morphology of single Au NPS particle

In continuation of our previous efforts for the development of beneficent methodologies for the synthesis of various moieties [26] herein, at first attempt we tried the reaction of equimolar quantity of vanillin, aniline and indole in favour of MOPS and Au NPs in ethyl alcohol separately as a model reaction at room temperature as well as at reflux temperature on magnetic stirrer. But there was not considerable conversion of product we observed.

Further, while optimizing the reaction conditions and stoichiometry of catalyst concentration we coupled Au NPs and MOPS under ultrasonic condition in ethanol. We realized that coupling of Au-MOPS is really a suitable catalyst for the proposed transformation at reflux temperature (Scheme 1).

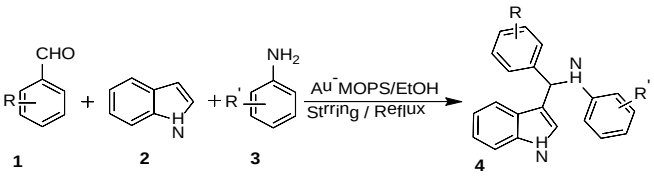

Scheme 1. Model reaction for 3-aminoalkylated indole.

Whereas, by considering the reaction time and product yield Au-MOPS were found to be the most capable catalyst. Au NPs provides active surface area on which all the reactants adsorbs chemically and MOPS initiates the reaction through ionic mechanism by protonating carbonyl oxygen so that condensation occurs between benzaldehyde and anilines to form imines intermediate. In 20 mL Au NPs solution following quantity (in mmol) of MOPS were added and the solutions were sonicated for 30 min. Which is then used as Au-MOPS catalyst for the screening of catalyst concentration and optimized concentration is further used for the synthesis of targeted products (Table 1).

Table 1. Screening of catalyst concentration for the synthesis of 3-aminoalkylated indoles

Sr. No	Catalyst (mmol) in 20 mL Au NPs solution	Time, h	Yield, %
1	0.4	8.5	55
2	0.6	8.5	62
3	0.8	8.5	70
4	1.0	8.5	85
5	1.2	8.5	85

Reaction conditions: vanillin (0.306 g), aniline (0.234 g), indole (0.186 g) stirred in ethyl alcohol (25 mL) at reflux temperature.

Table 2. Selection of suitable solvent for the synthesis of 3-aminoalkylated indoles

Sr. No	Solvent	Time, h	Yield, %
1	Water	24	20
2	Methanol	10	65
3	Isopropyl alcohol	15	60
4	Amyl alcohol	15	20
5	**Ethyl alcohol**	**8.5**	**85**
6	Aqueous Alcohol (1:1)	15	45
7	Acetone	10	68

Reaction condition: vanillin (0.306 g), aniline (0.234 g), indole (0.186 g) and MOPS (0.06 g) stirred at reflux temperature.

Table 3. MOPS catalyzed synthesis of 3-aminoalcylated indoles

Entry	R/Aldehyde	R´/Amine	Time, h	Yield, %	M.P., °C
4a	H	H	8	85	180-182
4b	4-Cl	H	8	82	124-126
4c	4-OH	H	8	82	144-146
4d	4-CH_3	H	8	85	132-134
4e	4-OH, 3-OCH_3	H	8.5	85	163-165
4f	3-Cl	H	9	75	129-131
4g	2-Cl	H	8.5	80	128-130
4h	4-$N(CH_3)_2$	H	8	82	110-102
4i	Acetaldehyde	H	9	70	103-105
4j	Furfuraldehyde	H	8.5	78	140-142
4k	H	Furfurylamine	9	70	98-101

Reaction condition: vanillin (0.306 g); aniline (0.234 g); indole (0.186 g) and Au MOPS (0.06 g) stirred at reflux temperature.

Keeping the sustainability aspects in mind we screened various solvents for the model reaction we found that ethyl alcohol is the best solvent for the sake of yield of the product, easy work-up, water soluble solvent and user friendly nature (Table 2).

With this examination Au-MOPS in ethyl alcohol was used to synthesize 3-aminoalkylated indoles from aromatic/heteroaromatic/aliphatic aldehydes, aniline and indole (Table 3).

We started the reaction by addition of MOPS in the alcoholic solution of vanillin and aniline. After stirring this reaction mixture at reflux temperature for one hour yellow colored precipitation observed, that indicates formation Schiff's base followed by condensation reaction. Thence, to this reaction mixture we added calculated amount of indole portion wise with continued stirring at same temperature. After two hours red colored precipitation observed in the reaction vessel that confirms formation of targeted product commenced. After each half hour reaction was monitored by TLC. After successful derivatization it has been observed that, there is no remarkable substituent effect. Both ring activating and deactivation substituted precursors reacted smoothly and resulted into the good to the better yield of the products.

To launch the scope and generality of the reaction aromatic aldehydes with electron donating and electron withdrawing substituent at different positions to the aromatic ring reacted smoothly and give a good to best yield of the product. Alongside, the heteroaromatic aldehydes are also proved to be amenable to these reaction conditions and did not show significant effect on the yield and reaction time. On the other hand, aliphatic aldehyde resulted comparatively less yield and took more time for transformation. The formation of products was confirmed by their physical constant and structures were elucidated by spectroscopic analysis.

CONCLUSIONS

We have developed a straight forward, beneficent and user friendly synthetic protocol for pharmacodynamic 3-aminoalcylated indoles favored by gracious catalyst Au-MOPS coupled catalyst in ethyl alcohol. Au NPs have a substantial percentage of atoms on the surface that become an advantage to bound reactants less tightly on its surface and could easily detaches from the products. This synthetic strategy also covers the advantages of one-pot multicomponent transformations which will make this research work practical and economically feasible and provides foresight for sustainability.

ACKNOWLEDGMENTS

Authors are thankful to the Director of the MGM's IBT College, Aurangabad for providing lab infrastructure and facilities for this research work.

REFERENCES

[1]Polshettiwar, V., Varma, R. S., Aqueous microwave chemistry: a clean and green synthetic tool for rapid drug discovery, *Chem. Soc. Rev.*, **2008** *37*, 1546-1557. https://doi.org/10.1039/b716534j

[2]Cioc, R. C., Ruijter, E., Orru, R. V. A., Multicomponent reactions: advanced tools for sustainable organic synthesis, *Green Chem.*, **2014,** *16*, 2958-2975. https://doi.org/10.1039/C4GC00013G

[3]Li, C. J., Anastas, P. T., Green Chemistry: present and future, *Chem. Soc. Rev.*, **2012**, *41*, 1413-1414. https://doi.org/10.1039/c1cs90064a

[4]Wang, J., Gu, H., Novel Metal Nanomaterials and Their Catalytic Applications, *Molecules*, **2015**, *20*, 17070- 17092. https://doi.org/10.3390/molecules200917070

[5]Chand, S., Sandhu, J. S., ZnO Nanoparticles: An efficient green reusable catalyst for the synthesis of 3-formyl benzopyranones chalcones by Claisen-Schmidt reaction under solvent-free condition, *Indian J. Chem.*, **2015,** *54B*, 1350-1354. http://hdl.handle.net/123456789/33037

[6]Li, Z. X., Luo, D., Li, M. M., Xing, X. F., Ma, Z. Z., Xu, H., Recyclable Fe3O4 Nanoparticles Catalysts for Aza-Michael Addition of Acryl Amides by Magnetic Field, *Catalysts*, **2017**, *7*, 219-230. https://doi.org/10.3390/catal7070219

[7]Marios, K., Manolis, S., Gold‐Nanoparticle‐Catalyzed Mild Diboration and Indirect Silaboration of Alkynes without the Use of Silylboranes, *Eur. J. Org. Chem.*, **2017**, 4265-4271. https://doi.org/10.1002/ejoc.201700754

[8]Leloup, M., Nicolau, R., Pallier, V., Yepremian, C., Cathalifaud, G. F., Organic matter produced by algae and cyanobacteria: Quantitative and qualitative characterization, *J. Environ. Sci.*, **2013**, *25*, 1089. https://doi.org/10.1016/S1001-0742(12)60208-3

[9]Cicekli, S. U., Onkol, T., Ozgen, S., Sahin, M. F., Schiff bases of 3-[(4-amino-5-thioxo-1,2,4-triazole-3-yl) methyl]-2(3H)-benzoxazolone derivatives: Synthesis and biological activity, *Rev. Roum. Chim*., **2012**, 57, 187-195.

[10]Rabbany, A. B. M. G., Mizutani, F., Chikaizumi, S., Effect of essential oils on in vitro activities of 1-aminocyclopropane-1-carboxylate (ACC) synthase and ACC oxidase from winter squash mesocarp, *Mem. Fac. Agr. Ehime Univ*., **2010**, 55, 1-6.

[11]Rozenman, M. M., Liu, D. R., DNA-templated synthesis in organic solvents, *Chem. Biol. Chem*., **2006**, *7*, 253-256.

[12]Jiang, B., Yang, G. C., Wang, J., Enantioselective Synthesis for the (−)-Antipode of the Pyrazinone Marine Alkaloid, Hamacanthin A, *J. Org. Chem*., **2001**, *66*, 4865-4869. https://doi.org/10.1021/jo010265b

[13]Bao, B., Sun, Q., Yao, X., Hong, J., Lee, C. O., Sim, C. J., Im, K. S., Jung, J. H., Cytotoxic Bisindole Alkaloids from a Marine Sponge Spongosorites sp., *J. Nat. Prod*., **2005**, *6(8)*, 711-715.https://doi.org/10.1021/np049577a

[14]Hibino, S., Choshi, T., Simple indole alkaloids and those with a nonrearranged monoterpenoid unit , *Nat. Prod. Rep*., **2002**, *19*, 148-180. https://doi.org/10.1039/b007740m

[15]Rao, V. K., Rao, M. S., Jain, N., Panwar, J., Kumar, A., Silver triflate catalyzed synthesis of 3-aminoalkylated indoles and evaluation of their antibacterial activities, *Org Med. Chem. Lett*., **2011**, *1(10)*, 1-7. https://doi.org/10.1186/2191-2858-1-10

[16]Radwan, M. A. A., Ragab, E. A., Sabry, N. M., El-Shenawy, S. M., Synthesis and biological evaluation of new 3-substituted indole derivatives as potential anti-inflammatory and analgesic agents, *Bioorg. Med. Chem*., **2007**, *15*, 3832-3841. https://doi.org/10.1016/j.bmc.2007.03.024

[17]Ekhlass, N., Synthesis, (in vitro) antitumor and antimicrobial activity of some pyrazoline, pyridine and pyrimidine derivatives linked to indole moiety, *J. Am. Sci*., **2010**, *6(8)*, 463-471.

[18]Radwan, M. A. A., Ragab, E. A., Shaaban, M. R., El-Nezhawy, A. O. H., Application of (2Z)-3-dimethylamino-2-(1H-indole-3-carbonyl) acrylonitrile in the synthesis of novel 3-heteroarylindoles: condensed meridianine analogs, *Arkivoc*, **2009**, (vii), 281-291.

[19]Deng, J., Sanchez, T., Neamati, N., Briggs, M. J., Dynamic Pharmacophore Model Optimization: Identification of Novel HIV-1 Integrase Inhibitors, *J. Med, Chem*., **2006**, *49*, 1684-1692. https://doi.org/10.1021/jm0510629

[20]Wynne, J. H., Stalick, W. M., Synthesis of 3-[(1-Aryl)aminomethyl]indoles, *J. Org. Chem*., **2002**, *67*, 5850-5853. https://doi.org/10.1021/jo020049i

[21]Jilla, S., Gaddam, S., Kumar, B. S. P. A., Yadavalli, V. D. N., β-Cyclodextrin catalyzed synthesis of substituted indoles in aqueous medium, *Eur. J. Chem*., **2014**, *5*, 668-670. https://doi.org/10.5155/eurjchem.5.4.668-670.1085

[22]Kumar, A., Kumar, P., Tripathi, V. D., Srivastava, S., A novel access to indole-3-substituted dihydrocoumarins in artificial sweetener saccharin based functional ionic liquids, *RSC Adv*., **2012**, *2*, 11641-11644. https://doi.org/10.1039/c2ra21284f

[23]Das, B., Kumar, J. N., Kumar, A. S., Satyalakshmi, G., Shinde, D. B., A distinct novel approach for the synthesis of 3-indolyl-methanamines starting from indoles, aldehydes and nitrobenzenes in water, *RSC Adv*., **2013**, *3*, 14308-14311. https://doi.org/10.1039/c3ra41131a

[24]Srihari, P., Singh, V. K., Bhunia, D. C., Yadav, J. S., One-pot three-component coupling reaction: solvent-free synthesis of novel 3-substituted indoles catalyzed by PMA–SiO_2, *Tetrahedron Lett*., **2009**, *50*, 3763-3766. https://doi.org/10.1016/j.tetlet.2009.02.176

[25]Palmieri, A., Petrini, M., Shaikh, R. R., Synthesis of 3-substituted indoles via reactive alkylideneindolenine intermediates, *Org. Biomol. Chem*., **2010**, *8*, 1259-1270.https://doi.org/10.1039/B919891A

[26]Sapkal, S. B., Shelke, K. F., Shingate, B. B., Shingare, M. S., Nickel nanoparticle-catalyzed facile and efficient one-pot synthesis of polyhydroquinoline derivatives via Hantzsch condensation under solvent-free conditions, *Tetrahedron Lett*., **2009,** 50, 1754-1756. https://doi.org/10.1016/j.tetlet.2009.01.140

Received: 11.03.2019.
Accepted: 01.03.2020.

SYNTHESIS OF A NOVEL IMINOPYRIMIDOOXAZINE AND THEIR DERIVATIVES

B. Sirsat Shivraj,[a]* G. Jadhav Anilkumar,[a] S. Jadhav Madhav[a] and S. Kale Prashant[a]

Keywords: Claisen-Schmidt condensation, Michael addition reaction, 2-(bis (methylthio) methylene)malononitrle, urea.

We have synthesized 2-(4-chlorophenyl)-8-(methylthio)-6-imino-4-phenyl-2,6,9,9*a*-tetrahydropyrimido[2,1-*b*][1,3]oxazine-7-carbonitrile (**3**) by the reaction of 6-(4-chlorophenyl)-4-phenyl-6H[1,3]oxazin-2-amine (**2**) with 2-(bis (methylthio)methylene)malononitrile in the presence of catalytic amount of potassium carbonate in DMF under reflux condition. The aminooxazine was prepared by the reaction of chalcone (**1**) with urea in the presence of ethanol and sodium hydroxide under reflux condition. The synthesized compounds were characterized by spectral methods. The compound (**3**) possesses replaceable methylthio (-SCH_3) group at 8 position. The compound (**3**) react with various nucleophiles like substituted aromatic amines, aromatic phenols, hetarylamines and active methylene compounds to give 2-(4-chlorophenyl)-8-(substituted)-6-imino-4-phenyl-2,6,9,9*a*-tetrahydropyrimido[2,1-*b*][1,3]oxazine-7-carbonitriles in good yields.

* Corresponding Authors
E-Mail: sbs.igm@gmail.com
[a] P. G. Research Centre, Department of Chemistry, Yeshwant Mahavidyalaya, Nanded 431602, India

INTRODUCTION

The six-membered heterocyclic compounds containing one oxygen and one nitrogen atom,[1] having important bio-active properties are known as oxazine or unsaturated oxazine derivatives. These molecules exist many isomeric structures such as 1,2-, 1,3- or 1,4-oxazines,[2] depending upon the relative position of these two atoms and the carbon-carbon double bond. The presence of oxygen, nitrogen heteroatoms in various relative positions along with a carbon-carbon double bonds in their structural moieties[3] have enhanced the important medicinal activities.

1,3-Oxazines attract more attention as they constitute an important class of both natural and non-natural products. Heterocycles containing the oxazine nucleus are found to possess a wide range of valuable biological properties like analgesic, anti-inflammatory, anti-leukemic, antimalarial,[4-6] antipyretic, anticonvulsant and antimicrobial activities.[7-11]

The synthesis of novel oxazine derivatives remains a main focus of research in the field of medicinal chemistry. Oxazine derivatives have been reported to possess antifungal,[12] antibacterial,[13] cytotoxic,[14] antiviral[15] and analgesic activity.[16] The structures of the various synthesized compounds have been assigned on the basis of IR, ^{1}H NMR, ^{13}C NMR and mass spectral data. In the view of this observation and extension of earlier work, we have synthesized 2-(4-chlorophenyl)-6-imino-8-(methylthio)-4-phenyl-2,6,9,9*a*-tetrahydropyrimido[2,1-*b*][1,3]oxazine-7-carbonitrile by using 6-(4-chlorophenyl)-4-phenyl-6*H*[1,3]oxazin-2-amine[17-18] and 2-bis(methylthio)-methylene)malononitrile. The aminooxazine was prepared by the reaction of chalcone[19-20] with urea in the presence of ethanol and sodium hydroxide under reflux conditions.

EXPERIMENTAL

Melting points were determined in open capillary tubes and are uncorrected. The silica gel F_{254} plates were used for thin layer chromatography (TLC), the spots were examined under UV light and then developed with iodine vapour. Column chromatography was performed with silica gel (BDH 100-200 mesh). Solvents were purified according to standard procedures. IR spectra were obtained, with KBr pellets, on a Perkin-Elmer RX1 FT-IR spectrophotometer. ^{1}H NMR, were recorded with a 400 MHz Varian Gemini 200 instrument and reported as δ in ppm with TMS as internal standard.

Synthesis of 2-(4-chlorophenyl)-6-imino-8-(methylthio)-4-phenyl-2,6,9,9*a*-tetrahydropyrimido [2,1-*b*] [1,3]oxazine-7-carbonitrile (3)

Step 1: A 50 % solution of KOH is added to a solution of acetophenone (0.01 mol) and 4-chlorobenzaldehyde (0.01 mol) in 95 % ethanol, under energetic stirring at room temperature. The reaction is left overnight under stirring then diluted with water and acidified. The precipitate is separated by filtration, dried under vacuum and crystallized from ethanol to yield the chalcone, i.e., 3-(4-chlorophenyl)-1-phenylprop-2-en-1-one (**1**).

Step II: A mixture of chalcone (**1**) (2.42 g, 0.01mol) and urea (0.60 g 0.01 mol) was dissolved in ethanolic potassium hydroxide solution (10 mL). It was heated for 4 h, then it was poured into cold ice water to yield 6-(4-chlorophenyl)-4-phenyl-6*H*-1, 3-oxazin-2-amine (**2**).

Step III**:** A mixture of (**2**) and 2-(bis (methylthio)methylene) malononitrile in DMF was refluxed for 6 h, in the presence of catalytic amount of potassium carbonate (10 mg). The reaction was monitored by TLC. After completion, the reaction, mixture was set to cool to room temperature, washed with water and extracted with ethyl acetate.

The extract was concentrated and the residue was subjected to column chromatography (silicagel, n-hexane-ethyl acetate 8:2) to obtain pure solid compound (**3**). The structure of compound (**3**) was confirmed by IR, ^{1}H NMR, ^{13}C NMR and MS analytical data (Scheme 1).

IR (KBr): 3350, 2240, 1650,760 cm^{-1}. ^{1}H NMR (DMSO-d_6, 400 MHz) δ = 2.32 (s, 3H, SCH_3), 5.89 (s, 1H, N-H), 8.32 (s, 1H, =NH), 5.36 (s,1H =CH, 5.62(s, 1H, CH), 4.48(s, 1H, CH), 7.10 (s, 5H, Ar-H), 7.28 (dd, 2H, Ar-H), 7.36 (dd, 2H, Ar-H). S (ESI-MS): *m/z* ($M^{+)}$ 408 (M+2) 410. Mol. Formula: $C_{21}H_{17}ClN_4O_3S$, Mol. Wt: 408 and 410.

Synthesis of derivatives

General procedure

A mixture of (**3**) (1 mmol) and various substituted aromatic amines, aromatic phenols, hetarylamines or active methylene compounds (1 mmol) in DMF (10 mL) and in the presence of anhydrous potassium carbonate (10 mg) was reflux for 4 to 6 h. The reaction mixture was cooled to room temperature and then poured into ice cold water. The separated solid product was filtered, washed with water and recrystallized using ethanol.

2-(4-Chlorophenyl)-6-imino-8-phenoxy-4-phenyl-2,6,9,9*a*-tetrahydro pyrimido[2,1-*b*][1,3]oxazine-7-carbonitrile (3a)

IR (KBr) :3350,2240, 650,760 cm^{-1}. ^{1}H NMR (DMSO-d_6, 400 MHz) δ = 7.27 (s, 5H, Ar-H), 5.78 (s, 1H, N-H), 8.36 (s, 1H, =NH), 5.32 (s, 1H, =CH), 5.54 (s, 1H, CH), 4.42 (s, 1H, CH), 7.14 (s, 5H, Ar-H), 7.26 (dd, 2H, Ar-H), 7.38 (dd, 2H, Ar-H). MS (ESI-MS): *m/z* ($M^{+)}$ 454, (M+2) 456. $C_{26}H_{19}ClN_4O_2$. MW: 454 and 456.

8-(4-Bromophenoxy)-2-(4-chlorophenyl)-6-imino-4-phenyl-2,6,9,9*a*-tetrahydropyrimido[2,1-*b*][1,3]oxazine-7-carbonitrile (3b)

IR (KBr): 3350, 2240, 1650, 760, 650 cm^{-1}. ^{1}H NMR (DMSO-d_6, 400 MHz) δ = 5.81 (s, 1H, N-H), 8.36 (s, 1H, =NH). 5.50 (s, 1H, =CH), 5.51 (s, 1H, CH), 4.40 (s, 1H, CH), 7.24 (s, 5H, Ar-H), 7.26 (dd, 2H, Ar-H), 7.40 (dd, 2H, Ar-H), 6.72(dd, 2H, Ar-H), 7.34 (dd 2H, Ar-H). MS (ESI-MS): *m/z* ($M^{+)}$ 532, (M+2) 534. $C_{26}H_{18}BrClN_4O_2$. Mw: 532 and 534.

2-(4-Chlorophenyl)-6-imino-8-(4-nitrophenoxy)-4-phenyl-2,6,9,9*a*-tetrahydropyrimido[2,1-*b*][1,3]oxazine-7-carbonitrile (3c)

IR (KBr): 3350, 2260, 1650, 760, 1510 cm^{-1}. ^{1}H NMR (DMSO-d_6, 400 MHz) δ = 5.77 (s, 1H N-H), 8.39 (s, 1H =NH), 5.55 (s, 1H, =CH), 5.44 (s, 1H, CH), 4.32 (s, 1H, CH), 7.30 (s, 5H, Ar-H), 7.36 (dd, 2H, Ar-H), 7.27 (dd, 2H, Ar-H), 7.16 (dd, 2H, Ar-H), 8.03 (dd, 2H, Ar-H). MS (ESI-MS): *m/z* (M^+) 499 (M+2) 501. $C_{26}H_{18}ClN_5O_4$. . Mw: 499 and 501.

2-(4-Chlorophenyl)-6-imino-4-phenyl-8-(phenylamino)-2,6,9,9*a*-tetrahydro pyrimido[2,1-*b*][1,3]oxazine-7-carbonitrile (4a)

IR (KBr): 3350, 2240, 1650, 760, 3250 cm^{-1}. ^{1}H NMR (DMSO-d_6, 400 MHz) δ = 5.76 (s, 1H, N-H), 8.42 (s, 1H, =NH), 6.34 (s, 1H, N-H), 5.53 (s, 1H, =CH), 4.51 (s, 1H, CH), 5.68 (s, 1H, CH), 7.25 (s, 5H, Ar-H), 7.28 (dd, 2H, Ar-H), 7.42 (dd, 2H, Ar-H), 7.04 (s, 5H, Ar-H). Mass (ESI-MS): *m/z* (M^+) 453, (M+2) 455. $C_{26}H_{20}ClN_5O$. Mw: 453 and 455.

8-((4-Bromophenyl) amino)-2-(4-chlorophenyl)-6-imino-4-phenyl-2,6,9,9*a*-tetrahydropyrimido [2,1-*b*]*[1,3]*oxazine-7-carbonitrile (4b)

IR (KBr): 3350, 2240, 1650, 3250, 640, 760 cm^{-1}. ^{1}H NMR (DMSO-*d*6, 400 MHz) δ = 5.74 (s, 1H, N-H), 8.35 (s, 1H, =NH), 6.27 (s, 1H, N-H), 5.48 (s, 1H, =CH), 4.42 (s, 1H, CH), 5.72 (s, 1H, CH), 7.32 (s, 5H, Ar-H), 7.34 (dd, 2H, Ar-H), 7.45 (dd, 2H, Ar-H), 6.48 (dd, 2H, Ar-H), 7.22 (dd, 2H, Ar-H). Mass (ESI-MS): *m/z* ($M^{+)}$ 531 (M+2) 533. $C_{26}H_{19}BrClN_5O$. Mw: 531 and 533 .

2-(4-Chlorophenyl)-6-imino-8-((4-nitrophenyl) amino)-4-phenyl-2, 6, 9,9*a*-tetrahydropyrimido[2,1-*b*][1,3]oxazine-7-carbonitrile (4c)

IR (KBr): 3350, 2240, 1650, 3250, 1480, 760 cm^{-1}. ^{1}H NMR (DMSO-d_6, 400 MHz) δ = 5.71 (s, 1H, N-H), 8.46 (s, 1H, =NH), 6.20 (s 1H, N-H), 5.44 (s, 1H, =CH), 4.49(s, 1H, CH), 5.78 (s, 1H, CH), 7.24 (s, 5H, Ar-H), 7.30 (dd, 2H, Ar-H), 7.40 (dd, 2H, Ar-H), 6.54 (dd, 2H, Ar-H), 7.92 (dd, 2H, Ar-H). MS (ESI-MS): *m/z* ($M^{+)}$ 498 (M+2) 500. $C_{26}H_{19}ClN_6O_3$. Mw: 498 and 500.

2-(4-Chlorophenyl)-6-imino-4-phenyl-8-(pyrrolidin-1-yl)-2,6,9,9*a*-tetrahydropyrimido[2,1-*b*][1,3]oxazine-7-carbonitrile (5a)

IR (KBr): 3350, 2240, 1650, 760 cm^{-1}. ^{1}H NMR (DMSO-d_6, 400 MHz) δ = 5.77 (s, 1H, N-H), 8.42 (s, 1H, =NH), 5.54 (s, 1H, =CH) 4.52 (s, 1H, CH), 5.68 (s, 1H, CH), 7.23 (s, 5H, Ar-H), 7.34 (dd, 2H, Ar-H), 7.40 (dd, 2H, Ar-H), 2.54 (t, 4H), 1.62 (m, 4H). MS (ESI-MS): *m/z* ($M^{+)}$ 431 (M+2) 433. $C_{24}H_{22}ClN_5O$. Mw: 431 and 433.

2-(4-Chlorophenyl)-6-imino-4-phenyl-8-(piperidin-1-yl)-2,6,9,9*a*-tetrahydropyrimido[2,1-*b*][1,3]oxazine-7-carbonitrile (5b)

IR (KBr): 3350, 2240, 1650, 760 cm^{-1}. ^{1}H NMR (DMSO-d_6, 400 MHz) δ = 5.88 (s, 1H, N-H), 8.49 (s, 1H, =NH), 5.46 (s, 1H, =CH) 4.62 (s, 1H, CH), 5.62 (s, 1H, CH), 7.25 (s, 5H, Ar-H), 7.30 (dd, 2H, Ar-H), 7.36 (dd, 2H, Ar-H), 3.08 (t, 4H), 1.50 (m, 6H). MS (ESI-MS): *m/z* ($M^{+)}$ 445 (M+2) 447. $C_{25}H_{24}ClN_5O$. Mw: 445 and 447.

2-(2-(4-Chlorophenyl)-7-cyano-6-imino-4-phenyl-2,6,9,9*a*-tetrahydropyrimido[2,1-*b*][1,3]oxazin-8-yl)malononitrle (6a)

IR (KBr, cm^{-1}): 3350, 2240, 1650, 2950, 760 cm^{-1}. ^1H NMR (DMSO-d_6, 400 MHz) δ =5.82 (s, 1H, N-H), 8.46 (s, 1H, =NH), 5.41 (s, 1H, =CH) 4.52 (s, 1H, CH), 5.70 (s, 1H, CH), 7.21 (s, 5H, Ar-H), 7.28 (dd, 2H, Ar-H), 7.38 (dd, 2H, Ar- H), 4.12 (s, 1H, act-CH). MS (ESI-MS): *m/z* ($M^{+)}$ 426 (M+2) 428. $C_{23}H_{15}ClN_6O$. Mw: 426 and 428.

Ethyl 2-(2-(4-chlorophenyl)-7-cyano-6-imino-4-phenyl-2,6,9,9*a*-tetrahydropyrimido[2,1-*b*][1,3]oxazin-8-yl)-2-cyanoacetate (6b)

IR (KBr, cm^{-1}): 3350, 2240, 1650, 1950, 1710, 760 cm^{-1}. ^1H NMR (DMSO-d_6, 400 MHz) δ = 5.79 (s, 1H, NH), 8.46 (s, 1H, =NH), 5.52 (s, 1H, =CH), 4.39 (s, 1H, CH), 5.59 (s, 1H, CH), 7.23 (s, 5H, Ar-H), 7.30 (dd, 2H, Ar-H), 7.41 (dd, 2H, Ar-H), 3.96 (s, 1H, act-CH), 4.16 (q, 2H), 1.21 (t, 3H). Mass (ESI-MS): *m/z* ($M^{+)}$ 473 (M+2) 475. $C_{25}H_{20}ClN_5O_3$. Mw: 473 and 475.

RESULT AND DISCUSSION

Synthesis of 2-(4-chlorophenyl)-6-imino-8-(methylthio)-4-phenyl-2,6,9,9*a*-tetrahydropyrimido[2,1-*b*][1,3]oxazine-7-carbonitrile (**3**) as starting material has been performed with refluxing 6-(4-chlorophenyl)-4-phenyl-6H[1,3]oxazin-2-amine and 2-(bis(methylthio)methylene)malononitrile in DMF in presence of K_2CO_3.

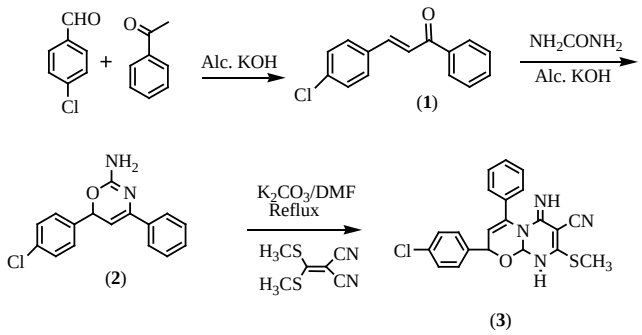

Scheme 1. Synthesis of 2-(4-chlorophenyl)-6-imino-8-(methylthio)-4-phenyl-2,6,9,9*a*-tetrahydropyrimido[2,1-*b*][1,3]oxazine-7-carbonitrile (**3**).

A 50 % solution of KOH is reacted with a solution of equimolar amount of acetophenone and 4-chlorobenzaldehyde in 95 % ethanol with stirring at room temperature. The chalcone, i.e., 3-(4-chlorophenyl)-1-phenylprop-2-en-1-one (**1**) was reacted with 1 equiv. of urea dissolved in ethanolic potassium hydroxide solution with 4 h heating to yield 6-(4-chlorophenyl)-4-phenyl-6*H*-1, 3-oxazin-2-amine (**2**). A mixture of (**2**) and 2-(bis (methylthio)methylene)malononitrile in DMF was refluxed for 6 h, in the presence of catalytic amount of potassium carbonate to yield the target compound (Scheme 1).

The synthesized compound acts as electrophilic species, reacting with various substituted aromatic amines and phenols to give 2-(4-chlorophenyl)-6-imino-8-(substituted)-4-phenyl-2,6,9,9*a*-tetrahydropyrimido[2,1-*b*][1,3]oxazine-7-carbonitrile derivatives in good yields (Schemes 2).

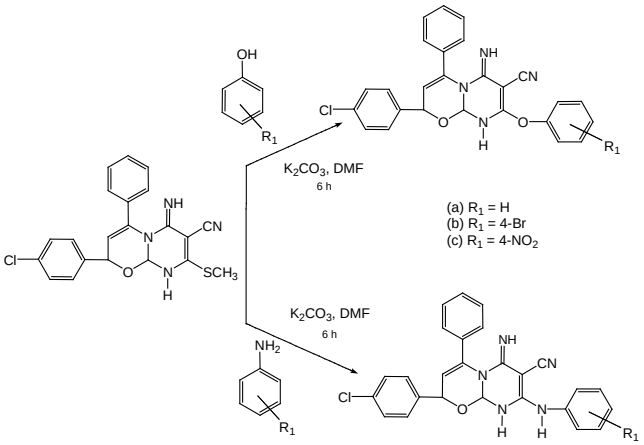

Scheme 2. Synthesis of ether and amino derivatives from compound **3.**

Analogous recations of compound **3** with hetaryl amines and active methylene compounds resulted ring-N attached substitution and ring-condensed derivatives, respectively (Scheme 3 and 4).

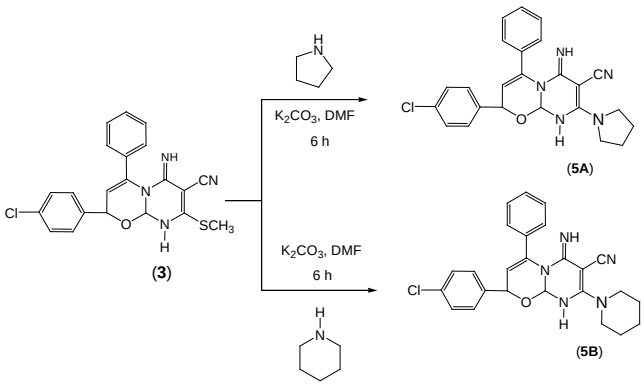

Scheme 3. Synthesis of heterocyclic derivatives from compound **3**.

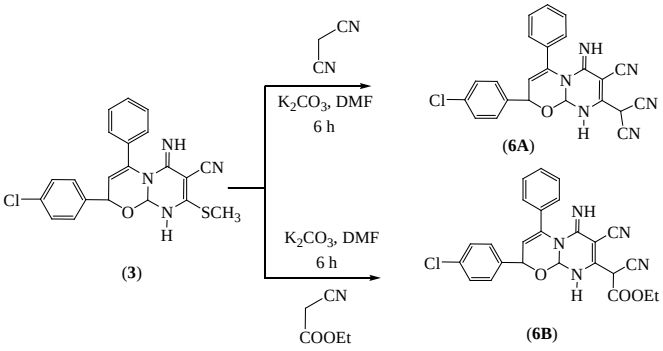

Scheme 4. Reaction products of compound **3** with active methylene compounds

The spectroscopic parameters of the synthesized new compounds (IR, NMR and MS) are given in the experimental section.

CONCLUSION

Several new 2-(4-chlorophenyl)-8-(substituted)-6-imino-4-phenyl-2,6,9,9*a*-tetrahydropyrimido[2,1-*b*][1,3]oxazine-7-carbonitrile are synthesized by using simple and efficient chemistry and this synthesized compounds possesses methylthio group at 8-position which is a good leaving group and, therefore, acts as an electrophilic species and reacting with various nucleophiles. In compound **3,** cyano and thiomethyl groups are at adjacent position it also undergo cyclization to give polycyclic heterocyclic compound.

ACKNOWLEDGEMENTS

The authors are grateful to Dr. G.N. Shinde, Principal, Yeshwant Mahavidyalaya, Nanded, for providing laboratory facilities & Vishnu Chemicals Ltd., Hyderabad, for providing spectral data.

REFERENCES

[1]Thompson, A. M., Sutherland, H. S., Palmer, B. D., Kmentova, I., Blaser, A., Franzblau, S. G., Wan, B., Wang, Y., Ma, Z., Denny, W. A., Synthesis and structure-activity relationships of varied ether linker analogues of the antitubercular drug (6S)-2-nitro-6-{[4-(trifluoromethoxy)benzyl]oxy}-6,7-dihydro-5H-imidazo[2,1-b][1,3]oxazines. *J. Med. Chem*, **2011**, *54*, 6563-6585. https://doi.org/10.1021/jm200377r

[2]Yakovlev, I. P., Prep'yalov, A. V., Ivin, B. A. , Unsaturated 4H-1, 3-Oxazines (Review). *Chem. Heterocyclic. Compd.*, **1994**, *30(3)*, 255-271.

[3]Manjula, M., Rai, K., Gaonkar, M. L., Ravesha, S. L., Satish, K.A., Synthesis of new series of 5, 6-dihydro-4*H*-1, 2-oxazines via hetero Deils-Alder reaction and evaluation of antimicrobial activity. *Eur. J. Med. Chem*, **2009**, *44*, 280-288.

[4]Takimoto C.H., Calvo E., *Principles of oncologic pharmacotherapy in cancer Management: A multidisciplinary approach*, UBM Medica Londen, **2008**, 42-58.

[5]Kalirajan, R., Sivakumar, S.U., Jubie, S., Gowramma, B., Suresh, B., Synthesis and biological evaluation of some heterocyclic derivatives of Chalcones, *Int. J. Chem. Tech. Res*, **2009**, *1(1)***,** 27- 34.

[6]Vennerstrom, J. L., Makler, M. T., Angerhofer, C. K., Williams, J. A., Antimalarial dyes revisited: Xanthenes, azines, Oxazine and thiazines, Antimicrobial, *Agents Chemother.*, **1995**. 2671-2677. doi.org/10.1128/aac.39.12. 2671.

[7]Singh C., Parwana H. K., Singh G., Synthesis of 3,6-diaryl-2h,3h,4h,5h,6h- [1, 3]- Oxazine-2-Thiones as potential anticonvulsants, *Indian J. Pharm. Sci.*, **1995**, *57*,198-202

[8]Latif N., Mishriky N., Assad F. M., Carbonyl and Thiocarbonyl compounds, XIX. Intramolecular cyclization of (2-nitroethenyl)aryl N-arylcarbamates: Synthesis of newer series of 3,4-dihydro-2H[1,3]oxazin-2-ones and their antimicrobial activities, *Aust. J. Chem.*, **1982**, *35*, 1037-1043**.** doi.org/10.1071/ch9821037.

[9]Cassady, J. M., Chan, K. K., J. M., Floss, H. G., Leistner, E., Recent developments in the Maytansinoid antitumor agents, *Chem. Pharm. Bull.*, **2004**, *52*, 1-26. doi.org/10.1002/chin.200427222.

[10]Turgut Z., Pelit E., Koycu A., Synthesis of new 1,3-disubstituted-2,3-dihydro-1*H*-naphth[1,2-*e*][1,3]oxazines, *Molecules*, **2007**, *12*, 345-352. doi.org/10.3390/12030345.

[11]Salwa, F. M., Mohamed, M. Y., Abd El-Galil, E. A., Eman, R. K., Antimicrobial Activities of some synthesized pyridines, Oxazine and Thiazole from 3-Aryl-1-(2-naphthyl)prop-2-en-1-ones, *Sci. Pharm.*, **2008**, *76*, 279-303. doi.org/10.3797/scipharm.0804-09.

[12]Beena, K. P., Design, synthesis, characterization and evaluation of 1,3-oxazine derivatives as potent antifungal agents, *Der Pharm. Lett.*, **2013**, *5*, 257-260.

[13]Prasad, D., Rohilla, R., Roy, N., Nath, M., Synthesis and antibacterial evaluation of benzazoles tethered dihydro-[1,3]oxazines. *Indian J. Chem.*, **2012**, *51B (5)*, 739-745.

[14]Temple, C. Jr., Wheeler, G. P., Comber, R. N., Elliott, R. D., Montgomery J. A., Synthesis of potential anticancer agents. Pyrido [4, 3-b] [1, 4] oxazines and pyrido [4, 3-b] [1, 4] thiazines. *J. Med. Chem*, **1983**, *26 (11)*, 1614-1619. Doi.10.1021/jm00365a012

[15]Selvam, P., Sridharan, D., Murugesh, N., Chandra Mohan, M., Witurouw, M., Synthesis and anti-hiv activity of some novel 2, 3-disubstituted quinazolin 4(3*h*)-ones, *Int. J. Chem. Sci.*, **2008**, *6*, 1196-1201.

[16]Sindhu, T. J., Arikkatt, S. D., Vincent, G., Chandran, M., Bhat, A. R., Krishna Kumar, K., Biological activities of Oxazine and its derivatives: A Review., *Int. J. Pharm. Sci. Res.*, **2013**, *4*, 134-143.

[17]Sawant R. L., Bhangale, L., Wadekar, J., Gaikwad, P., Substituent Selection for Design and Synthesis of Antimicrobial 1,3-Oxazine, a Topliss Modified Approach, *Farmacia*, **2012**, *60***,** 3-39.

[18]Kategaonkar, A. H., Sonar, S. S., Shelke, S. K., Shingate, B. B., Shingare, M. S., Ionic liquid catalyzed multicomponent synthesis of 3,4-dihydro-3-substituted-2*H*-naphthol[2,1-*e*][1,3]oxazine derivatives, *Org. Commun.*, **2010**, *3*, 1-7.

[19]Lafta, S. J., Abd, H. J., Abdulla, A., Synthesis, characterization, antimicrobial evaluation and docking study of new chalcone derivatives containing 1,3,5-triazinane-1,3,5-triyl moiety, *Int. J. Chem. Sci.*, **2016**, 141.

[20]Prasad, Y. R., Kumar, P. P., Ravi Kumar, P., Srinivasa Rao, A., Synthesis and antimicrobial activity of some new chalcone of 2-acetylpyridine, *J. Chem.*, **2008**, ***5(1)***, 144-148. doi.org/10.1155/2008/602458.

Received: 12.01.2020
Accepted: 04.04.2020

DRUG DELIVERY SYSTEMS BETWEEN METAL, LIPOSOME, AND POLYMER-BASED NANOMEDICINE: A REVIEW

Saad S. M. Hassan,[a*] Ayman H. Kamel,[a*] Heba M. Hashem[a] and E. M. Abdel Bary[b]

Keywords: Drug delivery system; nano-medicine; metallic nano-material; polymeric nanomaterial, polymeric structures.

Herein, the drug delivery systems (DDS) based on nanomedicine proofed high potential and wide applicability that have distinct features related to Nano-sized. Enhancement of bioavailability and pharmacokinetics after oral administration via utility of natural/synthetic biodegradable polymeric nanomaterials. Improving biocompatibility, safety, enhanced permeability, better retention time, lower toxicity and efficient transportation of drugs to desired tissues or cells. These nanomaterials based on different types including metallic and polymeric Nano-medicine that can hydride with each other to gain new and unique features increase the efficiency of drug delivery and decrease patient compliance.

*Corresponding Authors
Fax: (+20)1222162766
E-Mail: saadsmhassan@sci.asu.edu.eg(S.S.M.H.); ahkamel76@sci.asu.edu.eg (A.H.K.)
[a] Chemistry Department, Faculty of Science, Ain Shams University, Cairo, Egypt
[b] Chemistry Department, Faculty of Science, Mansoura University, Mansoura, Egypt

INTRODUCTION

The therapeutic delivery in our bodies can be achieved by temporal and spatial drug delivery systems, which ensure effective and efficient transportation for the drugs into the desired cells and tissues.[1,2] Since 1500 BC, using the pills as a form of administration of drugs had the precedence.[3] Pill administration concept involves swallowing the pill and dissolving it in the stomach which is absorbed in the intestines and goes into circulation. Some limitations have been encountered in this approach, in cases of drugs which can break down in the stomach such as insulin. Consequently, insulin is injected into the fatty tissues and is then absorbed into the systemic circulation.[4] There are several other ways of drug administration such as transdermal, ocular and gastrointestinal or stimuli-reactive routes.[5] The first and second routes were applied, respectively, for avoiding the drawbacks of oral administration of pills. Later on, the sustained release was a desirable objective for developing the therapeutic profile by maintaining the drug levels in blood and tissues by a gradual release of medication for a prolonged interval of time, after single-dose administration.

The sustained-release phenomenon was achieved first in the late 1940s and early 1950s when the pills were coated with a talc-mucilage composition that converts the pills into shape looked alike pearls.[6] These coatings were hydrophobic and non-swelling at acidic pH of the stomach but are converted to ionized form in slightly alkaline pH of the intestinal region of the gastrointestinal tract, then get dissolved and release the drug. The prolonged time of drug release from the stomach to the small intestine, protect the stomach from the drug and protect the drug from being destroyed by digestive enzymes in the stomach.[7] However, these systems had some shortcomings due to their sensitivity for different physiological parameters such as pH, gastric emptying and so on.[8] The trials until the 1950s were unsuccessful to control drug release.

By progressing the drug release process, SmithKline Beecham developed the oral predetermined-release formulation as Spansules®.[9] Spansules® could sustain the release kinetics of dextroamphetamine sulfate (Dexedrine®) up to 12 h. Hence, the term of controlled release was achieved by developing the design of the tablets to prolong the time of therapeutic release through the introduction of different drug release mechanisms (dissolution-controlled, diffusion-controlled, osmosis-controlled, and ion-exchange-controlled mechanisms).

Introducing Spansules® as capsules containing micro-pellets coated with water-soluble wax, developed this design. Then the liposomes were considered as one of the earliest targeted systems, which were discovered in the 1960s. The anticancer agent was discovered as the liposomal-encapsulated formulation of doxorubicin (Doxil) in the 1990s which was approved first by the US Food and Drug Administration (FDA).[10]

The watershed in the drug delivery occurred in 1976 when Robert Langer and Judah Folkman discovered the large molecules could be delivered over days and weeks from polymer matrices.[3] The development was the replacement of waxy coatings with reproducible synthetic and more stable polymers that get gradually dissolved[7, 11] to insure the sustained level of effective drug concentration in the blood and enhance the control on drug release with obviously efficient new DDSs.[12,13]

DEVELOPMENT OF DDSs FROM BENCH-SIDE TO MARKET

Through the rigorous steps of the process of drug development from the laboratory bench to the pharmacies, we can understand the drug discovery and draw attention to

the tremendous amount of scientific effort that goes into the production and development of modern medicines before they reach the pharmacies. There are four stages from bench to the patient as shown: (1) drug discovery, (2) drug development, (3) regulatory review and approval, and (4) marketing.[14]

Drug discovery

The key to both academic biomedical research and the pharmaceutical industry is explicitly associated with the discovery and exploitation of new drug targets. An appropriate target, which can be called 'druggable' is categorized into biomolecule and protein receptors that can be determined according to disease conditions or pathology.[15] This step is followed by confirmation of its impact on disease progression with target validation and identification. To completely understand this aspect, the effect of interaction of another molecule with the target molecule/receptor is studied.

Drug development

The term 'drug candidate' is the best term of identification of the picked compounds through its dosage, efficacy, safety, and toxicity. There are two phases to ensure drug acceptance and confirm its features.[16] Firstly, the preclinical phase, which composed of two ways to study desired compounds pharmacodynamics and pharmacokinetics, features. These are simulated in cells (in vitro) and in animals (in vivo), which confirm the compound's profiles from its absorption, metabolism, excretion, and toxicity. The best and promising compounds have no toxicity, high absorption, effective distribution into desired cells and highly efficient metabolism. Secondly, a clinical phase which investigated in patients through 3 phases as following 1) testing in a small group of healthy volunteers, 2) testing in a small group of patients and finally 3) testing in a large group of patients to show its efficacy.[14]

Regulatory review and approval

Approval, by the food and drug administration agency (FDA), and marketing of the new drugs involve two phases. The first one is pre-approval (pre-market), FDA continues its oversight of drug safety and effectiveness in the drug's proposed use; appropriateness of the proposed labelling; and adequacy of manufacturing methods to assure the drug's identity, strength, quality, and purity. Second, the phase of post-approval (post-marked) that the drug introduced finally in the markets.[17]

NANOMEDICINE IN DRUG RELEASE

Recently developed, the multidisciplinary nanotechnology field has a considerable potential for solving many problems in therapeutic delivery systems. These advanced technologies overcome different therapeutic issues of conventional formulations like its poor bioavailability, drug instability or insolubility.[18] Nanomaterial with size below 350 nm has high efficiency and the ability for enhancing both medical devices and therapeutic areas due to its unique working mechanism and specific properties. There are different types of nanomaterial and their conjugates, for example, polymeric nanomaterial, metallic nanomaterial, metal-metal nanocomposites or hybrids, and metal-polymer nanocomposites.[19] For a clear understanding of the types of nanomaterial, they have been divided into two broad categories.

Metal-based nanomedicine

The noticeable potential of drug release is related directly to nano-carriers for drug transportation into the desired cells and tissues, and this is based on the type of materials used. Metallic composites have high efficacy in the drug delivery and release that depend on the abundance of metals such as gold, silver, porous iron oxide, zinc oxide, nano-titanium dioxide, and nano-silica etc.[20] Various categories of metal-based nano-medicine have great potential and an obvious role in drug release that included the two broad applicable types, carbon nanotubes and mesoporous silica nanoparticles.

Carbon-based nanomedicine

Unique and distinct chemical and physical properties of carbonaceous materials allow them to penetrate the drug release domain. These compounds have variability in their shape and several characters and are able to be an efficient part of active gradients of many therapeutic molecules. At first, the sp^2 hyperdization of carbon materials allowed them to have exclusive features for the drug release, according to its valence.

The different types of carbon-based- materials show different shapes and dimensions ranged from zero, 0D, to 3D dimensions such as 0D fullerenes and graphene clusters, 1D carbon nanotubes (CNTs) and graphene nanoribbons, 2D graphene surface and 3D graphite crystal and nanotube networks.[21] CNTs cylindrical morphology is formed by rolling one or multiple graphene layers. It is classified as single-walled carbon nanotubes (SWCNTs), and multiple-walled carbon tubes (MWCNs). SWCNs consist of one single cylinder of graphite sheet, with a diameter ranging from 0.4 to 3.0 nm.[22] On the other hand, MWCNs are conventionally depicted as an array of tubes that are coaxially aligned around a central hollow with the uniformed distance between layers. The numbers of layers dictate the diameters of MWCNs: the inner diameter can change from 0.4 nm to a few nanometers, while the outer diameter ranges from 2 to 100 nm.[21,23] The drug loading mechanism on CNTs is due to its unique properties of high surface area and spherical shape that ensure the remarkable loading of drug molecules. Hydrophilic or amphiphilic polymeric materials can be used for enhancement of the drug loading of CNTs and can affect the drug loading mechanism.Various approaches can illustrate the drug loading mechanism on CNTs such as encapsulation inside the cavities of the tubes,[24] functionalization of the surface, and adsorption on the wall or among the walls of CNTs.[25]

Mesoporous silica nanoparticles (MSNs)

Platforms based on silica nanoparticles are efficient designs for enhancement of drug release. These platforms

have unique features and characteristics such as robustness, easy surface modification, high surface area large pore volume and its tunable shape provide the drug release profile. For the first time, MCM-41 (Mobil Composition of Matter No. 41) was introduced as a novel drug system in 2001. This material was introduced to develop advanced nano-therapeutics.[26-28]

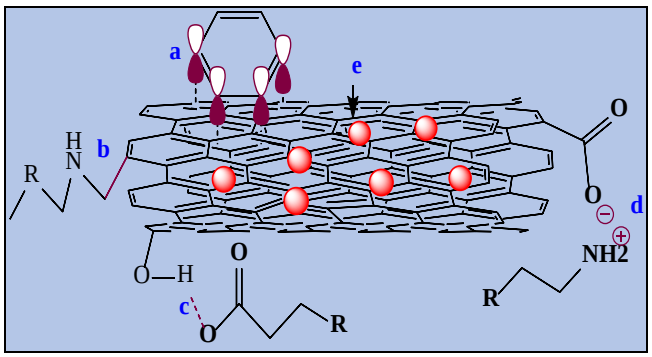

Figure 1. Overall approaches of attaching the drug to the outer surface of CNTs, a) π-π interaction n,b) Covalent bond, c) Hydrogen bonding, d) Ionic interaction and e) encapsulation inside the cavity.

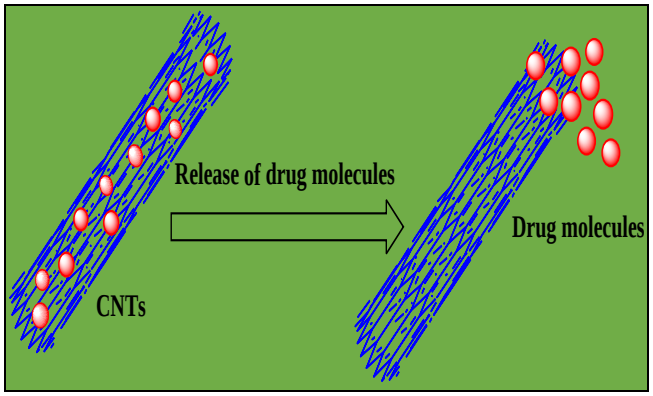

Figure 2. Drug release from carbon nanotubes.

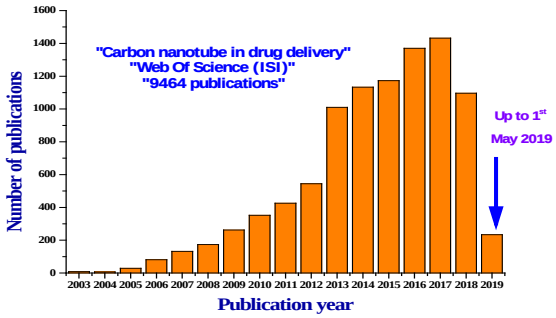

Figure 3. The number of publications per year indexed in the ISI Web of Science on the topic of "carbon nanotube in drug delivery" up to 1st May 2019.

Their therapeutics index and promising features as high drug loading capacity, protection and transportation of drugs to the target site to enhance the drug release. The high surface area of MSNs ensures a high percentage of contact area with guest molecules. MSNs architecture such as tuneable pore diameters, large surface areas and pore volumes, and high chemical and thermal stabilities has a crucial role in their combination therapies and influence the performance of drugs with these nano platforms.[29] Their pore diameter, which acts as a limiting factor, manipulates diffusion processes of drug molecules to the physiological environment. The pore diameter of the mesoporous cavities acts as selector of size of biologically active molecules that are loaded in these cavities. Besides, their Chemical composition and versatile chemistry for surface functionalization make them good hosts for accommodating guests biologically active molecules of various sizes, shapes, and functionalities.[30,31]

Polymer and Liposome-Based Nano-medicine

Polymeric ano-carriers are considered an essential part of manufacture of drug and are of two types, Liposomes and lipid-based polymers, and (2) Carbohydrate and lipid-based polymers

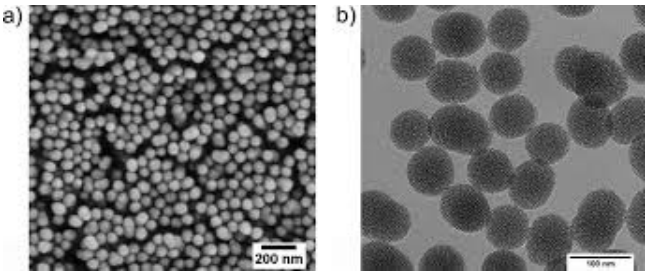

Figure 4. SEM image of mesoporous silica nanoparticles.[1]

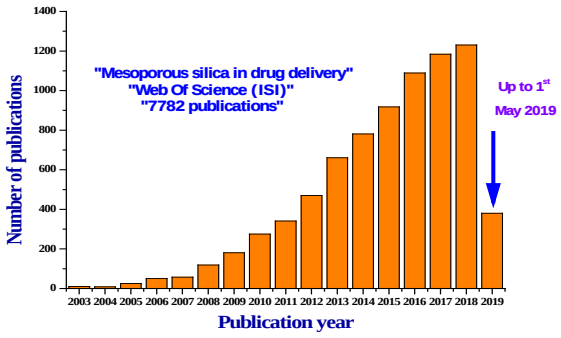

Figure 5. The number of publications per year indexed in the ISI Web of Science on the topic of "mesoporous silica in drug delivery" up to 1st May 2019.

They were discovered by Alec D. Bengham at the University of Cambridge in 1964 and were considered as the most efficient nano-carriers of drugs. Lipid bilayer structure or membrane that surrounds an aqueous compartment is the simple definition of the liposome. Main advantage of the liposomes in drug delivery systems is a core-shell design, for example, a typical phospholipid-based liposome, which allows a better encapsulation strategy for the sustained drug release. Phospholipid-based liposome has smart design as the hydrophilic or aqueous core that allows encapsulation of hydrophilic drugs, while the lipid membrane can encapsulate hydrophobic drugs. Thus, the advantage of the liposomal smart design is the encapsulation proficiency of both hydrophilic as well as hydrophobic drugs.

Table 1. Summary of some drug loaded metal-based nanoparticles together with their properties.

Nano system	Physicochemical properties and drug release efficiency	Synthesis method	Carried Drugs	Ref.
Silica-gold nanoshell and gold nanoparticles	Nanoshell sized in a range about 70-120 nm. Nanoshell drug loading efficiency and drug release profile revealed 87.5 and 99.0 % respectively.	Sol-gel method	Levofloxacin	33-35
Nano diamond-silk fibroin (ND-SF) hybrid	Nanodiamond (ND) is a new member of nanocarbon allotropes with truncated octahedral architecture that are about 2 to 8 nm in diameter. NDs are non-toxic, chemically and biologically inert, biocompatible and highly efficient in drug release.	Co-flow device	Doxorubicin	36
Porous silicon (pSi)	Revealed the tunable and versatile nature of pSi permitting high surface areas (up to 850 m^2g^{-1}), low-cost and reproducible fabrication, large pore volumes (>0.9 cm^3g^{-1}) and exhibited enhanced biocompatibility and biodegradation.	Anodic electrochemical etching in specific mixtures of hydrofluoric acid (HF) and ethanol thus enabling a 'top-down' approach	Doxorubicin and daunorubicn	37
Selenium nanoparticles carried on ruthenium polypyridyl (RuPOP)	Biocompatible, straightforward synthesis, low-toxicity, degradability in vivo, excellent antioxidant activity and chemopreventative effects	Pluronic F-127 surface modification for hydrophobic Ru complexes	5-Fluorouracil (5-FU) and doxorubicin	38, 39
Quantum dots (QDs)	(QDs) are type of stable semiconductor nanoparticles (NPs) such as g CdTe/CdS Q with a size of 2–10 nm that can easily emit strong fluorescence under irradiation. QDs possess great potential in intracellular imaging of living cells, good stability; high quantum yields (QYs), resistance to photobleaching, size-dependent emission spectra, and good biocompatibility.	Ex-situ growth approach	Folic acid (FA)	40, 41
Polyvinylpyrrolidone (PVP)-coated spherically clustered porous gold-silver alloy nanoparticle (PVP-SPAN)	PVP-SPAN provided 10 times higher loading capacity for oligonucleotide than conventional hollow Nanoshells due to increased pore diameter and surface-to-volume ratio	By low temperature mediated, partially inhibited galvanic replacement reaction followed by silver etching process	Doxorubicin	42
Polyethylene glycol-coated metal oxide nanoparticles (Fe_3O_4, NiO, CoO and SnO)	Better physiochemical properties have been achieved by surface modification of magnetic nanoparticles using various polymers, silica, different surfactant, or various organic compounds. Sufficient amount of drug can be loaded onto the stable surfaced nanoparticles with magnetic core shell structure and penetrating into Blood Brain Barrier. Low toxicity and better biodegradability	Precipitation method	Doxorubicin	43, 44
Oxidized multiwalled carbon nanotubes (MWCNT-COOH)	Enhanced delivery efficiency into cancer cells with reduced cytotoxicity. Release profiles demonstrated that approximately 98 % of BA could be released within 22 hours. Biocompatibility studies revealed that MWCNT-BA at concentrations <50 µg mL^{-1} expressed no cytotoxicity	Drug loading on (MWCNT-COOH)	Betulinic acid (BA)	45

TiO_2 film on TLM alloy	(TLM) alloys are Ti–25Nb–3Mo–2Sn– 3Zr consisting of biocompatible elements Nb, Mo, Sn, and Zr has good mechanical properties and biological compatibilities	Two-step anodization	Dexamethasone (DXM)	46
Single-walled carbon nanotubes (SWCNTs)	SWCNT provides enhanced biocompatibility, stability, and solubility in physiological solutions.	SWCNT complexes	Curcumin, gambogicacid and doxorubicin	47-49
Mesoporous silica nanoparticles (MSNs) and organic-inorganic hybrid on mesoporous silica nanoparticles	Excellent vehicle to carry drugs molecule. high thermal/chemical stability, tunable biocom-patibility/degradability and resistance to corrosion under extreme condition	Co-condensation and post –grafting method	Ibuprofen, hydrophilic and hydrophobic anticancer drugs	50-52
Mesoporous bioactive glass nanoparticles	Bioactive glass nanoparticles (BGn) have recently gained potential usefulness to load and deliver therapeutic molecules (drugs and particularly genes). Spherical BGn with sizes of 80–90 nm were produced to obtain 3–5 nm sized mesopores	Sono-reacted sol–gel process	Chemical drug (Na-ampicillin) and gene (small interfering RNA; siRNA)	53

They were discovered by Alec D. Bengham at the University of Cambridge in 1964 and were considered as the most efficient nano-carriers of drugs. Lipid bilayer structure or membrane that surrounds an aqueous compartment is the simple definition of the liposome. Mainadvantage of the liposomes in drug delivery systems is a core-shell design, for example, a typical phospholipid-based liposome, which allows a better encapsulation strategy for the sustained drug release. Phospholipid-based liposome has smart design as the hydrophilic or aqueous core that allows encapsulation of hydrophilic drugs, while the lipid membrane can encapsulate hydrophobic drugs. Thus the advantage of the liposomal smart design is the encapsulation proficiency of both hydrophilic as well as hydrophobic drugs. Nevertheless, there are some disadvantages of this design also e.f., nano-carriers containing lipids undergo severe degradation and then the toxicity level increases. Lately, there are approximately 12 clinically approved liposomal nano-medicine and around 80 under clinical investigation.

Secondly, carbohydrate and protein-based polymers type have promising clinical progress and results. This type containing polysaccharide polymers can be natural or synthetic such as cellulose, gelatin, chitosan, heparin, polylactic acid, polyglycolic acid, and their copolymer poly (lactic-co-glycolic acid) (PLGA). Natural degradation by the enzymes in the body and highly biocompatibility are the most inherent features of carbohydrate based polymers. Combining two or more polymers to form a core-shell design of polymeric micelles by is an alternate strategy used in the formulation of polymeric nano-medicine, which are currently under clinical investigations.

Classification of Polymers

Natural and synthetic classes are the essential two categories of polymeric materials that are used in the drug delivery system with broad applicability. Natural polymers are classified into two subdivisions as polysaccharide-based and protein-based polymers, which synthetic polymers have different subdivisions as polyesters, polyether, poloxamers, and recombinant protein-based polymers.[54]

Natural polymers in drug delivery

Natural polymers have an important role in drug release and in delivering therapeutic agents to the target tissue. Special features of natural polymers that are attractive in drug delivery are their biodegradability, lack of toxicity, inexpensive, great economic features and safety. There are various sources for natural polymers, mainly polysaccharides, including plants, microbes, algae, and fungus. Chemical character of some polymers is neutral and the carboxylate or sulfate groups have negative charges (Carrageenan, Chondroitin, and Dermatan) but Chitosan is the only cationic polysaccharide currently known. Various origins of natural polymers are described below:

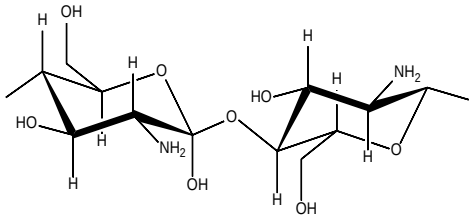

Chitosan

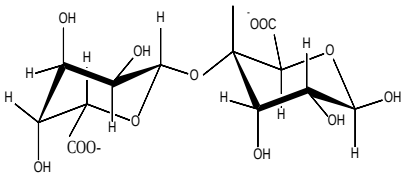

Alginate

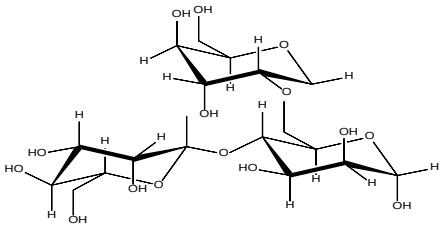

Guar gum

Figure 6. Structures of some natural polymers.

Synthetic polymers in drug delivery:

Synthetic biodegradable polymers have a wide and distinct impact on drug delivery and tissue engineering fields. Synthetic polymers, due to their structure, are devoid of certain disadvantages of natural polymers such as microbial contamination. Many natural polymers are exposed to external environment and there are chances of microbial contamination. Industrial production is a controlled procedure with definite quantities of ingredients, while the natural polymers are dependent on environmental and seasonal factors.[60] Unstable climate conditions and differences in the regions lead to an uncontrolled rate of hydration and different times of harvest collection of natural materials. There are commonly used synthetic polymers in drug delivery such as PLA (polylactic acid), PGA (polyglycolic acid), PCL (poly (e-caprolactone)), PHB (poly hydroxybutyrate), PLGA (Poly (lactide-co-glycolide), PDS (Polydioxanone) and Polyamide etc. Biocompatibility and degradability are the required important features of the polymers, which are selected for incorporation into the drug delivery system. Biocompatible polymers offer a highly efficient transition of desired drugs into the tissues or organs without issues in biological systems. Biodegradable polymers disintegrate with the cleavage of covalent bonds between the drug molecule and the polymer. This erosion of the polymer is due to the dissolution of linking chains without causing any change in the chemical structure of the drug molecule.

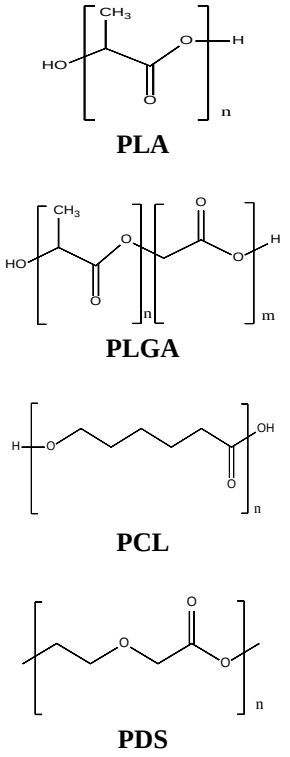

PLA

PLGA

PCL

PDS

Figure 7. Structures of some synthetic polymers.

Table 2. The origins of some natural polymers.

Polymer origin	Examples of polymers	Composition of polymers	Ref.
Plant origin	Starch, hemicellulose, cellulose, agar, pectin, guar gum	Guar gum is natural polysaccharide composed of the sugar's galactose and mannose. Pectin is a natural, non-toxic and anionic polysaccharide extracted from cell walls of most plants	55
Microbial origin	Curdlan, gellan, xanthan	Xanthan is an extracellular heteropolysaccharide produced by fermentation of the bacterium Xanthomonascampestris. Gellan gum is a bacterial exopolysaccharide commercially prepared by aerobic submerged fermentation of *Sphingomonas elodea.*	55
Algal origin	Alginate, carrageenan	Alginate is cross-linked as Ca salt; It incorporated in different application, their derivatives such as polyethylene glycol–anthracene modified alginate, photocross-linked heparin-alginate hydrogels, alginate–guargum hydrogel, micelles/sodium alginate composite gel beads and chitosan-Ca-alginate microspheres.	56-58
Fungal origin	Chitin, pullulan, scleroglucan	Chitosan is linear polysaccharide composed of -1,4-linked 2-amino-2-deoxy-*D*-glucose (N-acetyl glucosamine). It is insoluble at high pH conditions. Chitosan itself is nontoxic, biodegradable, and biocompatible	55, 59

Table 3.Methods of preparation of polymeric nanomedicine

Method of preparation	Definition	Examples	Ref.
Coacervation or ionic gelation of hydrophilic polymers	Coacervation is an electrostatic interaction between two aqueous media in which the liquid-to-gel (i.e., ionic gelation) transition occurs at normal conditions.	The cationic (amino groups of chitosan are positively charged) interaction with anions (tripolyphosphates are negative charged) to form coacervates.	61-63
Interfacial polymerization	The interfacial polymerization of two reactive monomers in two different phases (i.e., disperse and continuous) with the cross-linking of interfacial reactions.	Radical polymerization, polycondensation, or polyaddition	64, 65
Emulsification-solvent evaporation	Two-step process consists of polymeric emulsification in an aqueous medium followed by solvent evaporation from the polymer and nanoparticle precipitation.	Poly(lactic-co-glycolic acid) (PLGA), poly-*D*,*L*-lactic acid (PLA), poly(ε-caprolactone) (PCL), ethyl cellulose, poly(β-hydroxybutyrate) etc.	66
Salting out	This phenomenon based on separation of the water-miscible phase (solvent) from the aqueous phase by the salting-out method	PLA, poly (methacrylic) acids, and ethyl cellulose nanospheres.	62, 67

Some smart platforms of polymeric Nanomedicine in drug delivery systems

Polymeric nano-materials have distinct characteristics that qualify them to be good sources for sustained and controlled release. These materials offer required perquisites, which ensure the efficient drug delivery system such as biocompatibility, biodegradability, high accuracy and efficiency, a high loading capacity of the desired drug and finally temporal and spatial directing of the drug into the desired cell or tissue with limited cytotoxicity and side effects.

The entrapment of the drug either physically or covalently bound to the polymer matrix is controlled by the method of preparation and the final shape and properties of the materials. Hyperbranched macromolecules (dendrimers), Polymeric micelles (amphiphilic core/shell) and drug-conjugates are the different shapes of polymeric nanomaterial conjugated with the drug.

Dendrimers

These three-dimensional, well-organized nanoscopic and highly branched polymers of less than 10 nm size were was discovered in 1978 by Vogtle as a novel and highly efficient nanotechnology platforms for drug delivery.[68] Their constructions take place via two different approaches, a divergent method and a convergent approach. A typical dendrimer structure consists of mainly three parts that are core molecule, multiple layers or generations of branched molecules and surface molecules.[69]

Encapsulation or loading mechanism of the drug within the dendrimers is through two ways that are as shown in figure 9. Drug molecules can be loaded both in the interior of the dendrimers as well as attached to the surface groups (terminal groups). Dendrimers are highly efficient vehicles for drug molecules either by encapsulating drugs within the dendritic structure or by inter-acting with drugs at their terminal functional groups via electrostatic or covalent bonds.[70]

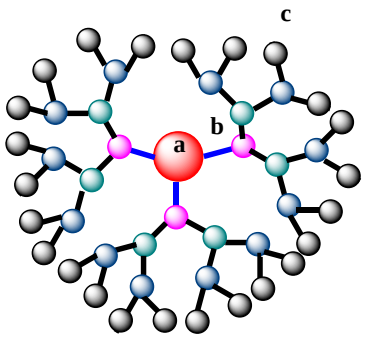

Figure 8. Dendrimer shape consists of a) core, b) multilayers (generations) and c) surface groups.

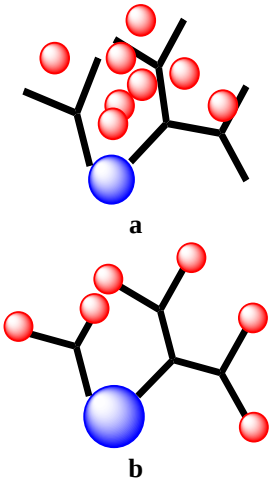

Figure 9. Dendrimer molecule with drug molecules a) Encapsulated within branches and b) loaded at terminal surface of branches.

Micelles (core-shell)

Micelles represent spherical lipid NSs consists of two parts (hydrophobic and hydrophilic parts) like a sheet folded back onto itself. According to the surrounding medium, micelle or reverse micelle can be arranged. Micelle remains with hydrophobic chains on the inside with the polar heads on the outside when the surrounding is an aqueous medium. However, if the surrounding medium is organic, then the components of the micelle are reversed-hence the name becomes reverse micelle. The polar heads are in interior, and the hydrophobic chains are outside.[71]

Polymeric micelles are emerging as a powerful design in the field of nano-medicine for drug release and act as a carrier for different drugs due to their tunable size, in vivo stability, and efficiency in solubilizing water-insoluble drugs, small particle size, good thermodynamic stability in solution and extended-release of various drugs.[72]

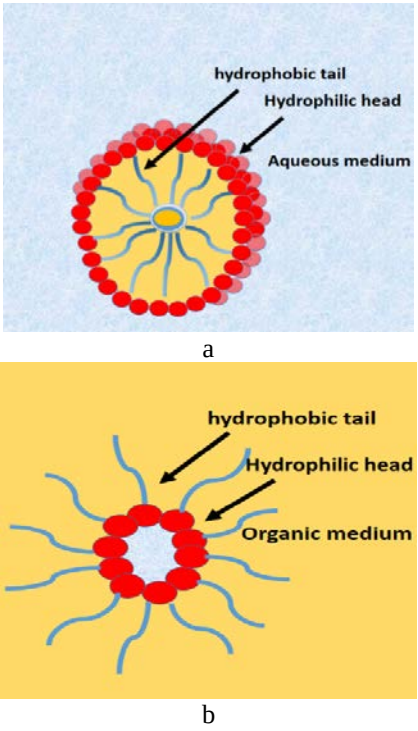

Figure 10. Structure of (a) micelle and (b) reverse micelle.

Hydrogels

Hydrogels are biocompatible hydrophilic networks that can be constructed from both natural and synthetic materials. Some unusual properties of hydrogels make them more attractive and efficient for drug delivery and tissue engineering. Their high-affinity for water and high swelling property, relatively low cytotoxicity, injectability, biodegradability, mucoadhesiveness, and tuneable bioadhesive properties are the most beneficial property of hydrogel for enhancement of drug delivery system.[73] Some widespread polymers used to synthesize hydrogels are poly(N-isopropyl acrylamide), poly(L-lactic-co-glycolic acid), poly ethylene glycol), methacrylated poly (glycerol succinic acid) dendrimers, and hen egg-white lysozyme.[74,75] (N-isopropyl acrylamide) (pNIPAm)-based microgels are stimuli-responsive microgels that reversible pNIPAm's volume phase transition temperature (VPTT) at 32 °C. "Breathing-in" technique is the most effective encapsulation of insulin as one of the hydrogel applications in the drug delivery system when compared to more common encapsulation methods in which the gel is re-hydrated in the aqueous solution of the desired material. Its permeability is controlled by lowering the temperature or increasing pH that increases the swelling degree of the desired drug.[73]

Molecularly imprinted polymer (MIP)

Recently, the investigations of new drug delivery vehicles have been directed on the development of some "intelligent" drug delivery devices that can increase the transportation efficiency of the desired drug and decrease patient non-compliance. MIPs have high potential and selectivity for drug delivery to desired tissue and cells without exposure of another cells, which has definite and selective cavities to the desired material. The molecular imprinting phenomenon is related to three steps of synthesis that started with the creation of a pre-polymerization complex of selected functional monomer(s) and a template molecule. It is followed by cross-linking of the complex via polymerization process and finally removing the template from the matrix leaving the well-defined three-dimensional cavities,[76,77] attaching the template with MIPs via a covalent or non-covalent approach. The non-covalent approach is the most widely adopted in the case of a drug delivery system in which, there are no interactions between the template and the functional monomers that ensure the efficiency of the drug release.

CONCLUSION AND FUTURE PERSPECTIVES

From this review, it can be shown that there are various methods for the preparation of DDS that have different potential and impacts in the release efficiency and desired requirements for efficient DDS. Nano-medicine is highly sophisticated and triggered vehicles for enhancement of DDS efficacy that has definite features as biocompatibility, efficient cargo of desired drugs, transportation efficiency that help in decreasing the administration times of drug and reducing the patient compliance. Types of nanomaterial include metallic and polymeric based nanomedicine, which refers to a wide range of applicability of nanomaterial, hence there are different preparation methods and different properties of synthesized materials. Therefore, it can be expected that there is tremendous development in DDS and therapeutic recognition and monitoring according to the new trends and objectives.

Hybrid polymeric smart platforms such as fibrous material, dendrimer, micelle (core-shell), stimuli-responsive hydrogel and MIPs with metallic nanomaterial can ensure the best behaviour and unique properties of DDS. These hypotheses can be studied for further objectives and able to have new trends and prove to be promising biomedical devices in the future.

Table 4. Some applications of molecular imprinted polymers in DDS.

Matrix	Polymerization	Functional monomer/s	Cross- linker	Template	Ref.
MIP- bromhexine	bulk polymerization	MAA	EGDMA	Bromhexine	[78]
MIP- tramadol	bulk polymerization	MAA	EGDMA	Tramadol	[79]
MIP-S-propranolol	copolymerisation	MAA	EGDMA	S-propranolol	[80]
β-cyclodextrin (β-CD)-grafted chitosan (CS) (CS-g-β-CD) microsphere/MIP	bulk polymerization	MAA	EGDMA	Sinomenine hydrochloride (SM)	[81]
MIP- glycyrrhizic acid	bulk polymerization	MAA, dimethylamino-ethyl methacrylate and hydroxyethyl methacrylate	EGDMA	glycyrrhizic acid	[82]
Acetylsalicylic acid-loaded polyDEGDMA in supercritical carbon dioxide	supercritical polymerization	EGDMA	In CO2	Acetylsalicylic acid-	[83]
Magnetic MIPs- aspirin	co-polymerization	MAA and trimethylolpropane-trimethacrylate (TRIM)	-	Aspirin	[84]
Polystyrene-MIP- S-naproxen	precipitation polymerization	MAA	EGDMA	S-naproxen	[85]
MIP- Sulpiride	bulk polymerization	itaconic acid	EGDMA	Sulpiride	[86]
5-FU imprinted microspheres MIP-CS-g-PMMA	free radical polymerization	methyl methacrylate	-	5-fluorouracil (5-FU)	[87]

REFERENCES

[1]Jain, K. K., Drug delivery systems-an overview, in "*Drug delivery systems*", Springer, **2008**, 1-50. https://doi.org/10.1007/978-1-59745-210-6_1

[2]Webster, J. G., *Encyclopedia of medical devices and instrumentation*, John Wiley & Sons, Inc. **1990**.

[3]Lavik, E. B., Kuppermann, B. D., Humayun, M. S., Drug Delivery in Retina, Elsevier, **2013**, 734-745. https://doi.org/10.1016/B978-1-4557-0737-9.00038-2

[4]Frid, A., Hirsch, L., Gaspar, R., Hicks, D., Kreugel, G., Liersch, J., Letondeur, C., Sauvanet, J.-P., Tubiana-Rufi, N., Strauss, K., New injection recommendations for patients with diabetes. *Diabetes Metab.*, **2010**, *36*, 3-18. https://doi.org/10.1016/S1262-3636(10)70002-1

[5]Zaidi, S. A., Molecular imprinted polymers as drug delivery vehicles, *Drug Deliv.*, **2016**, *23*, 2262-2271.

[6]Rezaie, H. R., Esnaashary, M., Arjmand, A. A., Öchsner, A. A., *Review of Biomaterials and Their Applications in Drug Delivery*, Springer, **2018**.

[7]Hillery, A.M.; Park, K.; *Drug Delivery: Fundamentals and Applications*. CRC Press, **2016**. https://doi.org/10.1201/9781315382579

[8]Akiti, O., Jimoh, A. G., Wise, D. L., Barabino, G. A., Trantolo, D. J., Gresser, J. D., Multiphasic or "Pulsatile" controlled release system for the delivery of vaccines, in *Human Biomaterials Applications*, Springer, **1996**, 319-343. https://doi.org/10.1007/978-1-4757-2487-5_14

[9]Rezaie, H. R., Esnaashary, M., Öchsner, A., *The History of Drug Delivery Systems, in A Review of Biomaterials and Their Applications in Drug Delivery*, Springer, **2018**, 1-8.

[10]Lian, T., Ho, R. J., Trends and developments in liposome drug delivery systems, *J. Pharm. Sci.*, **2001**, *90*, 667-680. https://doi.org/10.1002/jps.1023

[11]Zhang, W., Zhao, Q., Deng, J., Hu, Y., Wang, Y., Ouyang, D., Big data analysis of global advances in pharmaceutics and drug delivery1980-2014, *Drug Discov. Today*, **2017**, *22*, 1201-1208. https://doi.org/10.1016/j.drudis.2017.05.012

[12]Park, K., Controlled drug delivery systems: past forward and future back, *J. Control. Release*, **2014**, *190*, 3-8. https://doi.org/10.1016/j.jconrel.2014.03.054

[13]Park, K., Drug delivery of the future: Chasing the invisible gorilla, *J. Control. Release*, **2016**, *240*, 2-8. https://doi.org/10.1016/j.jconrel.2015.10.048

[14]Agrawal, P., Drug discovery and development: an insight into pharmacovigilance, *J. Pharmacovigil.*, **2014**, 2-3. DOI:10.4172/2329-6887.1000e120

[15]Rask-Andersen, M., Almén, M.S., Schiöth, H.B., Trends in the exploitation of novel drug targets, *Nature Rev. - Drug Discov.*, **2011**, *10*, 579-590. https://doi.org/10.1038/nrd3478

[16]Elhassa, G. O., Alfarouk, K. O., Drug development: stages of drug development, *J. Pharmacovigil.* **2015**, *3*, 1-3. https://doi.org/10.4172/2329-6887.1000e141

[17]Thaul, S., How FDA approves drugs and regulates their safety and effectiveness, *Congressional Research Service*, 7-5700, R41983, Report, **2012**.

[18]Anton, N., Jakhmola, A., Vandamme, T. F., Trojan microparticles for drug delivery, *Int. J. Pharm.*, **2012**, *4*, 1-25. https://doi.org/10.3390/pharmaceutics4010001

[19]Steinhoff, G., *Regenerative medicine-from protocol to patient: 5. Regenerative therapies II*, Springer, **2016**. https://doi.org/10.1007/978-3-319-28293-0

[20]Kaushik, A., Jayant, R. D., Nair, M., *Advances in Personalized Nanotherapeutics*, Springer, **2017**. https://doi.org/10.1007/978-3-319-63633-7

[21]Keservani, R. K., Sharma, A. K., *Nanoconjugate Nanocarriers for Drug Delivery*, CRC Press., **2018**.

https://doi.org/10.1201/9781351171045

[22]Iijima, S., Helical microtubules of graphitic carbon. *Nature*, **1991,** *354*, 56-58. https://doi.org/10.1038/354056a0

[23]Ajayan, P., Ebbesen, T., Nanometre-size tubes of carbon, *Rep. Prog. Phys*., **1997**, *60*, 1025-1062.

https://doi.org/10.1088/0034-4885/60/10/001

[24]Arsawang, U., Saengsawang, O., Rungrotmongkol, T., Sornmee, P., Wittayanarakul, K., Remsungnen, T., Hannongbua, S., How do carbon nanotubes serve as carriers for gemcitabine transport in a drug delivery system? *Mol. Graph. Model*, **2011**, *29*, 591-596.

https://doi.org/10.1016/j.jmgm.2010.11.002

[25]Das, M. C., Xu, H., Wang, Z., Srinivas, G., Zhou, W., Yue, Y.-F., Nesterov, V.N., Qian, G., Chen, B., A Zn 4 O-containing doubly interpenetrated porous metal–organic framework for photocatalytic decomposition of methyl orange, *Chem. Commun*., **2011**, *47*, 11715-11717.

https://doi.org/10.1039/c1cc12802g

[26]Tang, F., Li, L., Chen, D., Mesoporous silica nanoparticles: synthesis, biocompatibility and drug delivery, *Adv. Mater*., **2012**, *24*, 1504-1534.

https://doi.org/10.1002/adma.201104763

[27]Martínez-Carmona, M., Colilla, M., Vallet-Regí, M., Smart mesoporous nanomaterials for antitumor therapy. *Nanomaterials*, **2015**, *5*, 1906-1937. https://doi.org/10.3390/nano5041906

[28]Castillo, R. R., Colilla, M., Vallet-Regí, M., Advances in mesoporous silica-based nanocarriers for co-delivery and combination therapy against cancer, *Expert Opin. Drug. Deliv*., **2017**, *14*, 229-243.

https://doi.org/10.1080/17425247.2016.1211637

[29]Vallet-Regí, M., Colilla, M., González, B. Medical applications of organic–inorganic hybrid materials within the field of silica-based bioceramics. *Chem. Soc. Rev*., **2011**, *40*, 596-607. https://doi.org/10.1039/C0CS00025F

[30]Trewyn, B. G., Whitman, C. M., Lin, V. S.-Y., Morphological control of room-temperature ionic liquid templated mesoporous silica nanoparticles for controlled release of antibacterial agents, *Nano Lett.*, **2004**, *4*, 2139-2143.https://doi.org/10.1021/nl048774r

[31]Wang, L.-S., Wu, L.-C., Lu, S.-Y., Chang, L.-L., Teng, I.-T., Yang, C.-M., Ho, J.-a. A., Biofunctionalized phospholipid-capped mesoporous silica nanoshuttles for targeted drug delivery: improved water suspensibility and decreased nonspecific protein binding, *ACS Nano*, **2010**, *4*, 4371-4379. https://doi.org/10.1021/nn901376h

[32]Borisova, D., Möhwald, H., Shchukin, D. G., Mesoporous silica nanoparticles for active corrosion protection, *ACS Nano*, **2011**, *5*, 1939-1946. https://doi.org/10.1021/nn102871v

[33]Kaur, R., Dhari, J., Sharma, O.P., Gupta, G., Kharb, V., *Res. J. Pharm. Biol. Chem. Sci.*, **2012**, *3*, 1037-1041.

[34]Kumar, A., Zhang, X., Liang, X.-J., Gold nanoparticles: emerging paradigm for targeted drug delivery system, *Biotechnol. Adv*., **2013**, *31*, 593-606. https://doi.org/10.1016/j.biotechadv.2012.10.002

[35]Raghavendra, R.. Arunachalam, K., Annamlai, S. K., Aarrthy, M., Diagnostics and therapeutic application of gold nanoparticles. medicine (bio diagnostics, drug delivery and cancer therapy), *J. Pharm. Pharm. Sci.*, **2014**, *6(2)*, 74-82.

[36]Khalid, A., Mitropoulos, A. N., Marelli, B., Tomljenovic-Hanic, S., Omenetto, F.G., Doxorubicin loaded nanodiamond-silk spheres for fluorescence tracking and controlled drug release. *Biomed. Opt. Express*, **2016**, *7*, 132-147. https://doi.org/10.1364/BOE.7.000132

[37]Yazdi, I. K., Ziemys, A., Evangelopoulos, M., Martinez, J. O., Kojic, M., Tasciotti, E., Physicochemical properties affect the synthesis, controlled delivery, degradation and pharmacokinetics of inorganic nanoporous materials, Nanomedicine, **2015**, *10*, 3057-3075. https://doi.org/10.2217/nnm.15.133

[38]Liu, W., Li, X., Wong, Y.-S., Zheng, W., Zhang, Y., Cao, W., Chen, T., Selenium nanoparticles as a carrier of 5-fluorouracil to achieve anticancer synergism, *ACS Nano*, **2012**, *6*, 6578-6591. https://doi.org/10.1021/nn202452c

[39]Huang, Y., L. He, L., Liu, W., Fan, C., Zheng, W., Wong, Y.-S., Chen, T., Selective cellular uptake and induction of apoptosis of cancer-targeted selenium nanoparticles, *Biomaterials*, **2013**, *34*, 7106-7116. https://doi.org/10.1016/j.biomaterials.2013.04.067

[40]Zhao, M.X., Zeng, E.Z., Zhu, B.J., The biological applications of inorganic nanoparticle drug carrierr, *ChemNanoMat*, **2015**, *1*, 82-91. https://doi.org/10.1002/cnma.201500036

[41]Zhao, H., Ma, D., *Synthesis and Characterization of Quantum Dots, Biosensors Based on Nanomaterials and Nanodevices*, CRC Press, **2013**, p. 11.

[42]Jang, H., Min, D.-H, Spherically-clustered porous Au–Ag alloy nanoparticle prepared by partial inhibition of galvanic replacement and its application for efficient multimodal therapy, *ACS Nano*, **2015**, *9*, 2696-2703. https://doi.org/10.1021/nn506492s

[43]Javed, K. R., Ahmad, M., Ali, S., Butt, M.Z., Nafees, M., Butt, A. R., Nadeem, M., Shahid, A., Comparison of doxorubicin anticancer drug loading on different metal oxide nanoparticles, *Medicine*, **2015**, *94*, 1-6. https://doi.org/10.1097/MD.0000000000000617

[44]Liu, J., Huang, C., He, Q., Pharmaceutical application of magnetic iron oxide nanoparticles, *Sci. Adv. Mater*., **2015**, *7*, 672-685. https://doi.org/10.1166/sam.2015.1887

[45]Tan, J.M., Karthivashan, G., Arulselvan, P., Fakurazi, S., Hussein, M. Z., Characterization and in vitro studies of the anticancer effect of oxidized carbon nanotubes functionalized with betulinic acid, *Drug Des. Dev. Ther*., **2014**, *8*, 2333-2343. https://doi.org/10.2147/DDDT.S70650

[46]Zhang, Y., He, F., Sun, Z., Li, L., Huang, Y., Controlled delivery of dexamethasone from TiO_2 film with nanoporous structure on Ti–25Nb–3Mo–2Sn–3Zr biomedical alloy without polymeric carrier, *Mater. Lett.*, **2014**, *128*, 384-387. https://doi.org/10.1016/j.matlet.2014.04.149

[47]Li, H., Zhang, N., Hao, Y., Wang, Y., Jia, S., Zhang, H., Zhang, Y., Zhang, Z., Formulation of curcumin delivery with functionalized single-walled carbon nanotubes: characteristics and anticancer effects in vitro, *Drug Deliv*., **2014**, *21*, 379-387. https://doi.org/10.3109/10717544.2013.848246

[48]Saeed, L. M., Mahmood, M., Pyrek, S. J., Fahmi, T., Xu, Y., Mustafa, T., Nima, Z. A., Bratton, S. M., Casciano, D., Dervishi, E., Single-walled carbon nanotube and graphene nanodelivery of gambogic acid increases its cytotoxicity in breast and pancreatic cancer cells, *J. Appl. Toxicol.*, **2014**, *34*, 1188-1199. https://doi.org/10.1002/jat.3018

[49]Liu, Z., Sun, X., Nakayama-Ratchford, N., Dai, H., Supramolecular chemistry on water-soluble carbon nanotubes for drug loading and delivery, *ACS Nano*, **2007**, *1*, 50-56. https://doi.org/10.1021/nn700040t

[50]Dave, P. N., Chopda, L. V, A review on application of multifunctional mesoporous nanoparticles in controlled release of drug delivery, in *Mater. Sci. Forum, Multi-Functional Nanomaterials and their Emerging Applications, Trans. Tech. Publ.*, **2014**, p. 17, https://doi.org/10.4028/www.scientific.net/MSF.781.17

[51]Chen, Y., Chen, H., Shi, J., Drug delivery/imaging multifunctionality of mesoporous silica-based composite nanostructures, *Expert Opin. Drug. Deliv.*, **2014**, *11*, 917-930. https://doi.org/10.1517/17425247.2014.908181

[52]Chen, Z., Li, Z., Lin, Y., Yin, M., Ren, J., Qu, X., Biomineralization inspired surface engineering of nanocarriers for pH-responsive, targeted drug delivery, *Biomaterials*, **2013**, *34*, 1364-1371. https://doi.org/10.1016/j.biomaterials.2012.10.060

[53]El-Fiqi, A., Kim, T.-H., Kim, M., Eltohamy, M., Won, J.-E., Lee, E.-J., Kim, H.-W., Capacity of mesoporous bioactive glass nanoparticles to deliver therapeutic molecules, *Nanoscale*, **2012**, *4*, 7475-7488. https://doi.org/10.1039/c2nr31775c

[54]Hamid Akash, M. S., Rehman, K., Chen, S., Natural and synthetic polymers as drug carriers for delivery of therapeutic proteins, *Polym. Rev.*, **2015**, *55*, 371-406. https://doi.org/10.1080/15583724.2014.995806

[55]Jana, S., Gandhi, A., Sen, K., Basu, S., Natural polymers and their application in drug delivery and biomedical field, *J. Pharm. Sci. Tech.*, **2011**, *1*, 16-27.

[56]El-Sherbiny, I. M., Abdel-Mogib, M., Dawidar, A.-A.M., Elsayed, A., Smyth, H. D., Biodegradable pH-responsive alginate-poly (lactic-co-glycolic acid) nano/micro hydrogel matrices for oral delivery of silymarin, *Carbohydr. Polym.*, **2011**, *83*, 1345-1354. https://doi.org/10.1016/j.carbpol.2010.09.055

[57]Mennini, N., Furlanetto, S., Cirri, M., Mura, P., Quality by design approach for developing chitosan-Ca-alginate microspheres for colon delivery of celecoxib-hydroxypropyl-β-cyclodextrin-PVP complex, *Eur. J. Pharm. Biopharm.*, **2012**, *80*, 67-75. https://doi.org/10.1016/j.ejpb.2011.08.002

[58]Pongjanyakul, T., Puttipipatkhachorn, S., Modulating drug release and matrix erosion of alginate matrix capsules by microenvironmental interaction with calcium ion, *Eur. J. Pharm. Biopharm.*, **2007**, *67*, 187-195. https://doi.org/10.1016/j.ejpb.2006.12.009

[59]Hwang, D.-C., Damodaran, S., Selective precipitation and removal of lipids from cheese whey using chitosan, *J. Agric. Food Chem.*, **1995**, *43*, 33-37. https://doi.org/10.1021/jf00049a008

[60]Bourne, D., Banker, G., Rhodes, C., *Modern Pharmaceutics, Informa Healthcare*, New York, **2002**, 67-92.

[61]Jana, S., Jana, S., Natural polymeric biodegradable nanoblend for macromolecules delivery, in *Recent Developments in Polymer Macro, Micro and Nano Blends*, Elsevier, **2017**, 289-312.https://doi.org/10.1016/B978-0-08-100408-1.00010-8

[62]Pal, S. L., Jana, U., Manna, P. K., Mohanta, G. P., Manavalan, R., Nanoparticle: An overview of preparation and characterization, *J. Appl. Pharm.*, **2011**, *1*, 228-234.

[63]Dustgania, A., Vasheghani Farahani, E., Imani, M., Preparation of chitosan nanoparticles loaded by dexamethasone sodium phosphate, *Iranian J. Pharm.*, **2008**, *4*, 111-114.

[64]Scott, C., Wu, D., Ho, C.-C., Co, C. C., Liquid-core capsules via interfacial polymerization: a free-radical analogy of the nylon rope trick, *J. Am. Chem. Soc.*, **2005**, *127*, 4160-4161. https://doi.org/10.1021/ja044532h

[65]Crespy, D., Stark, M.; Hoffmann-Richter, C., Ziener, U., Landfester, K., Polymeric nanoreactors for hydrophilic reagents synthesized by interfacial polycondensation on miniemulsion droplets, *Macromolecules*, **2007**, *40*, 3122-3135. https://doi.org/10.1021/ma0621932

[66]Song, C., Labhasetwar, V., Murphy, H., Qu, X., Humphrey, W., Shebuski, R., Levy, R., Formulation and characterization of biodegradable nanoparticles for intravascular local drug delivery. *J. Control. Release*, **1997**, *43*, 197-212. https://doi.org/10.1016/S0168-3659(96)01484-8

[67]Kadian, R., Nanoparticles: a promising drug delivery approach, *Asian J. Pharm. Clin. Res.*, **2018**, *11*, 30-35. https://doi.org/10.22159/ajpcr.2018.v11i1.22035

[68]Buhleier, E., Wehner, W., Vögtle, F., "Cascade"- and "Nonskid-Chain-like" Syntheses of Molecular Cavity Topologies, *Synthesis*, **1978**, *2*, 155-158. https://doi.org/10.1055/s-1978-24702

[69]Tolia, G. T., Choi, H. H., The role of dendrimers in topical drug delivery, *Pharm. Technol. Int.*, **2008**, *32*, 88-98.

[70]Rai, A.K., Tiwari, R.;, Maurya, P., Yadav, P., Dendrimers: a potential carrier for targeted drug delivery system, *Pharm. Biol. Evaluat.*, **2016**, *3*, 275-287.

[71]Singh, A. K., Yadav, T. P., Pandey, B., Gupta, V., Singh, S. P., *Engineering Nanomaterials for Smart Drug Release: Recent Advances and Challenges, in Applications of Targeted Nano Drugs and Delivery Systems*, Elsevier, **2019**, 411-449. https://doi.org/10.1016/B978-0-12-814029-1.00015-6

[72]Gundloori, R. V., Singam, A., Killi, N., *Nanobased Intravenous and Transdermal Drug Delivery Systems, in Applications of Targeted Nano Drugs and Delivery Systems*. Elsevier, **2019**, 551-594. https://doi.org/10.1016/B978-0-12-814029-1.00019-3

[73]Schwall, C., Banerjee, I., Micro-and nanoscale hydrogel systems for drug delivery and tissue engineering, *J. Mater. Sci.*, **2009**, *2*, 577-612. https://doi.org/10.3390/ma2020577

[74]Söntjens, S. H., Nettles, D. L., Carnahan, M. A., Setton, L. A., Grinstaff, M. W., Biodendrimer-based hydrogel scaffolds for cartilage tissue repair, *Biomacromolecules*, **2006**, *7*, 310-316. https://doi.org/10.1021/bm050663e

[75]Shi, G., Cai, Q., Wang, C., Lu, N., Wang, S., Bei, J., Fabrication and biocompatibility of cell scaffolds of poly (L-lactic acid) and poly (L-lactic-co-glycolic acid). *Polym. Adv. Technol.*, **2002**, *13*, 227-232.https://doi.org/10.1002/pat.178

[76]Cormack, P. A., Elorza A. Z., Molecularly imprinted polymers: synthesis and characterisation, *J. Chromatogr. B*, **2004**, *804*, 173-182. https://doi.org/10.1016/j.jchromb.2004.02.013

[77]Kamel, A. H., Mohammad, S. G., Awwad, N. S., Mohammed, Y. Y., Survey on the Integration of Molecularly Imprinted Polymers as Artificial Receptors in Potentiometric Transducers for pharmaceutical Drugs, *Int. J. Electrochem.*, **2019**, *14*, 2085-2124. https://doi.org/10.20964/2019.02.23

[78]Azodi-Deilami, S., Abdouss, M., Javanbakht, M., The syntheses and characterization of molecularly imprinted polymers for the controlled release of bromhexine, *Appl. Biochem. Biotechnol.*, **2011**, *164*, 133-147. https://doi.org/10.1007/s12010-010-9121-y

[79]Azodi-Deilamia, S., Abdoussa, M., Seyedib, S.R., Synthesis and characterization of molecularly imprinted polymer for controlled release of tramadol, *Open Chem.*, **2010**, *8*, 687-695. https://doi.org/10.2478/s11532-010-0035-x

[80]Bodhibukkana, C., Srichana, T., Kaewnopparat, S., Tangthong, N., Bouking, P, Martin, G. P., Suedee, R., Composite membrane of bacterially-derived cellulose and molecularly imprinted polymer for use as a transdermal enantioselective controlled-release system of racemic propranolol, *J. Control. Release*, **2006**, *113*, 43-56. https://doi.org/10.1016/j.jconrel.2006.03.007

[81]Chen, H., Zhang, W., Yang, N., Chen, C., Zhang, M., Chitosan-Based Surface Molecularly Imprinted Polymer Microspheres for Sustained Release of Sinomenine Hydrochloride in Aqueous Media, *Appl. Biochem. Biotechnol.*, **2018**, *185*, 370-384. https://doi.org/10.1007/s12010-017-2658-2

[82]Cirillo, G., Parisi, O. I., Curcio, M., Puoci, F., Iemma, F., Spizzirri, U.G., Picci, N., Molecularly imprinted polymers as drug delivery systems for the sustained release of glycyrrhizic acid, *J. Pharm. Pharmacol.*, **2010**, *62*, 577-582. https://doi.org/10.1211/jpp.62.05.0003

[83]Duarte, A. R. C., Casimiro, T., Aguiar-Ricardo, A., Simplício, A. L., Duarte, C. M., Supercritical fluid polymerisation and impregnation of molecularly imprinted polymers for drug delivery, *J. Supercrit. Fluids*, **2006**, *39*, 102-106. https://doi.org/10.1016/j.supflu.2006.01.013

[84]Kan, X., Geng, Z., Zhao, Y., Wang, Z., Zhu, J.-J., Magnetic molecularly imprinted polymer for aspirin recognition and controlled release, *Nanotechnology*, **2009**, *20*, 165601-165608. https://doi.org/10.1088/0957-4484/20/16/165601

[85]Li, X. X., Hao, L.F., Huang, Y. P., Duan, H. Q., Liu, Z.S., Release evaluation of molecularly imprinted polymers prepared under molecular crowding conditions, *Polym. Eng. Sci.*, **2012**, *52*, 1440-1449. https://doi.org/10.1002/pen.23086

[86]Zhang, W., She, X., Wang, L., Fan, H., Zhou, Q., Huang, X., Tang, J. Z., Preparation, Characterization and Application of a Molecularly Imprinted Polymer for Selective Recognition of Sulpiride, *J. Mater. Sci.*, **2017**, *10*, 475-490. https://doi.org/10.3390/ma10050475

[87]Zheng, X.-F.. Lian, Q., Yang, H., Wang, X., Surface molecularly imprinted polymer of chitosan grafted poly (methyl methacrylate) for 5-fluorouracil and controlled release, *Sci. Rep.*, **2016**, *6*, 21409-21420. https://doi.org/10.1038/srep21409

Received: 09.02.2020
Accepted: 04.04.2020

3,4,5-TRIHYDROXYCYCLOHEXYL METHANOL - A NEW REDUCED DERIVATIVE FROM STRUCTURAL ACTIVITY RELATIONSHIP STUDIES (SARS) ON GALLIC ACID

Olawale H. Oladimeji[a]*, Magdalene A. Anwana[a], Emmanuel E. Attih[a] and Daniel E. Effiong[b]

Keywords: Gallic acid; esterification; reduction; ethyl gallate; 3,4,5-trihydroxycyclohexyl methanol.

Gallic acid or 3,4,5-trihydroxybenzoic acid is a poly-hydroxyl compound with potential therapeutic effects in the treatment/management of oxidative stress implicated in cancers, cardiovascular and neurodegenerative diseases amongst many others. The identity, purity, integrity and suitability of the acid were ascertained and established prior to the preparation of derivatives. Furthermore, a simple titrimetric method for its assay was designed. The esterification and selective reduction of the acid led to two derivatives coded ME and MA whose identities have been established to be ethyl gallate and 3,4,5-trihydroxycyclohexylmethanol (possibly a new reduction derivative) respectively using the IR spectral technique. Gallic acid and MA demonstrated minimal antioxidant activity at IC_{50} of 0.76 and 0.89 µg mL^{-1}, respectively. However, ME was remarkably active at 0.37 µg mL^{-1} which compare favourably with 0.34 µg mL^{-1} elicited by Vitamin C (a standard antioxidant drug). The obtained results indicate that esterification enhances the antioxidant activity of gallic acid.

* Corresponding Authors
Tel.: +2348146306558; +2347038916740
E-Mail: wale430@yahoo.co.uk;
hakeemoladmeji@uniuyo.edu.ng
[a] Department of Pharmaceutical & Medicinal Chemistry, Faculty of Pharmacy, University of Uyo, Uyo, Nigeria
[b] Department of Pharmaceutics & Pharmaceutical Technology, Faculty of Pharmacy, University of Uyo, Uyo, Nigeria

INTRODUCTION

Free radicals which can be reactive oxygen species (ROS), reactive nitrogen species (RNS) and many others are atoms, molecules, or ions that have unpaired valance electrons which make them chemically very reactive.[1] These chemical species are unstable and have short life time.[1-2] The ROS especially can be produced from either endogenous or exogenous sources. The endogenous sources of ROS include cellular organs/ organelles such as mitochondria, peroxisomes, endoplasmic reticulum while the exogenous sources include pollution, alcohol, tobacco smoke, heavy transition metals amongst many others.[3] It could be a daunting task for humans to avoid damage by free radicals. Hence, the is an everpressing need for antioxidants which are substances that when present in low concentrations compared with that of an oxidized substrate *w*ould significantly delay or prevent the oxidation of that substrate.

The oxidized substrate may be any molecule that is found in foods or biological materials, including carbohydrates, DNA, lipids and proteins.[4] However, some of the antioxidant drugs in clinical practice are toxic, poorly active and expensive. Hence, there is need to prospect for templates with little or no toxicities, better activities and which are affordable for general people. A known chemical substance with antioxidant activity is gallic acid. It is a white crystalline substance found in gallnuts, witch-hazel tea leaves, oak bark, strawberries, grapes, bananas and vinegars[5,6] amongst many other plants. The name is derived from oak galls, which were historically used to prepare tannic acid. It is found both free and as part of hydrolysable tannins. The gallic acid groups are usually bonded to form dimers such as ellagic acid. Hydrolysable tannins break down on hydrolysis to gallic acid and glucose or ellagic acid and glucose.[7] In addition, gallic acid has been isolated from a number of plants such as *Cynimcrium coccineum*, *Myriophyllum spicatum*, *Caesulpina nimosoida* and *Boswellia dalzieli* [8-11] amongst many others. The interest in this compound is due to its pharmacological activity as a radical scavenger which has been proved to have potential preventive and therapeutic effects in many diseases such as convulsion, microbial diseases, cardio-vascular diseases, cancer, neuro-degenerative disorders[12-14] and etc. where oxidative stress has been implicated. Consequently, gallic acid was considered as a promising lead compound for structural activity relationship studies (SARS).

In the present study, the acid was chemically modified to its ethyl ester and reduced derivatives by esterification and reduction respectively. The acid and synthesized products were tested for antioxidant activities using the DPPH (2,2-diphenyl-1-picrylhydrazyl hydrate) reagent and the obtained antioxidant activities (IC_{50}) were compared.

EXPERIMENTAL

Reagents/chemicals

Gallic acid and DPPH (2, 2-diphenyl-1-picryl hydrazyl hydrate**)** were obtained from Tianjin Kernel Chemical Reagent Company, China and Sigma Aldrich Chemicals, Germany, while acetic acid, chloroform, diethyl ether, dichloromethane, ethanol, hydrochloric acid, magnesium sulphate, methanol, iodine, petroleum ether, sodium borohydride, sulphamic acid, sodium hydroxide, sulphuric acid and tetrahydrofuran were obtained as AnaLAR Grade Chemicals from BDH Chemicals Limited, Poole, England. NaOH (1 M) solution used was standardized with sulfamic acid in the presence of phenolphthalein indicator.

Dissolution studies of gallic acid was done in chloroform, ethanol, dichloromethane, diethyl ether, methanol, petroleum ether and distilled water. Melting points were determined[15] using an Electro-thermal Melting Point apparatus (Electro-thermal Engineering Limited, England). Gallic acid content was determined by dissolution of sample in 0.5 M NaOH added, the mixture was heated in a water water-bath for 10 minutes, cooled and titrated with 0.5 M HCl in the presence of phenolphthalein as indicator.

The optical rotation and refractive index of gallic acid dissolved in ethanol were measured with using a Polarimeter type ADP-220 (Bellingham Stanley, England) and a refractometer type WAY-15 (Abbe, England) at the wavelength (λ) of sodium D line (589.3 nm) at 20.5 °C. The optical rotation and refractive indices of the derivatives being liquids were measured directly without dissolution in any solvents.[16] IR characteristics were measured by using the FTIR 84005 Spectrophotometer (Shimadzu, Japan).

To prepare a calibration curve for DPPH reagent (2,2-diphenyl-1-picrylhydrazyl hydrate), DPPH (4 mg) was weighed and dissolved in methanol (100 mL) to produce the stock solution (0.004 % w/v). Serial dilutions of the stock solution were carried out and the absorbance of each of the sample was taken at 512 nm using the UV spectrophotometer (Jenway 6405, USA). Methanol without DPPH was served as the blank.

Esterification of gallic acid

Gallic acid (m.p. 258-260 °C. $[n]_D^{20}$ 1.704, $[\alpha]_D^{20}$ +38°, FTIR: 1615 (Ar-C=C), 1705 (-C=O), 2854 (-CH stretching), 2922 (-CH stretching), 3281 (-OH) and 3361 (-OH) cm^{-1} (1.0 g) was added to 50 mL of ethanol and the mixture was stirred with a glass rod for 20 min until the particles were completely dissolved to obtain a clear solution. To the solution in the flask, another 50 mL of ethanol was added to ensure complete dissolution of the particles. Concentrated sulphuric acid (10 mL) was added to the solution which served as a catalyst. The flask containing the solution was corked with aluminum foil to prevent air. The reacting mixture was kept for two weeks in a refrigerator at 4 °C to ensure complete esterification.[17] Ethyl gallate (ME) was given as yellow liquid. $[n]_D^{20}$ 1.730, $[\alpha]_D^{20}$ +46°, d=1.73 g cm^{-3}. FTIR: 1037 (C-O-C, ether linkage), 1633 (Ar-C=C), 1715 (C=O), 3440 (-OH) and 3851 (-OH) cm^{-1}).

Reduction of gallic acid

Gallic acid (1.5 g) was dissolved in 20 mL of THF. The resultant solution was slowly added to a suspension of $NaBH_4$ (0.45 g) in 200 mL of THF at room temperature for 10 min. The mixture was stirred until evolution of gas ceased. 0.63 g of iodine and 20 mL of THF were carefully added to the mixture immersed in an ice-bath with the evolution of more gas. The mixture was further stirred for 1 h. Dilute HCl (5 mL) was added carefully and the mixture extracted several times with ether. The combined ether extract was washed with 3 M NaOH (30 mL), brine and dried over anhydrous MgSO4. Evaporation of the organic layer gave the reduced product.[18]

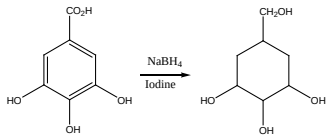

Scheme 2. Reduction of gallic acid.

3,4,5-Trihydroxycyclohexyl methanol (MA) was given as colourless liquid. $[n]_D^{20}$ 1.6111, $[\alpha]_D^{20}$ +30°, d=1.30 g cm^{-3}. FTIR: 2922 (CH stretching) and 3437 (-OH) cm^{-1}).

Antioxidant activity

Substances which are capable of donating electrons or hydrogen atoms can convert the purple-colored DPPH radical (2,2-diphenyl-1-picrylhydrazylhydrate) to its yellow-colored non-radical form, 1,1-diphenyl-2-picryl hydrazine.[19,20] This property was used to determine the antioxidant activity of derivatives of gallic acid and vitamin C. To determine the antioxidant activity of gallic acid, derivatives and vitamin C, 2 mg or 2 mL (liquids derivatives) each of sample was dissolved in 50 mL of methanol. Serial dilutions were carried out and 5 mL of each solution was incubated with 5 mL of 0.004 % w/v methanolic DPPH solution for optimal analytical accuracy. After an incubation period of 30 min in the dark at room temperature (25±2 °C), observation was made for a change in the color of the mixture from purple to yellow. The absorbance of each of the test samples was then taken at 512 nm. The Radical Scavenging Activity (RSA %) or Percentage Inhibition (PI %) of free radical DPPH was thus calculated:

$$RSA\ \%\ (PI\ \%) = [(A_{blank} - A_{sample})/A_{blank}] \times 100 \qquad (1)$$

where A_{blank} is the absorbance of the control reaction (DPPH solution without the test sample and A_{sample} is the absorbance of DPPH incubated with the sample. Vitamin C was used as a standard antioxidant drug. MGA/ME/MA/Vitamin C concentration providing 50 % inhibition (IC_{50}) was calculated from a graph of inhibition percentage against the concentration of the MGA /ME/MA/Vitamin C.[22-23]

Antioxidant activity

A calibration curve was prepared for DPPH reagent with an aim of confirming its purity, integrity and suitability for use in the antioxidant determinations. The Beer-Lambert's Law is the basis of all absorption spectrophotometry. Therefore, a plot of absorbance against concentration for a cell of unit thickness should give a linear graph. The reduction of the DPPH radical was determined by taking its absorption at a wavelength of 512 nm. It was observed that the absorbance of DPPH decreased as the concentration of added free radical scavenger (MGA/ME/MA/Vitamin C) increased which suggested that the DPPH reagent was being reduced. Table 1 shows radical scavenging activity (RSA %) or percentage inhibition (*PI* %) and the computed values of IC_{50} of MGA, ME, MA and Vitamin C.

RESULTS AND DISCUSSION

Gallic acid employed in this study was put through some monographic determinations with a view to ascertaining and establishing its identity, purity, integrity and suitability. Hence, its solubility profile and melting point determination were carried out. The acid was soluble in all the organic solvents used except petroleum ether while its melting point was observed 258-260 °C. These observed results are comparable with standard values in the literature. Prior to this study, there was no titrimetric method for assaying gallic acid. Hence, its assay was carried out using NaOH solution. Furthermore, the technique known as back-titration was used because direct titration of an acid against an alkali may sometimes be difficult. Partial hydrolysis could take place leading to the formation sodium gallate as a side product. Consequently, the excess NaOH was titrated against HCl. Also, a blank titrimetric determination was done without the sample of gallic acid. The percentage purity of the sample of gallic acid was computed to be 98.60 % w/w. Gallic acid gave a refractive of 1.704 and demonstrated an optical rotation of +38º. Diagnostic IR peaks at 3361, 3281, 2922, 2854, 1705 and1615 cm^{-1} indicate the characteristic -OH, -CH,-C=O and Ar-C=C stretchings respectively as can be seen in the IR spectrum of MGA.

Ethyl gallate (ME) was synthesized as a yellow liquid with a pleasant fruity smell which is characteristic of esters. This derivative showed a refractive index of 1.730 and gave an optical rotation of +46º. In addition, the IR spectroscopic analyses of ME show peaks at 3851, 3440, 1715, 1633 and 1054 cm^{-1} which are characteristic of -OH, -C=O, Ar-C=C (which was observed to absorb higher than that seen in MGA) and -C-O-C stretchings respectively.

MA was synthesized by the reduction method.[18] This procedure converts a carboxylic acid to an alcohol using sodium borohydride. This derivative gave a refractive index of 1.611 and an optical rotation of +30º. IR peaks at 3437 and 2922 cm^{-1} reveal the OH stretching and –CH absorptions respectively as are found in the IR spectrum of MA. It is instructive to state that this reduction method was primarily supposed to selectively reduce the –C=O group of the COOH to a $-CH_2$ (methylene). Furthermore, in addition to the removal of the –C=O peak at 1705 cm-1, the IR spectrum also shows that the 3 endocyclic aromatic C=C bonds represented by the peak at 1615 cm-1 disappeared indicating that the aromaticity of the gallic acid had been lost. This indicates that saturation of the three C=C bonds had taken place. Comprehensive database search of organic compounds was carried out and no piece of information or data about 3,4,5-trihydroxycyclohexyl methanol were obtained. Hence, it could be safe to infer that the compound is probably a new derivative of the reduction of gallic acid.

It is interesting to note that gallic acid and its derivatives showed optical rotations of +38°, +46° and +30° respectively, indicating that the three compounds are optically active. All these compounds rotate plane of polarized light in the clockwise directions. Hence, the compounds can demonstrate dextrorotation.

In antioxidant studies, the RSA % is an indicator of the antioxidant activity of MGA / ME/ MA/ vitamin C. Both gallic acid and MA demonstrated marginal antioxidant activity, IC_{50} of 0.76 and 0.89µg mL^{-1} respectively compared with ethyl gallate which was remarkably active at 0.37 µg mL^{-1}. Furthermore, the activity recorded by ME was not surprising because this compound is highly lipophilic due to the presence of the ethyl group moiety which enables it transverse the lipid membrane much easily and readily to the allosteric (active) sites better and faster than gallic acid to effect the pharmacological action of anti-oxidation. It must be stated that the ester showed an IC_{50} close to that shown to vitamin C (standard antioxidant drug) at 0.34 µg mL^{-1}. Interestingly, ethyl gallate isolated from *Acalypha wilkesiana* var. *laceacalypha* (Muell and Arg.) was observed to possess antimicrobial activity against *Bacillus subtilis*, *Staphylococcus aureus*, *Escherichia coli*, *Pseudomonas aeriginosa*, and *Salmonella typhi*.[23]

CONCLUSION

This present study reports the synthesis of a probably new derivative from the reduction of gallic acid with a marginal (minimal) antioxidant activity. However, the esterification of gallic acid enhances its antioxidant activity as the ester obtained therefrom demonstrated an antioxidant activity which compare favourably with the activity elicited by a standard antioxidant drug, Vitamin C.

ACKNOWLEDGEMENTS

The authors are grateful for the kind gesture of the Department of Pharmaceutical and Medicinal Chemistry, University of Uyo for the use of its Jenway 6405UV/VS Spectrophotometer in the antioxidant assays. We aslo acknowledge the contribution of the University of Ibadan, Nigeria in obtaining the IR spectra with the use of their facilities.

Table 1. Radical Scavenging activity (Percentage Inhibition) of samples at different concentrations and IC_{50} of the compounds.

Sample	Concentration, mg mL^{-1}					IC_{50} µg mL^{-1}
	0.0004	0.0008	0.0012	0.0016	0.0020	
MGA	36.16	57.55	58.78	59.18	78.98	0.76
ME	81.22	81.62	82.64	83.27	84.13	0.37
MA	38.35	38.78	57.95	58.10	58.98	0.89
Vitamin C	88.10	88.47	88.65	89.28	89.68	0.34

REFERENCES

[1]Hayyan, M., Hashim, M., Alnashef, I., Superoxide ion: Generation and chemical implications, *Chem. Rev.*, **2016,** *116(5)*, 3029-3085. DOI: 10.1021acs.chemrev.5b00407.

[2]Cheeseman, K., Slater, T., An introduction to free radicals chemistry, *Brit. Med. Bull.*, **1993,** *49(3)*, 481-493. DOI: org/10.1093/oxfordjournals.bmb.a072625.

[3]Speed, N., Blair, I., Cyclooxygenase and lipoxygenase-mediated DNA damage, *Cancer Metastasis Rev.*, **2011,** *30(34)*, 437-472. DOI: org/10.1007/510555-011-9298-8.

[4]Wanasundara, P., Shahidi, F., *Antioxidants: Science, Technology and Applications. Bailey's Industrial Oil and Fat Products*, **2005,** John Wiley and Sons, Inc., 1-11. ISBN: 9780471678496, DOI: 10.1002/047167849X

[5]Hodgson, J., Morton, L., Puddy, I., Beilin, L., Croft, K., Gallic acid metabolites are markers of black tea intake in humans, *J. Agric. Food Chem.*, **2000,** *48(6)*, 2276-2280. DOI: org/10.1021/Jf0000895.

[6]Pathak, S., Niranjan, K., Padh, H., Rajani, M., TLC densitometric method for the quantification of eugenol and gallic acid in clove, *Chromatography*, **2004,** *60(3)*, 241-244. DOI: 10.1365/510337-004-0373-y.

[7]Andrew, J., Availability of non-carotenoid antioxidants affects the expression of a carotenoid-based sexual ornaments, The role of antioxidants in photo-protection, *J. Am. Acad. Dermatol.*, **2004,** *67(5)*, 1013-1024. DOI: 10.1016/j.jacid.2019.12.077.

[8]Nakai, S., *Myriophyllum spicatum*-released allelopathic polyphenols inhibiting growth of blue-green algae *Microcystics aeruginosa*, *Water Res.*, **2000,** *34(11)*, 3026-3032. DOI: org/10.1016/50043-1354 (00)00039-7.

[9]Alemika. T. E., Onawunmi, G. O., Olugbade, T. A., Isolation and characterization of incensole from *Boswellia dalzielli* stem bark, *J. Pharm. Biores.*, **2004**, *1(1)*, 7-11. 001:10.4314/jpb.rlil.32041.

[10]Chanutheesuk, A., Teerawutgulrag, A., Kilburn, J., Rakariyatham, N., Antimicrobial gallic acid from *Caesalphina minosoides* bark, *Food Chem.*, **2007,** *100(3)*, 1044-1048. DOI: org/110.1016/j.foodchem.2020.126226.

[11]Zucca, P., Antonella, R., Carlo, T., Rinaldi, A., Enrico, S., Maria, D., Antonio, R., Evaluation of antioxidant potential of Maltese mushroom (*Cynomorium coccincum*) by means of multiple chemical and biological assays, *Nutrients*, **2013,** *5(1)*,149-161. DOI : org/10.3390/nu5010149.

[12]Duibedy, B., Gyamfi, A., Yonamine, Y., Aniya, Y., Free-radical scavenging action of medicinal herbs from Ghana: *Thonningia sanguinea* on experimentally-induced liver injuries, *Gen. Pharmacol.*, **1999,** *32(6)*, 661-667. DOI: org/10.1016/S0306-3623 (98)00238-9.

[13]Anurag, R. Allison, M., Lackey, L., McDougle, R., Brown, W., Law, E., Harris, R., Temiz, N., Refls, E., Kotandeiya, D., Nikas, B., Birns, M., Carpenter, M., Tretyakova, W., Temic, N., APOBEC3B is an enzymatic source of mutation in breast cancer, *Nature*, **2013,** *494(7437)*, 366-370. DOI: 10.1038/nature11881.

[14]Locatelli, C., Branco, F., Creczynski-Pasa, T., Alkyl esters of gallic acid as anticancer agents, *Eur. J. Med. Chem.*, **2013,** *60*, 233-239. DOI: org/10.1016j.ejnech.2012.056.

[15]*British Pharmacopeia*, *Appendix VA*, *A109*, The Pharmaceutical Press London, **1993**, 754.

[16]Olaniyi, A. A., *Principles of quality assurance and pharmaceutical analysis*, Mosuro Publishers, **2000**.

[17]Morrison, R.T, Boyd, R.N, *Organic chemistry*, Prentice-Hall Inc., New York, **1973**, 602-603; 672-673.

[18]Bhaskar-Kanth, J. V, Periasamy, M., Selective reduction of carboxylic acids into alcohols using $NaBH_4$ and I_2, *J. Org. Chem.*, **1991**, *56(20)*, 5964-5965. DOI:10.1021/jo00020a052.

[19]Nagalapur, S. K., Paramjyothi, S., *In-vitro* antioxidant activity of *Launaea pinnatifida* Cass leaves, *The Bioscan*, **2010**, *5(1)*, 105-108. www.the bioscan.in /journals/abs2010.5nl_105_108 htm.

[20]Guangrong, H., Jiaxin, J., Dehui, D., Anti-oxidative and antibacterial activity of the methanol extract of Artemisia anomala S. Moore, *Afr. J. Biotech*., **2008**, *7(9)*, 1335-1338. DOI: 10.1011060.8245 and rep.repl.

[21]Lebeau, J., Furman, G., Bernier, J. L., Durietz, P., Teissier, E., Cotelle, N., Antioxidant properties of di-tert-butylhydroxylated flavonoids. *Free-Radical Biology and Med*., **2000**, *29(9)*, 900-912. https://doi.org/10.1016/s0891-5849 (00)00390-7.

[22]Leitao, G. G., Leitao, S. G., Vilegas, W., Z. Quick preparative separation of natural naphthoquinones with antioxidant activity by high speed counter current chromatography, Z. *Naturforsch*., **2002**, *57C*, 1051-1055. https://doi.org/10.1515/znc-2002-11-1217.

[23]Oladimeji H. O., Tom, E. U., Attih, E. E., Ethyl gallate and Pyrogallol from *Acalyphawilkesiana* var. laceacalypha (Muell & Arg.), *Eur. Chem. Bull.*,**2014,** *3(8)*, 788-791.DOI: 10.17628/ecb.2014.3.788.

Received: 22.01.2020.
Accepted: 11.03.2020.

N-DERIVATIVES OF FORMALDIMINES: THE REASON FOR THE HIGH NITROGEN INVERSION BARRIERS IN N-METHYL- AND N-CHLOROIMINES

Yuliya A. Chertykhina[a], Nataliya V. Kutsik-Savchenko[a], Bohdan V. Murashevych[a], Oleg S. Lebed[a], Alexander V. Tsygankov[b], Igor I. Melnik[b] and Alexander V. Prosyanik[a]*

Keywords: Imines, inversion barriers, intramolecular interactions, electronegativity, correlations.

The energy and electronic parameters of the nitrogen inversion in imines $H_2C{=}NXH_n$ (XH_n = CH_3, NH_2, OH, F, SiH_3, PH_2, SH, Cl) have been calculated with the DFT method (B3LYP 6-311+G(d,p)) in terms of natural bond orbital. It has been established that the interactions of the nitrogen lone pair (LP) with the bond orbitals at the imino carbon atom are practically independent of the X atom and contribute to the decrease of the inversion barriers ($\Delta E_i^{\neq}$). While $nN\rightarrow\sigma^*_{X-H}$, $nN\leftrightarrow\sigma_{X-H}$ and $nN\leftrightarrow nX$ interactions substantially depend on the heteroatom type and promote the increase in the $\Delta E_i^{\neq}$ values with the rise in electronegativity of the X atom. The contribution of the interactions of the nitrogen LP with the Rydberg orbitals of the C=N–X group atoms is small and they cannot be the main reason of the decrease in the $\Delta E_i^{\neq}$ values when X atoms of the second period are replaced by atoms of the third period of the same group. The interactions of the LP of the X atoms and the X–H bond orbitals with the C=N bond orbitals have the main influence on the inversion barriers. The contribution of $nX\rightarrow\pi^*_{C=N}$ interactions to the $\Delta E_i^{\neq}$ values is dominant. The main reason of the "anomalous" inversion barriers of N-methyl- and N-chloroformaldimines is the destabilization of inversion transition states because of the reduction in the energies of $\sigma_{X-H}\rightarrow\pi^*_{C=N}$ and $nX\rightarrow\pi^*_{C=N}$ interactions and the rise in the energies of $nN\leftrightarrow nCl$ interactions. The contributions of electronegativity of XH_n substituents and energies of intramolecular interactions to the $\Delta E_i^{\neq}$ values have been determined.

* Corresponding Authors
E-Mail prosyanykav@gmail.com
[a] Ukrainian State University of Chemical Technology, Dnipro city, Ukraine
[b] National Technical University «Kharkiv polytechnic institute», Kharkiv city, Ukraine

INTRODUCTION

The nitrogen atom inversion is one of the classic problems of stereochemistry. Special attention is paid to the *Z,E*-isomerization process in imines occurring, as a rule, by an inversion. The energetic barrier of this inversion determines the electronic and steric effects of the substituents at the C=N-bond.[1-3] These effects are often hard to separate one from another, so in most cases only a qualitative description of the substituent's influence on the inversion barriers is possible. The quantitative influence of the substituents at imino-group and some intramolecular interactions on the nitrogen inversion barriers have been reviewed.[4-12] It has been established that the inversion barriers of the NH- and N-alkylamines decrease with the increase in electronegativity of the substituents on the carbon atom of the amino group, a positive charge on it and with a decrease in the population of the nitrogen lone pair (LP). The main influence on the inversion barriers is exerted by the interactions between the nitrogen LP and the bond orbitals of the imino carbon atom.[4-10]

In general, intramolecular interactions in N-substituted formaldimines reduce the inversion barriers. However, their contribution decreases with an increase in electronegativity of the XH_n substituents containing elements of the second period (except C) and increases for the XH_n substituents containing elements of the third period (except Cl).

The opposite vectors of changes in the energies of intramolecular interactions are mainly conditioned by the interactions of the X heteroatoms LP with the C=N bond orbitals; $nN\rightarrow$3d interactions are insignificant and have practically no effect on the nitrogen inversion barriers. Compared to other formaldimines, the N-methyl- and N-chloroderivatives showed abnormally low orbital energies of the C–H σ-bonds of the methyl group and nitrogen LP. The absence of correlations between the charge on the imino carbon atom and other parameters has been noted.[11,12]

In general, quantum chemical computations of ordinary imines, primarily N-derivatives of formaldimines, allow accurate estimate of the impact of the electron factors and intramolecular interactions on their structure and properties, including nitrogen inversion barriers. This can be largely facilitated by analyzing the correlational equations between the calculated properties of the imines (inversion barriers, charges, orbital energies) and the empiric parameters of the substituents (for example, electronegativity and Hammett constants), which allow predicting the changes of the calculated magnitudes depending on parameters used.

The purpose of the current study is to find out the factors responsible for the abnormal properties of N-methyl- and N-chloroformaldimines, which are manifested in the correlations disorders between their inversion barriers with electronic parameters and intramolecular interactions, as well as to determine their relative contributions to the inversion barriers.

COMPUTATIONAL METHODS

We have chosen isoelectronic N-derivatives of formaldimine as the objects of the study in which the steric effect of the substituents on the imino-carbon atom on the inversion barriers is minimized:

$H_2C{=}NXH_n$ (n = 0–3),

XH_n = CH_3 (I), NH_2 (II), OH (III), F (IV), SiH_3 (V), PH_2 (VI), SH (VII), Cl (VIII).

All calculations have been made using the DFT method (B3LYP[13,14]) in the basic set of atomic functions 6-311+G(d,p) through the software package Firefly 8.2.0.[15,16] Geometry optimizations has been performed for all systems. The accordance of the computed points to the minima and saddle points of the potential energy surfaces has been confirmed by vibrational frequency calculations. Standard basis set 6-311+G(d,p) as has been used is sufficient for the purposes mentioned above and for the better comparability with the results of the previous studies and experimental data. The obtained wave functions have been analyzed in terms of Natural Bond Orbital method using the program NBO 5.9 G[17] implemented in the Firefly 8.2.0. package.

Calculated values of the nitrogen inversion barriers in the formaldimines I-VIII ($\Delta E_i^{\neq}$) have been defined as the difference between the energies of the transition (TS) and ground (GS) states (Table 1).

Table 1. Inversion barriers of the imines I-VIII ($H_2C{=}NXH_n$)

Imine	XH_n	$\Delta E_i^{\neq}$, kJ mol^{-1}	χ[18]	σ_i[19]
I	Me	117.9	2.55	0.01
II	NH_2	141.8	3.12	0.08
III	OH	237.6	3.55	0.33
IV	F	311.7	4.00	0.45
V	SiH_3	30.9	1.90	0.06
VI	PH_2	47.3	2.17	0.09
VII	SH	89.6	2.65	0.30
VIII	Cl	194.4	3.05	0.42

The influence of intramolecular interactions on the inversion barriers has been estimated using the approach described.[7,10] We have divided all analyzed intramolecular into 5 groups, composed, as a rule, based on alternative donor-acceptor and repulsive interactions of the same bonds (Table 2) i.e. the nitrogen LP with the orbitals of the methylene group on the imino carbon atom (group 1), with the orbitals of the X–H bonds and the LP of substituents X (group 2), with the Rydberg orbitals of the imino group (group 3), the X-H bond orbitals and methylene group of the imine fragment (group 4), the orbitals of the bonds C=N and X–H, as well as C=N, and the LP of the atom X (group 5).

Donor-acceptor interactions that stabilize the GS (TS) are taken with a minus (–) sign, and repulsive interactions that destabilize the considered states are taken with a plus (+) sign. The intramolecular interactions energies (E_i) in the imines I-VIII are given in the article.[11] The influence of each interaction on the inversion barrier (ΔE_i) has been calculated as the difference between the energies of the transition and ground states. The additivity of the contributions of the energies ΔE_i to the changes of $\Delta E_i^{\neq}$ is assumed a priori, i.e. regardless of the type of intramolecular interactions energies (E_i) (donor-acceptor or repulsive) and the type of orbitals involved, any change in the energies ΔE_i causes a proportional change in inversion barriers. The total effect of interactions on the inversion barrier in each group ($\Delta\Sigma E_i$) has been obtained by the formula $\Delta\Sigma E_i = \Sigma E_i(TS) - \Sigma E_i(GS)$. The values of $\Sigma\Delta\Sigma E_{1-5}$ have been obtained by summation of the corresponding values of $\Delta\Sigma E_i$ in all groups. Negative values of $\Delta\Sigma E_i$ and $\Sigma\Delta\Sigma E_{1-5}$ indicate a decrease of the inversion barrier due to the considered interactions, and positive ones indicate its increase.

RESULTS AND DISCUSSION

The calculated values of the inversion barriers of formaldimines I-VIII satisfactorily correlate with the electronegativity of the substituents (χ)[18] on the nitrogen atom (Table 3, Eqn. 1). With a separate consideration of the data for the imines I-IV, which contain elements of the second period on the nitrogen atom, as well as for the imines V-VIII, which contain elements of the third period, correlations deteriorate (Table 3, Eqns. 2, 3). Graphical analysis (Figure 1) shows that the correlations violate the data for N-methyl- (I) and N-chloroformaldimines violate (VIII), which have anomalously high inversion barriers. If these data are excluded, the $\Delta E_i^{\neq}$ values of the imines II-IV and V-VII perfectly correlate with the values of χ-constants of substituents (Table 3, Eqns. 4, 5). Since the equations obtained describe the dependence of the inversion barriers on the electronegativity of the substituents on the nitrogen atom, by substituting the values of the χ-constants for the methyl group and the chlorine atom in them we can determine the theoretical inversion barriers for the imines I and VIII, which are conditioned only by the electronegativity of the substituents. The latter are respectively 36.1 and 120.2 kJ mol^{-1}, which is 81.8 and 74.2 kJ mol^{-1} less than the calculated values of $\Delta E_I^{\neq}$ and $\Delta E_{VIII}^{\neq}$. Consequently, it is more correct to speak of the abnormally high values of the inversion barriers for imines I and VIII and not of their decrease, for example, when an S atom is introduced instead of a C atom at the nitrogen atom, basing on comparable electronegativities of S and C atoms.

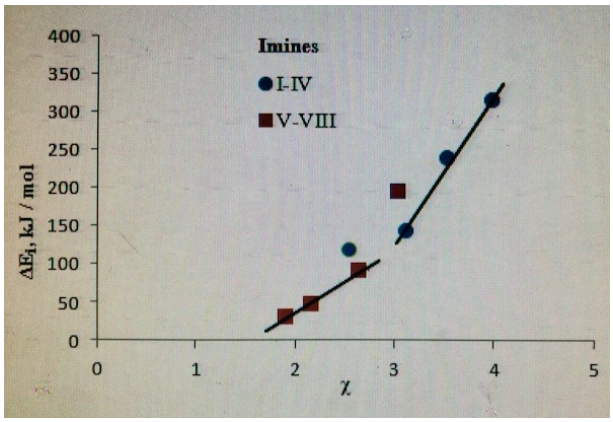

Figure 1. Dependence of the inversion barriers on the electronegativity of substituents X.

Table 2. The energies of intramolecular interactions in the imines I-VIII, kJ mol^{-1} $H_2C{=}NXH_n$

Gr.	Interaction/XH_n	Me(I)	NH_2(II)	OH(III)	F(IV)	SiH_3(V)	PH_2(VI)	SH(VII)	Cl(VIII)
1	$\Delta\Sigma E_1$[a)]	-74.1	-50.5	-62.9	-65.8	-52.8	-50.2	-33.0	-49.3
2	$\Delta\Sigma E_2$[b)]	-21.5	-38.8	40.4	74.6	-31.7	-24.7	-21.0	72.4
3	$\Delta\Sigma E_3$[c)]	4.3	12.1	10.1	17.9	-2.5	-11.7	-23.1	-28.3
4	$\Delta\Sigma E_4$[d)]	-27.4	-37.0	-32.6	-23.4	-16.2	-14.3	-19.2	-14.5
5	$\Delta\Sigma E_5$[e)]	-50.0	-153.1	-115.4	-96.4	-11.8	-63.6	-115.5	-84.5
-	$\Sigma\Delta\Sigma E_{1\text{-}4}$	-118.7	-114.2	-45.0	3.3	-103.2	-100.9	-96.3	-19.6
-	$\Sigma\Delta\Sigma E_{1\text{-}5}$	-168.7	-267.3	-160.4	-93.1	-115.0	-164.5	-211.8	-104.1
5.1	$\Delta\Sigma E$[$nX(\sigma_{XH})\rightarrow\pi^*_{C=N}$]	-13.8	-152.6	-130.7	-78.4	-6.5	-28.9	-81.3	-53.3
5.2	ΔE[$nX\rightarrow\pi^*_{C=N}$]	-	-160.5	-141.7	-78.4	-	-14.5	-81.3	-53.3

Note – following interactions have been considered[11]: [a)] $nN\rightarrow\sigma^*_{C-H1,2}$, $nN\leftrightarrow\sigma_{C-H1,2}$; [b)] $nN\rightarrow\sigma^*_{X-H}$, $nN\leftrightarrow\sigma_{X-H}$, $nN\leftrightarrow nX$; [c)] $nN\rightarrow RY^*_{C=}$, $nN\rightarrow RY^*_{X}$; [d)] $\sigma_{N-X}\rightarrow\sigma^*_{C-H1,2}$, $\sigma_{C-H1,2}\rightarrow\sigma^*_{N-X}$, $\sigma_{N-X}\leftrightarrow\sigma_{C-H1,2}$; [e)] $\sigma_{X-H}\rightarrow\sigma^*_{C=N}$, $\sigma_{X-H}\rightarrow\pi^*_{C=N}$, $\pi_{C=N}\rightarrow\sigma^*_{X-H}$, $\sigma_{X-H}\leftrightarrow\pi_{C=N}$, $\sigma_{X-H}\leftrightarrow\sigma_{C=N}$, $nX\rightarrow\sigma^*_{C=N}$, $nX\rightarrow\pi^*_{C=N}$, $n_X\leftrightarrow\sigma_{C=N}$, $n_X\leftrightarrow\pi_{C=N}$.

Table 3. Parameters of the dependence of the inversion barriers of the imines I-VIII on the χ- and σ_i-constants of the XH_n substituents and the energies of intramolecular interactions (Y=ρX+C).

Eqns. No	Imines	X	Y	ρ	C	*s*	*r*
1	I-VIII	χ	$\Delta E_i^{\neq}$	134.5111	-240.03	22.05	0.974
2	I-IV	χ	$\Delta E_i^{\neq}$	139.1	-257.49	24.48	0.962
3	V-VIII	χ	$\Delta E_i^{\neq}$	137.1	-244.34	22.65	0.951
4	II-IV	χ	$\Delta E_i^{\neq}$	192.8	-455.53	6.02	0.996
5	V-VII	χ	$\Delta E_i^{\neq}$	79.4	-121.96	2.20	0.996
6	I-IV	σ_i	$\Delta E_i^{\neq}$	429.3	108.88	9.75	0.994
7	V-VIII	σ_i	$\Delta E_i^{\neq}$	403.5	2.79	24.12	0.945
8	II-IV	$\sum\Delta\sum E_{1\text{-}5}$	$\Delta E_i^{\neq}$	0.968	398.43	3.96	0.998
9	V-VII	$\sum\Delta\sum E_{1\text{-}5}$	$\Delta E_i^{\neq}$	-0.604	-43.03	6.42	-0.966
10	II-IV	$\Delta\sum E_1$	$\Delta E_i^{\neq}$	-10.10	-372.95	18.6	-0.964
11	V-VII	$\Delta\sum E_1$	$\Delta E_i^{\neq}$	2.78	182.05	3.77	0.988
12	II -IV	$\Delta\sum E_2$	$\Delta E_i^{\neq}$	1.448	193.60	10.5	0.989
13	V-VII	$\Delta\sum E_2$	$\Delta E_i^{\neq}$	5.08	186.90	10.21	0.911
14	II-IV	$\Delta\sum E_3$	$\Delta E_i^{\neq}$	13.93	44.17	52.1	0.663
15	V-VII	$\Delta\sum E_3$	$\Delta E_i^{\neq}$	-2.88	20.08	4.62	-0.982
16	II-IV	$\Delta\sum E_4$	$\Delta E_i^{\neq}$	11.81	596.61	18.86	0.963
17	V-VII	$\Delta\sum E_4$	$\Delta E_i^{\neq}$	-9.62	-103.40	15.33	-0.785
18	II-IV	$\sum\Delta\sum E_{1\text{-}4}$	$\Delta E_i^{\neq}$	1.442	305.29	2.00	1.000
19	V-VII	$\sum\Delta\sum E_{1\text{-}4}$	$\Delta E_i^{\neq}$	8.606	917.64	1.47	0.998
20	I-IV	$\sum\Delta\sum E_{1\text{-}4}$	$\Delta E_i^{\neq}$	1.521	306.64	6.98	0.997
21	V-VIII	$\sum\Delta\sum E_{1\text{-}4}$	$\Delta E_i^{\neq}$	1.754	230.88	19.76	0.963
22	II-IV	$\Delta\sum E_5$	$\Delta E_i^{\neq}$	2.93	587.02	7.95	0.993
23	V-VII	$\Delta\sum E_5$	$\Delta E_i^{\neq}$	-0.566	19.91	6.09	-0.966
24	II-IV	$\Delta\sum E$[a)]	$\Delta E_i^{\neq}$	2.131	487.25	20.94	0.954
25	V-VII	$\Delta\sum E$[a)]	$\Delta E_i^{\neq}$	-0.789	25.25	0.54	-1.000

To determine the reasons for the inversion barrier increases in N-methyl- and N-chloroformaldimines, we have investigated the influence of electronic factors and intramolecular donor-acceptor and repulsive interactions.

The $\Delta E_i^{\neq}$ values of the imines I-VIII do not show a direct dependence on the induction constants of the substituents (σ_i),[19] although a certain correlation of values is observed (*r* = 0.765). With a separate consideration of imines containing elements of the second or third periods on the nitrogen atom, the values of $\Delta E_i^{\neq}$ correlate with σ_i-constants of substituents (Table 3, eqns. 6, 7), forming two almost parallel straight lines (Figure 2). Wherein, despite the comparable values of σ_i-constants for the substituents, the central atoms X of which are in the same group, the inversion barriers for the corresponding imines differ a lot. The difference in the values of $\Delta E_i^{\neq}$ obtained from equations 6 and 7, is 106.1 kJ mol^{-1} if σ_i = 0, and 117.7 kJ mol^{-1} if σ_i=0.45. It may mean that the inversion barriers mainly depend on the electronegativity of the XH_n substituents. The inductive effect has a subordinate impact. This fact indicates the incorrectness of the analysis of the imines inversion barriers values based on σ_i-constants of the substituents containing elements X of different periods or groups.

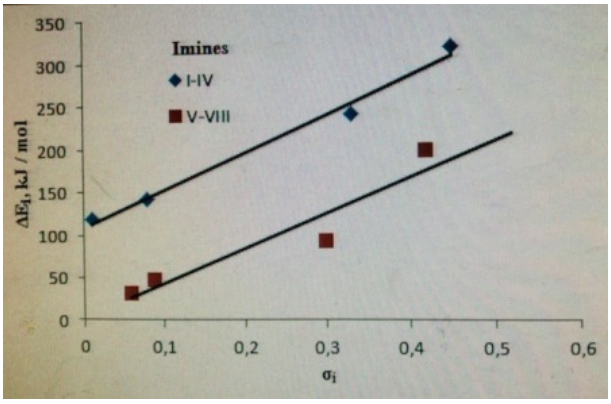

Figure 2. Dependence of the inversion barriers on the induction constants of substituents X.

The values of $\Delta E_i^{\neq}$ do not show any dependence on the sum of the energies of intramolecular interactions $\sum\Delta\sum E_{1\text{-}5}$ either by joint consideration of imines I-VIII (r = 0.32) or by separate consideration of the imines I-IV and V-VIII (r = 0.75 and 0.31, respectively). The correlations are observed only after exclusion of the data for the imines I and VIII (Figure 3, 4, Table 3, Eqns. 8, 9). At the same time, the change in the $\sum\Delta\sum E_{1\text{-}5}$ values with an increase of the electronegativity of the substituents contributes to an increase of the inversion barriers of imines II-IV and their decrease for imines V-VII. Since the Eqns. (8) and (9) describe the dependence of the inversion barriers on the sum of the energies of intramolecular interactions $\sum\Delta\sum E_{1\text{-}5,}$ by substituting the values of $\Delta E_I^{\neq}$ and $\Delta E^{\neq}_{VIII}$ into them it is possible to determine the theoretical values of the sums $\sum\Delta\sum E_{1\text{-}5(i)}^{theor}$, which would conform to the above correlations of the inversion barriers of the imines I and VIII. The corresponding values of $\sum\Delta\sum E_{1\text{-}5(i)}^{theor}$ for them are to be -289.2 and -395.7 kJ mol^{-1}, which is 120.5 and 291.6 kJ mol^{-1} less than the calculated values ($\Delta\sum\Delta\sum E_{1\text{-}5(i)} = \sum\Delta\sum E_{1\text{-}5(i)} - \sum\Delta\sum E_{1\text{-}5(i)}^{theor}$). Reductions in the stabilization of the inversion TS as a result of a change in the energies of intramolecular interactions may be the main reason for the observed increase in the inversion barriers of imines I and VIII.

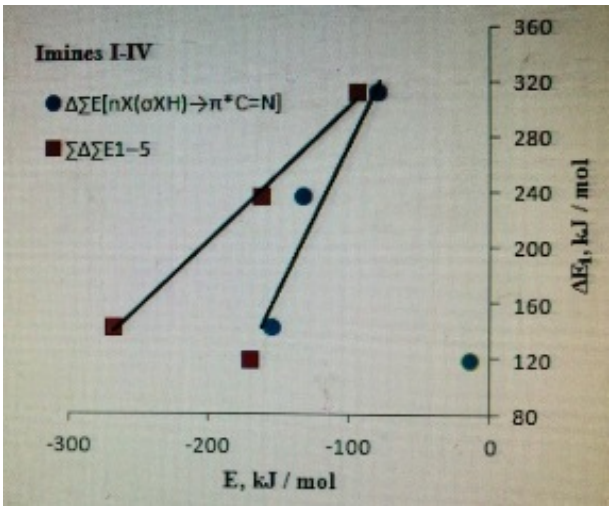

Figure 3. Dependence of the inversion barriers on the intramolecular interaction energies of substituents X of the second period.

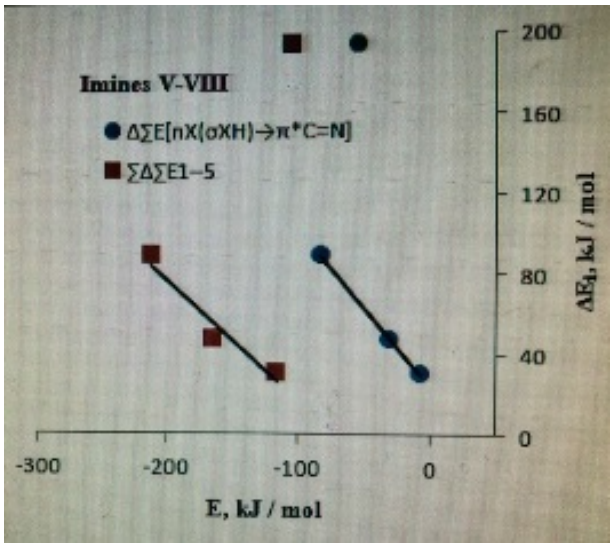

Figure 4. Dependence of the inversion barriers on the intramolecular interaction energies of substituents X of the third period.

To determine the intramolecular interactions responsible for increasing the calculated values of $\sum\Delta\sum E_{1\text{-}5}$, the analysis of changes in the $\Delta\sum\Delta E_i$ values for groups 1-5 has been carried out based on their correlations with the inversion barriers of the imines II-IV and V-VII.

The interactions of the nitrogen LP with the bond orbitals at the imino carbon atom (Table 2, Group 1) generally reduce the inversion barriers. An increase in electronegativity of X atom for the elements of the second period (subgroup A) contributes to a decrease in the $\Delta E_i^{\neq}$ values as a result of an increase in stabilization of the inversion TS, whereas for the elements of the third period (subgroup B), it contributes to an increase in the $\Delta E_i^{\neq}$ values because of a decrease in the TS stabilization (Table 3, eqns. 10, 11). Slope opposition of the changes in the values of $\Delta\sum E_1$ in subgroups A and B indicates the impossibility of a general correlation for them. In general, even though the interactions of group 1 contribute to a significant decrease in the inversion barriers, they do not have a significant effect on the change in the $\Delta E_i^{\neq}$ values depending on the heteroatom X (the relative change in the $\Delta\sum E_1$ values for subgroups A and B is 23.6 and 19.8 kJ mol^{-1}, respectively).

With the increase in the electronegativity of the X atom, the interactions of the nitrogen LP with the orbitals of the X–H bonds and the X heteroatoms LP (Table 2, Group 2) contribute to the increase of the inversion barriers in both subgroups due to the dominant influence of repulsive intramolecular interactions destabilizing the inversion TS (Table 3, Eqns. 12, 13). The interactions of the 2-nd group largely depend on the type of heteroatom X and have a significant effect on the change in the inversion barriers (the relative change in the $\Delta\sum E_2$ values for subgroups A and B is 96.1 and 104.1 kJ mol^{-1}, respectively). It is necessary to note an explicit, by 93.4 kJ mol^{-1}, change in the intramolecular interactions energy $\Delta\sum E_2$ upon transition from N-sulfhydrylimine VII to N-chloroimine VIII, which is approximate to the change in the values of $\sum\Delta\sum E_{1\text{-}5}$ for this pair of imines (107.7 kJ mol^{-1}). Undoubtedly, the repulsive interaction of nN↔nCl has a significant effect on increasing the inversion barrier of the N-chloroimine VIII. Based on

the $\Delta E_i^{\neq}$ values found for imines I, VIII, and the correlational equations 12 and 13, the theoretical values of the intramolecular interactions energies $\Delta\sum E_{2(i)}^{theor}$ should be -52.2 and 1.5 kJ mol^{-1}, respectively, which are 30.7 and 70.9 kJ mol^{-1} less than the calculated ones ($\Delta\Delta\sum E_{2(i)} = \Delta\sum E_{2(i)} - \Delta\sum E_{2(i)}^{theor}$). Thus, as a result of the intramolecular interactions of the 2-nd group, the inversion barriers of imines I, VIII must increase proportionally to the increase in the intramolecular interactions energies $\Delta\sum E_{2(i)}$. It should be noted that the influence of these interactions on the values of $\Delta E_i^{\neq}$ was not practically taken into account before.

On the contrary, the influence of the interaction of the nitrogen LP with 3d-orbitals of sulfur atoms and other heteroatoms of higher periods was intensively discussed. For example, it was pointed out that these interactions underlie the low inversion barriers of the sulfenyl-, sulfinyl-, and sulfonylimines.[20-23] The analysis of the interactions between the nitrogen LP and the Rydberg orbitals of the atoms of C=N-X group (Table 2, Group 3) shows that with an increase in electronegativity of X atoms in subgroup A, they contribute to a slight increase in the inversion barriers and their slight decrease in subgroup B (Table 3, Eqns. 14, 15). Moreover, upon the transition from the elements of the second period to the elements of the third period, the contribution of these interactions to the reduction of the inversion barriers for the IV-VII groups of the periodic system is relatively small and amounts to 6.8, 23.8, 33.2 and 46.2 kJ mol^{-1}, respectively. This is disparately insignificant in comparison with the observed change in the inversion barriers (87.0, 94.5, 148.0 and 117.3 kJ mol^{-1}). Consequently, these interactions cannot be the main reason for the decrease in the inversion barriers for the imines containing atoms of the third period.

The impact of interactions on the inversion barriers collected in the 4-th group has never been studied. Indeed, although these interactions contribute to decreasing of the inversion barriers (Table 3, Eqns 16, 17), they have insignificant effect on their change and, moreover, practically do not depend on the substituent at the nitrogen atom (the relative change in the $\Delta\sum E_4$ values for subgroups A and B is 13.6 and 4.9 kJ mol^{-1}, respectively).

The sums of intramolecular interactions energies $\sum\Delta\sum E_{1\text{-}4}$ perfectly correlate with the values of $\Delta E_i^{\neq}$ of the imines II-IV and V-VII (Table 3, Eqns. 18,19) and even more of the imines I-IV and V-VIII (Table 3, Eqns. 20, 21). This indicates a minor participation of these interactions in increasing the inversion barriers of N-methyl- (I) and N-chloroformaldimines (VIII) and reducing the energies $\sum\Delta\sum E_{1\text{-}5(i)}$ for them.

The interactions of the X–H bonds orbitals and the X atoms LP with the orbitals of the C=N bonds show the dominant impact on the change in the intramolecular interactions energies $\sum\Delta\sum E_{1\text{-}5}$ (Table 2, group 5). The energies of the intramolecular interactions of this group make the main contribution to the total energies of intramolecular interactions $\sum\Delta\sum E_{1\text{-}5}$ of the imines II-IV and V-VII. The values of $\Delta\sum E_5$ correlate completely with the values of $\Delta E_i^{\neq}$ of the imines II-IV and V-VII (Table 3, Eqns. 20, 21). In this case, the increase in electronegativity of the X atom in subgroup A contributes to the increase in the inversion barriers as a result of decreasing stabilization of the inversion TS, while in subgroup B it decreases the values of $\Delta E_i^{\neq}$ due to the increasing stabilization of the TS. Based on the values of $\Delta E_i^{\neq}$, found for the imines I, VIII, and the correlation equations 20 and 21, the theoretical energies $\Delta\sum E_{5(i)}^{theor}$ should be -160.1 and -306.1 kJ mol^{-1}, respectively, which is 110.1 and 221.6 kJ mol^{-1} less than the calculated ones ($\Delta\Delta\sum E_{5(i)} = \Delta\sum E_{5(i)} - \Delta\sum E_{5(i)}^{theor}$). Therefore, as a result of the intramolecular interactions of the 5-th group, the inversion barriers of imines I, VIII must increase significantly in proportion to the increase in the energies $\Delta\sum E_{5(i)}$.

In its turn, the dominant contribution to the change in the inversion barriers due to the interactions of the 5-th group is made by the energies of donor-acceptor interactions of electrons of the σ-bonds N-X and X heteroatoms LP with the π^*-orbital of the C=N bond (Table 2, Group 5.1), which are close to the total energies $\Delta\sum E_5$ of the corresponding imines and correlate completely with the values $\Delta E_i^{\neq}$ of the imines II-IV and V-VII (Table 3, Eqns. 24, 25). The similar values of the coefficients ρ in Eqns. 22 and 24, 23 and 25 indicate the dominant contribution of the interactions of group 5.1 to the total change in energies of the 5th group. The main contribution to the change in the values of $\Delta\Sigma E[nX(\sigma_{XH})\rightarrow\pi^*_{C=N}]$ is made by the interaction energy of the X atom LP with the π^*-orbital of the C=N bond ($nX\rightarrow\pi^*_{C=N}$, Table 2, group 5.2). Comparison of the dependences of the inversion barriers of imines I-IV and V-VIII on the $\sum\Delta\sum E_{1\text{-}5}$ and $\Delta\Sigma E[nX(\sigma_{XH})\rightarrow\pi^*_{C=N}]$ values (Fig. 3, 4, respectively) indicates the dominant influence of the latter especially clearly.

Almost equal for the imines I and VIII values of the energies $\Delta\sum\Delta\sum E_{1\text{-}5(i)}$ and the sum of energies $\Delta\Delta\sum E_{2(i)}$ and $\Delta\Delta\sum E_{5(i)}$, which are 120.5 and 140.8 (imine I) and 291.6 and 292.5 kJ mol^{-1} (imine VIII), respectively, confirm the correctness of the above arguments. On the other hand, it points that abnormally high nitrogen inversion barriers in N-methylformaldimine I and N-chloroformaldimine VIII are mainly conditioned by the decrease in the interaction energies of the electrons of the σ-bonds XH and X heteroatoms LP with antibonding orbitals of the C=N bonds ($\sigma_{X-H}\rightarrow\pi^*_{C=N}$ and $\pi_{C=N}\rightarrow\sigma^*_{X-H}$ (imine I) and $nX\rightarrow\sigma^*_{C=N}$, $nX\rightarrow\pi^*_{C=N}$ and $nX\rightarrow\sigma^*_{C=N}$, $nX\rightarrow\pi^*_{C=N}$ (imine IX)) and, to a lesser extent, by the increase in the interaction energies nN↔nCl. Therefore, we can assume that the calculated value of the inversion barrier of N-methylformaldimine I in the first approximation consists of the electronegativity of the methyl group (36.1 kJ mol^{-1}) and intramolecular interactions (81.8 kJ mol^{-1}). The electronegativity contributions of the chlorine atom and the intramolecular interactions for N-chloroformaldimine VIII are 120.2 and 74.2 kJ mol^{-1}, respectively. It is obvious that with the increase in the electronegativity of the XH_n substituent, its relative contribution to the nitrogen inversion barriers increases, and the contribution of intramolecular interactions decreases.

CONCLUSIONS

The investigation of the correlation dependencies of the nitrogen atom inversion barriers in N-derivatives of imines on electronegativity and χ-constants of substituents and intramolecular interactions has made it possible to establish that N-methyl- and N-chloroformaldimines have abnormally

high nitrogen inversion barriers. The main reason for such an increase of the barriers is a decrease in the stabilization of the transition states of the inversion as a result of a change in the energies of intramolecular donor-acceptor and repulsive interactions. The latter are mainly conditioned by the decrease in the energies of the interactions between the electrons of the σ-XH bonds and X heteroatoms LP and antibonding orbitals of C=N bonds ($\sigma_{X-H}\rightarrow\pi^*_{C=N}$, $\pi_{C=N}\rightarrow\sigma^*_{X-H}$ и $nX\rightarrow\sigma^*_{C=N}$, $nX\rightarrow\pi^*_{C=N}$, respectively) and, to a lesser extent, by the increase in the interaction energies $nN\leftrightarrow nCl$. In general, the main contribution to the change in the energies of intramolecular interactions has been made by the interactions of X atoms LP with the π^*-orbitals of the C=N bonds ($nX\rightarrow\pi^*_{C=N}$).

The magnitude of the inversion barriers depends on both the electronegativity of the substituents on the nitrogen atom and the energies of intramolecular interactions, and their relative contributions are 30–60 and 70–40 %, respectively. An increase in the electronegativity of substituents leads to the growth of its contribution to the barriers.

The interactions of the nitrogen LP with bond orbitals at the imino carbon atom contribute to the reduction of the inversion barriers, but they practically do not depend on the heteroatom X. On the contrary, the interactions of the nitrogen LP with the orbitals of the X–H bonds and the X heteroatoms LP significantly depend on the type of heteroatom. They have a great effect on the inversion barriers, contributing to their increase with the growth of electronegativity of the X atom as a result of the repulsive intramolecular interactions destabilizing inversion TS.

The interactions of the nitrogen LP with the Rydberg orbitals of the atoms of the C=N group promote an insignificant multidirectional change of the inversion barriers. The contribution of these interactions to the decrease of the inversion barriers in the transition from the elements of the second period to the elements of the third period for groups IV-VII is relatively small and cannot be the reason for their reduction in imines containing atoms of the third period.

The interactions of the orbitals of the X–H bonds and the X atoms LP with the orbitals of the C=N bonds have the main effect on the inversion barriers of N-substituted imines in comparison with other intramolecular interactions. An increase in electronegativity of X atoms for elements of the second period contributes to an increase in the inversion barriers resulting from a decrease in stabilization of the inversion TS; whereas, for the elements of the third period they decrease because of an increase in the stabilization of TS. The energies of donor-acceptor interactions of electrons of the N-X σ-bonds and X heteroatoms LP with the π^*-orbital of the C=N bond have made the dominant contribution to the change in the inversion barriers.

REFERENCES

[1]Lehn, J. M., Nitrogen inversion experiment and theory, *Top. Curr. Chem.*, **1970**, *15*, 311-377.

[2]McCarty, C. G., *The chemistry of the carbon-nitrogen double bond*, John Wiley & Sons, NY., **1970**, *9*, 363 – 464. https://doi.org/10.1002/9780470771204.ch9

[3]Kalinowski, H., Kessler, H., Fast Isomerizations About Double Bonds, *Top. Stereochem.*, **1973**, *7*, 295-383. DOI: 10.1002/9780470147160.ch4

[4]Blanco, F., Alkorta, I., Elguero, J., Barriers about Double Carbon-Nitrogen Bond in Imine Derivatives (Aldimines, Oximes, Hydrazones, Azines), *Croat. Chem. Acta.*, **2009**, *82*, 173-183. https://www.researchgate.net/publication/27221655

[5]Shuhua, H., Ying, T., Xiuchan, X., Lijuan, Z., Yanzhi, G., Menglong, L., Anmin, T., Xuemei, P., Ning-Bew, W., Substituent effects on electronic character of the C=N group and trans/cis isomerization in the C-substituted imine derivatives: a computational study, *J. Mol. Struct.*, THEOCHEM, **2010**, *951(1)*, 7-13. DOI: 10.1016/j.theochem.2010.03.029

[6]Prosyanik, A. V., Kutsik-Savchenko, N. V., Kol'tsov, N. Yu., Yukhno, A. G., Konovalova, S. A., Avdeyenko, A. P., Thermal Z, E-isomerization of imines. VII. N-arylsulfenylimines of acetone, mesoxal ester and tetramethylurea, *Vopr. Khim. Khim. Technol.*, **2012***(2)*, 14–24 (in Russian). http://nbuv.gov.ua/UJRN/Vchem_2012_2_4

[7]Kutsik-Savchenko, N. V., Lebed, O. S., Prosyanik, A. V., NH- i N-alkylimines of formaldehyde: the electronic structure and inversion barriers of nitrogen atom, *Vopr. Khim. Khim. Tekhnol.*, **2014***(1)*, 15-23 (in Russian). https://udhtu.edu.ua/public/userfiles/file/VHHT/2014/1/5.pdf

[8]Kutsik-Savchenko, N. V., Lebed, O. S., Prosyanik, A. V., The effect of C-substituents on the topomerization mechanism, inversion barriers and electronic character of C=N bond in N-alkylimines: A theoretical study, *Comput. Theor. Chem.* **2015**, *1072*, 15-20. DOI: 10.1016/j.comptc.2015.08.019

[9]Kutsik-Savchenko, N. V., Lebed, O. S., Prosyanik, A. V., Effect of substituents at the imine carbon on the nitrogen inversion barriers in the HN-imines, *Vopr. Khim. Khim. Tekhnol.*, **2015***(2)* 45-52 (in Russian). https://udhtu.edu.ua/public/userfiles//file/VHHT/2015/2/Kutsik-Savchenko.pdf

[10]Kutsik-Savchenko, N. V., Lebed, O. S., Prosyanik, A. V., The HN- and N-methylimines of formaldehyde, acetaldehyde and acetone: electronic structure and nitrogen inversion barriers, *Bull. Dnipropetrovsk Univ., Ser. Chem.*, **2015**, *23*, 21-29 (in Russian). DOI: https://doi.org/10.15421/081504

[11]Chertykhina, Yu. A., Kutsik-Savchenko, N. V., Prosyanik, A. V., N-Derivatives of formaldimine: the effect of electronegativity of substituents and intramolecular interactions on the inversion barriers of the nitrogen atom, *Vopr. Khim. Khim. Tekhnol.*, **2017***(4)*, 37-45 (in Russian). https://udhtu.edu.ua/public/userfiles/file/VHHT/2017/4/Chertihina.pdf

[12]Chertykhina, Yu. A., Kutsik-Savchenko, N. V., Tsygankov, A. V., Prosyanik, A. V., N-Derivatives of formaldimine: the relationship between donor-acceptor intramolecular interactions and the electronic parameters of atoms, *Vopr. Khim. Khim. Tekhnol.*, **2018***(1)*, 57-66 (in Russian), https://udhtu.edu.ua/public/userfiles/file/VHHT/2018/1/Chertihina.pdf

[13]Koch, W., Holthausen, M. C., *A chemists guide to density functional theory*, Wiley-VCH, Weinheim (Germany), **2001**, 300, ISBNs: 3-527-30372-3 (Softcover); 3-527-60004-3 (Electronic)

[14]Schuchardt, K. L., Didier, B. T., Elsethagen, T., Sun, L., Gurumoorthi, V., Chase, J., Li, J., Windus, T. L., Basis set exchange: a community database for computational sciences, *J. Chem. Inf. Model.*, **2007**, *47(3)*, 1045-1052, DOI:10.1021/ci600510j

[15]Granovsky, A. A., Firefly version 8.2.0., http://classic.chem.msu.su/gran/firefly/index.html.

[16]Schmidt, M. W., Baldridge, K. K., Boatz, J. A., Elbert, S. T., Gordon, M. S., Jensen, J. H., Koseki, S., Matsunaga, N., Nguyen, K. A., Su, S. J., Windus, T. L., Dupuis, M., Montgomery, J. A., General atomic and molecular electronic structure system, *J. Comput. Chem.*, **1993**, *14*, 1347-1363. https://doi.org/10.1002/jcc.540141112

[17]NBO 5.9/Gledening, E. D., Badenhoop, J. K., Reed, A. E., Carpenter, J. E., Bohmann, J. A., Morales, C. M., Weinhold, F., Theoretical Chemistry Institute, University of Wisconsin, Madison, *WI*, **2012**, http://www.chem.wisc.edu/~nbo5

[18]Mullay, J., Atomic and group electronegativities, *J. Am. Chem. Soc.*, **1984**, *106*, 5842–5847. https://doi.org/10.1021/ja00332a014

[19]Hansch, C., Leo, A., Taft, R. W., A survey of Hammett substituent constants and resonance and field parameters, *Chem. Rev.*, **1991**, *91*, 165–195. https://doi.org/10.1021/cr00002a004

[20]Davis, F. A., Slegeir, W. A. R., Kaminski, J. M., Sulfenimines: A new synthesis and barrier of stereomutation, *J. Chem. Soc., Chem. Commun.*, **1972**, *11*, 634–635. DOI: 10.1002/chin.1972502100

[21]Davis, F. A., Kluger, E. W., Chemistry of sulfur-nitrogen bond. 10. Barriers to planar inversion in N-(4,4-dimethylbenzophenylidene)arensulfenamides and selenenamides, *J. Am. Chem. Soc.*,**1976**, *98(1)*, 302–303. DOI: **10.1021/ja00417a084**

[22]Brown, C., Grayson, B. T., Hudson, R. F., Z-E isomerisation of N-sulphenylimines, *J. Chem. Soc., Perkin Trans. 2*, **1979**, 427-434. https://pubs.rsc.org/ja/content/articlelanding/1979/p2/p29790000427

[23]Bharatam, P. V., Kaur, A., Kaur, D., Electronic structure of N-sulfenylimines, *J. Phys. Org. Chem.*, **2003**, *104(3)*, 183–188. DOI: 10.1002/poc.592

Received: 22.02.2020
Accepted: 05.04.2020